CHAPTER 1

GENERAL INTRODUCTION

Traditional clinical methods for evaluating the circulation measure capillary refill time, arterial pulse or arterial pressure of superficial blood vessels. These methods are subjective or general estimates of the circulatory status. Angiography, scintigraphy, implanted electromagnetic or Doppler flowmeter can be used to investigate haemodynamics at deep locations in the body such as the splanchnic vessels[1,2], but these are somewhat invasive methods. Additionally angiography is attended by the potential risk of contrast agent toxicity; scintigraphy carries the risk of radiation injury; and implanted electromagnetic or Doppler flowmeter is not available for routine clinical work. Because of its safe and non-invasive nature, the introduction of transcutaneous Doppler ultrasonography marked a new era in the clinical evaluation of blood flow[3]. The technique can be used repeatedly to accurately determine haemodynamic patterns at a specific location within a vessel or cardiac chamber. Doppler ultrasonography provides information on blood flow direction, speed and velocity profile. The physiological-anatomical condition of the cardiovascular system can in turn be deduced from the haemodynamic information.

Currently three established modes of Doppler ultrasonography consisting of spectral, colour and power Doppler, are in use. A general use of Doppler ultrasonography is in differentiating anechoic non-vascular from vascular structure; or a vessel with blood flow from that without - all appearing as anechoic tubular or rounded structures during routine B-mode ultrasonography[4,5]. The clinical roles of Doppler ultrasonography in the investigation, diagnosis and management of localised peripheral or cerebrovascular disorders such as occlusions, shunts and arteriovenous anastomoses[6-8] or cardiac

and great blood vessel disorders such as congenital defects[9] in human patients is well established. In these roles, the three Doppler modalities compliment B-mode ultrasonography, and each other, for improved diagnostic capability.

Clinical uses or studies of Doppler ultrasonography in human patients have been extended to the diagnosis or investigation and management of splanchnic vessel disorders[4,10], differentiation of focal parenchymal[11-13] and hollow organ[4] lesions, and evaluation and management of physiological processes in obstetrics[14], urology[15,16] and digestion[17,18]

To-date little attention has been given to the potential utility of Doppler ultrasonography for investigating systemic conditions such as anaemia, metabolic disorders or infection. However, studies with foeto-maternal alloimmunisation due to rhesus blood group incompatibility have shown that Doppler ultrasonography may play an important role in the non-invasive diagnosis and management of human foetal anaemia[19]. Increased peak systolic velocity of the middle cerebral or splenic artery is considered to be a highly sensitive and specific test for the diagnosis and management of severe anaemia of alloimmunisation[20,21] or parvovirus infection[22] in the human foetus. Increased blood flow velocity of the middle cerebral artery in children suffering from cerebral malaria has also been reported[23].

Doppler ultrasonography is relatively new to the veterinary domain. Clinical applications are less established, but studies into potential applications have followed those listed for medical practice and suggest that uses similar to those in human patients can be found. Various studies that used Doppler ultrasonography for evaluating normal cardiac function[24] and investigating localised cardiac disorders[25] have been extensively reported. Fewer in the literature, however, are reports on

investigation of vascular disorders e.g. the abdominal aorta and caudal vena cava[26], and portal vein[27,28]. Other researchers have used Doppler ultrasonography for investigating focal or diffuse disorders of the kidneys[29-31]; liver[28,32]; spleen[33]; gastrointestinal tract[34]; spermatic cord and testis[35]; and prostate[36] of dogs. Use of Doppler ultrasonography for monitoring foetal viability in ewes and sows[37] or cows and mares[38]; for evaluating physiological processes of the uterus[39]; and of digestion[40,41] have been cited. A few studies have reported changes in renal Doppler patterns associated with systemic conditions such as anaesthesia[42] and Addison's disease (hypotension)[43]. Except for a Doppler investigation of cerebral haemodynamics in acutely anaemic newborn lambs[44], Doppler studies on anaemia, or anaemia-inducing conditions in domestic animals have not been reported.

Canine babesiosis (CB) in South Africa, like human falciparum malaria, is caused by a virulent haemoprotozoan parasite, Babesia canis rossi[45]. In addition to inducing anaemia, the disease may become complicated, making treatment difficult[46]. Death is inevitable in some of the complicated diseases, especially those presenting as cerebral forms or acute renal failure[46]. Haemodynamic disturbances are thought to play a significant role in the pathophysiology of complicated CB[47,48]. However, clinical evaluation of haemodynamic changes in the affected dogs is not routinely done. Studies using invasive methods in the dog have established significant influence of experimentally induced acute[49] or chronic[1] normovolaemic anaemia on systemic and regional haemodynamics, even though complications like those seen in CB have not been reported. In order to understand and evaluate the haemodynamic changes that lead to complications in CB, it is imperative to separate them from those that result from anaemia.

The aims of the current study were to investigate the influence of (1) experimentally induced canine normovolaemic anaemia (EA), and (2) uncomplicated CB on the abdominal aorta and splanchnic vessels using Doppler ultrasonography, and (3) to compare uncomplicated CB with experimental anaemia. Information generated from the study is expected to provide a necessary database for further investigations needed to improve an understanding of the pathophysiology of CB.

1.1 REFERENCES

1. Vatner SF, Higgins CB, Franklin D. Regional circulatory adjustments to moderate and severe chronic anaemia in conscious dogs at rest and during exercise. *Circulation Research*. 1972;30:731-740.
2. Guyton AC, Hall JE. The circulation. In: Guyton AC, Hall JE, eds. *Textbook of Medical Physiology*. Tenth ed. Philadelphia: W.B. Saunders Company; 2000:144-262.
3. Barber FE, Baker DW, Nation AWC, Strandness JDE, Reid JM. Ultrasonic duplex echo Doppler scanner. In: *IEEE Trans Biomed Eng*; 1974:109-113.
4. Kambergs J, Tabatabai G. Abdomen. In: Hofer M, ed. *Teaching Manual of Colour Duplex Sonography*. New York: Thieme New York; 2001:31-42.
5. Janthur M. Use of abdominal colour Doppler ultrasonography in dogs and cats. *Tierarztliche Praxis*. 2000;28:19-24.
6. Dietz A, Hofer M, Sitzer M. Cerebrovascular imaging. In: Hofer M, ed. *Teaching Manual of Colour Duplex Sonography*. New York: Thieme New York; 2001:17-24.
7. Turck J. Peripheral arteries. In: Hofer M, ed. *Teaching Manual of Colour Duplex Sonography*. New York: Thieme New York; 2001:69-76.
8. Saleh A. Peripheral veins. In: Hofer M, ed. *Teaching Manual of Colour Duplex Sonography*. New York: Thieme New York; 2001:77-84.
9. Krogman ON, Pieper M. Echocardiography. In: Hofer M, ed. *Teaching Manual of Colour Duplex Sonography*. New York: Thieme New York; 2001:85-97.
10. Hollenbeck M. Nephrology. In: Hofer M, ed. *Teaching Manual of Colour Duplex Sonography*. New York: Thieme New York; 2001:43-49.
11. Saleh A. Cervical lymph nodes and thyroid. In: Hofer M, ed. *Teaching Manual of Colour Duplex Sonography*. New York: Thieme New York; 2001:25-30.

12. Bartolozzi C, Lencioni R, Paolicchi A. Differentiation of hepatocellular adenoma and focal nodular hyperplasia of the liver: Comparison of power Doppler imaging and conventional colour Doppler sonography. *European Journal of Radiology*. 1997;7:1410-1415.

13. Hosten N, Pils R, Bechstein WO, Felix R. Focal liver lesions: Doppler ultrasound. *European Radiology*. 1999;9:428-435.

14. Reihs T, Hofer M. Obstetrics and gynaecology. In: Hofer M, ed. *Teaching Manual of Colour Duplex Sonography*; 2001:57-68.

15. Berman JM, Beidle TR, Kunberger LE, Letourneau, JG. Sonographic evaluation of acute intrascrotal pathology. *American Journal of Roentgenology*. 1996;166:857-861.

16. Antoch G. Urology. In: Hofer M, ed. *Teaching Manual of Colour Duplex Sonography*. New York: Thieme New York; 2001:50-56.

17. Qamar MI, Read AE, Mountford R. Increased superior mesenteric artery blood flow after glucose but not lactulose ingestion. *The Quarterly Journal of Medicine*. 1986;233:893-896.

18. Sieber C, Beglinger C, Jager K, Stadler GA. Intestinal phase of superior mesenteric artery blood flow in man. *Gut*. 1992;33:497-501.

19. Mari G, Adrignolo A, Abuhamad AZ, Pirhonen J, Jones DC, Ludomirsky A, Copel JA. Diagnosis of fetal anaemia with Doppler ultrasound in the pregnancy complicated by maternal blood group immunization. *Ultrasound in Obstetrics and Gynaecology*. 1995;5:400-404.

20. Teixeira JMA, Duncan K, Letsky E, Fisk NM. Middle cerebral artery peak systolic velocity in the prediction of fetal anaemia. *Ultrasound in Obstetrics and Gynaecology*. 2000;15:205-208.

21. Bahado-Singh R, Oz AU, Hsu CD, Kovanci E, Deren O, Onderoglu L, Mari G. Middle cerebral artery Doppler velocimetric deceleration angle as a predictor of foetal anaemia in

Rh-alloimmunised foetuses without hydrops. *American Journal of Obstetrics and Gynaecology*. 2000;183:746-751.

22. Cosmi E, Mari G, Chiaie LD, Detti L, Akiyama M, Murphy KJ, Stefos T, Ferguson JE, Hunter D, Hsu CD, Abuhamad AZ, Bahado-Singh R. Noninvasive diagnosis by Doppler ultrasonography of foetal anaemia resulting from parvovirus infection. *American Journal of Obstetrics and Gynaecology*. 2002;187:1290-1293.

23. Newton CR, Marsh K, Peshu N, Kirkham FJ. Perturbations of cerebral haemodynamics in Kenyans with cerebral malaria. *Pediatric Neurology*. 1996;15:41-49.

24. Bonagura DJ, Miller MW. Doppler echocardiography II. Colour Doppler imaging. *Veterinary Clinics of North America. Small Animal Practice*. 1998;28:1361-1389.

25. Kirberger RM, Berry WL. Atrial septal defect in a dog: The value of Doppler echocardiography. *Journal of the South African Veterinary Association*. 1992;63:43-48.

26. Mattoon JS, Nyland TG. Abdominal fluid, lymph nodes, masses, peritoneal cavity, and great vessel thrombosis. In: Nyland TG, Mattoon JS, eds. *Small Animal Diagnostic Ultrasound*. Second ed. Philadelphia: W.B. Saunders Company; 2002:82-91.

27. Szatmari V, Nemeth T, Kotai I, Voros K, Sotonyi P. Doppler ultrasonographic diagnosis and anatomy of congenital intrahepatic arterioportal fistula in a puppy. *Veterinary Radiology & Ultrasound*. 2000;41:284-286.

28. Lamb CR. Ultrasonographic diagnosis of congenital portosystemic shunts in dogs: Results of a prospective study. *Veterinary Radiology & Ultrasound*. 1996;37:281-288.

29. Morrow KL, Salman MD, Lappin MR, Wrigley RH. Comparison of the resistive index to clinical parameters in dogs with renal disease. *Veterinary Radiology & Ultrasound*. 1996;37:193-199.

30. Nyland TG, Mattoon JS, Herrgesell EJ, Wisner ER. Urinary tract. In: Nyland TG, Mattoon JS, eds. *Small Animal Diagnostic Ultrasound*. Second ed. Philadelphia: W.B. Saunders Company; 2002:158-195.

31. Rivers BJ, Walter PA, Polzin DJ, King VL. Duplex Doppler estimation of intrarenal Pourcelot resistive index in dogs and cats with renal disease. *Journal of Veterinary Internal Medicine*. 1997;11:250-260.

32. Nyland TG, Mattoon JS, Herrgesell EJ, Wisner ER. Liver. In: Nyland TG, Mattoon JS, eds. *Small Animal Diagnostic Ultrasound*. Second ed. Philadelphia: W.B.Saunders Company; 2002:93-127.

33. Saunders HM, Neath PJ, Brockman DJ. B-mode and Doppler ultrasound imaging of the spleen with canine splenic torsion: a retrospective evaluation. *Veterinary Radiology & Ultrasound*. 1998;39:349-353.

34. Kircher PR, Spaulding KA, Vaden SL, Lang J, Doherr M, Gaschen L. Doppler ultrasonographic evaluation of gastrointestinal haemodynamics in food hypersensitivities: a canine model. *Journal of Veterinary Internal Medicine*. 2004;18:605-611

35. Lee FT, Winter DB, Madsen FA, Zagzebski JA, Pozniak MA, Chosy SG, Scanlan KA. Conventional colour Doppler velocity sonography verses colour Doppler energy sonography for diagnosis of acute experimental torsion of the spermatic cord. *American Journal of Radiology*. 1996;167:785-790.

36. Newell SM, Neuwirth L, Ginn PE. Doppler ultrasound of the prostate in normal dogs and in dogs with chronic lymphocytic-lymphoplasmocytic prostatitis. *Veterinary Radiology & Ultrasound*. 1998;39:332-336.

37. Fraser AF, Robertson JG. Detection of foetal life in ewes and sows. *Veterinary Record*. 1967;80:528-529.

38. Mitchell D. Detection of foetal circulation in the mare and cow by Doppler ultrasound. *Veterinary Record*. 1973;93:365-368.

39. Waite LR, Ford SP, Young DF, Conley AJ. Use of ultrasonic Doppler waveforms to estimate changes in uterine artery blood flow and vessel compliance. *Journal of Animal Science*. 1990;68:2450-2458.

40. Kircher P, Lang J, Blum J, Gaschen F, Doherr M, Sieber C, Gaschen L. Influence of food composition on splanchnic blood flow during digestion in unsedated normal dogs: a Doppler study. *Veterinary Journal*. 2003;166:265-272.

41. Riesen S, Schmid V, Gaschen L, Busato A, Lang J. Doppler measurement of splanchnic blood flow during digestion in unsedated normal dogs. *Veterinary Radiology & Ultrasound*. 2002;43:554-560.

42. Rivers BJ, Walter PA, Letourneau JG. Duplex Doppler estimation of resistive index in arcuate arteries of sedated, normal female dogs: Implications for use in the diagnosis of renal failure. *Journal of the American Animal Hospital Association*. 1997;33:69-76.

43. Koch J, Jensen AL, Wenck A, Iversen L, Lykkegaard K. Duplex Doppler measurements of renal blood flow in a dog with Addison's disease. *Journal of Small Animal Practice*. 1997;38:124-126.

44. Taylor GA, Hudak ML. Colour Doppler ultrasound changes in small vessel diameter and cerebral blood flow during acute anaemia in the newborn lamb. *Investigative Radiology*. 1994;29:188-94.

45. Matjila PT, Penzhorn BL, Becker CPJ, Nijhof AM, Jongejan F. Confirmation of occurrence of Babesia canis vogeli in domestic dogs in South Africa. *Veterinary Parasitology*. 2004;122:119-125.

46. Reyers F, Leisewitz AL, Lobetti RG, Milner RJ, Jacobson LS, van Zyl M. Canine babesiosis in South Africa: more than one disease. Does this serve as a model for falciparum malaria? *Annals of Tropical Medicine and Parasitology*. 1998;92:503-511.

47. Jacobson LS, Lobetti RG, Vaughan-Scott T. Blood pressure changes in dogs with babesiosis. *Journal of the South African Veterinary Association*. 2000;71:14-20.

48. Malherbe WD, Parkin BS. Atypical symptomatology in Babesia canis infection. *Journal of the South African Veterinary Medical Association*. 1951;22:25-36.

49. Fowler NO, Holmes JC. Blood viscosity and cardiac output in acute experimental anaemia. *Journal of Applied Physiology*. 1975;39:453-456.

CHAPTER 2

LITERATURE REVIEW

2.1 DOPPLER ULTRASONOGRAPHY

Three ultrasonographic modalities of spectral, colour and power Doppler have been separately developed as ultrasound technology advanced. Spectral Doppler was developed first in the 1950's[1], followed by colour Doppler in the 1980's[2-4]. Power Doppler is the latest innovation, with the first reports of its use coming in the early 1990s[5-7]. Use of a combination of real-time, B-mode and Doppler ultrasonography (duplex Doppler) to provide anatomical and blood flow information was reported in the early 1970s[8]. Whereas all Doppler modalities provide blood flow information, differences exist in their methods of sampling, processing and display of information by computer software giving each modality a distinct role in the evaluation of haemodynamics, and the cardiovascular system.

2.1.1 The Doppler effect - When imaging blood flow, the ultrasound reflectors are moving red blood cells. The echo received back by the transducer has a different frequency from that of the transmitted incident ultrasound. If blood flows towards the transducer (ultrasound source), the echo frequency is higher than the incident frequency, but when the blood flows away from the transducer, the echo frequency is lower. This phenomenon is known as the “Doppler effect”. The difference between incident and echo frequencies may be positive or negative, and is known as the frequency shift, which is proportional to the speed and direction (velocity) of blood flowing parallel to the axis of

the ultrasound beam. The relationship between the magnitude of the frequency shift and the velocity of blood flow is expressed by the Doppler equation[9,10]:

$$Fd = Fi - Fe = \frac{2 \cdot Fi \cdot V \cdot \cos\theta}{C}$$

Where: Fd is the frequency shift, Fi is the frequency of incident ultrasound, Fe is the frequency of echoes, V is the velocity of blood flow, C is the speed of ultrasound in living tissue, and θ is the beam-vessel intercept angle.

The Doppler frequency shifts for incident frequencies in the range of 2–8 MHz and physiological blood flow velocities lie in the audible frequency range of 50–15000 Hz and is presented audibly and visually as positive and negative shifts.

2.1.2 Spectral Doppler imaging - Spectral Doppler mode uses a continuous or pulsed wave ultrasound source. In a continuous wave Doppler system, one transducer element constantly transmits ultrasound waves while another receives the echoes. It is not possible to determine the exact location or depth from which the echoes received originated. A continuous wave Doppler system is capable of accurately measuring very high frequency shifts and aliasing does not occur readily. In a pulsed wave system, a transducer crystal periodically transmits pulses of ultrasound and then interrupts its transmission to receive echoes from the transmitted sound waves. A pulsed wave system has the ability to select the depth at which ultrasound is reflected and detect the specific location of the vessel or cardiac chamber from which blood flow has been sampled. However, there is an upper limit of velocity that can be accurately measured by a pulsed wave system. Beyond this limit, aliasing occurs leading to inaccuracy in estimating the velocity of blood flow. In the pulsed wave mode, a single gate is placed within a vessel lumen or cardiac chamber to obtain information from a

sample of the flowing blood known as the sample volume. The size of the sample volume can be varied and the sample can be selected from anywhere along the cross section of a vessel, or it may include the entire cross section of the vessel lumen[9-12].

The spectral Doppler flow information is processed and analysed by the Fast Fourier Transformation software program and presented in the form of audible sound as well as a graphic tracing of the detailed profiles of the flow velocity known as Doppler spectrum or spectral tracing. The Doppler spectrum represents a plot of the blood flow velocity (Y-axis) against time (X-axis). The Y-axis has positive and negative values on either side of the Y equal to zero line that is commonly referred to as the baseline. A positive Doppler frequency shift indicating blood flow towards the transducer is seen as a tracing above the baseline while a negative shift indicating flow away from the transducer appears below the baseline. The baseline is the point where the speed of blood flow is zero. The flow speed increases on either side farther away from the baseline. A point on the Doppler spectrum corresponding to that time defines the speed of blood flow at any given time of the cardiac cycle[9,10].

The width of the Doppler spectrum at any point represents the velocity gradient across the vessel diameter at that time during the cardiac cycle. A narrow tracing of the velocity spectrum implies that all RBCs across the vessel diameter are moving at equal velocity, while a broad band indicates the presence of a wide range of velocities across the vessel diameter. The spectral width is usually narrower during the acceleration phase of systole (plug flow) than during the rest of the cardiac cycle, especially in the large arteries. This means during early systole, the flow speed of the laminae of RBCs across the vessel diameter is about equal due to the sudden rise in systolic pressure gradient. This is known as the "entrance effect". During the deceleration phase of systole the spectral width broadens as the blood flow stabilises to a parabolic profile. When parabolic flow is

present during early systole, the spectral width may be more or less equal throughout the cardiac cycle. In a disturbed or turbulent flow, the spectral width broadens as a wide range of flow speeds appears within the vessel. Random movement of RBCs is seen as irregular, poorly defined margins of the spectral band[9,10].

In a pulsatile flow profile, an "envelope" is produced by two arms of the Doppler spectrum that correspond to the acceleration and deceleration phases of systole as the speed of blood flow rises and falls steeply. When there is little or no velocity gradient across the vessel as in the case of plug flow, the spectral band is narrow and the envelope is "empty" or there is a spectral "window". As the velocity gradient across the vessel increases e.g. in parabolic, disturbed or turbulent flow, the velocity spectrum is said to broaden, and the envelope becomes filled or the spectral window is closed. The slopes of the conical envelope define the rate of acceleration and deceleration of blood flow velocity during early and late systole respectively. In a triphasic pulsatile flow, two envelopes, one produced by systole and the other by early diastole are present on either side of the baseline. Each envelope is normally a sharply pointed narrow cone. In the biphasic pulsatile flow profile, only one systolic envelope is present and it has more gentle slopes and is rounded or flattened at the top. An envelope should appear entirely on only one side of the baseline. When the tip of the envelope is cut off and becomes displaced on the opposite side of the baseline, it indicates the presence of aliasing that is associated with a high blood flow velocity[9,10].

From the Doppler spectrum, blood flow can be expressed by measurement or calculation of various parameters and indices. The blood flow velocity is equal to the frequency shift if the beam-vessel alignment is exactly parallel, i.e. intercept angle equals zero. For arterial flow, peak systolic velocity is measured directly from the Doppler spectrum by positioning the electronic callipers of the

ultrasound machine at the maximum systolic frequency shift. Pulsatility and resistive indices can be computed also from the Doppler spectrum using the program of the ultrasound machine. For venous flow, peak velocity is measured in the same way as for arterial flow, and a congestion index can be computed. Other useful blood flow parameters that can be computed from the Doppler spectrum are time-averaged mean velocity and blood flow, for both arterial and venous flows.

2.1.3 Peak systolic velocity, peak velocity, time-averaged mean velocity - The accuracy of peak systolic velocity (PSV), peak velocity, or time-averaged mean velocity measured or computed from the frequency shift depends on the beam-vessel alignment used at the time of obtaining the Doppler spectrum. Measurement of PSV, peak velocity or time-averaged mean velocity therefore requires that the blood vessel must be big enough to be clearly resolved, and remain steady for accurate positioning of the sample volume and for angle correction. Peak systolic velocity, peak velocity, or time-averaged mean velocity is expressed in metres or centimetres per second (m/s or cm/s).

2.1.4 Pulsatility index and resistive index - Both pulsatility index (PI) and resistive index (RI) express the resistance to blood flow by vessels that are located further distal to the site of interrogation of blood flow. They may be calculated from values of frequency shift or velocity. They are not influenced by the angle of beam-vessel alignment. The PI and RI can therefore be used for semi-quantitative evaluation of the blood flow of arteries that are not well resolved on B-mode ultrasonography, or those that are tortuous and do not permit angle correction[13]. For low resistance vessels, they are computed electronically as follows[14]:

$$PI = \frac{A - B}{Mean}$$

$$RI = \frac{A - B}{A}$$

Where: A is the peak systolic frequency shift (peak velocity), B is the end diastolic frequency shift, and "mean" is the time-averaged value over the same cardiac cycle.

2.1.5 Blood flow - Is computed using the equation[15-17]:

$$BF = \frac{CSA \times TAV_{mean}}{\text{Body weight}} \quad \text{or} \quad \frac{CSA \times PV \times 0.57}{\text{Body weight}}$$

Where: BF is the volume flow, CSA is vessel cross sectional area, and time-averaged mean velocity is the mean blood flow velocity, PV is peak velocity, and 0.57 is a correction factor.

The blood flow is expressed in units of ml/min/kg. This measurement requires calculation of both the vessel cross sectional area and blood flow velocity measured at the same location of the vessel. Measurement of vessel diameter introduces significant errors, and the method is particularly not suited for use in vessels with small diameters.

2.1.6 Congestion index - Is computed as[18]:

$$CI = \frac{CSA}{TAV_{mean}}$$

Where: CI is congestion index, CSA is cross sectional area, TAV_{mean} is time-averaged mean velocity.

2.1.7 Colour Doppler imaging - Only uses pulsed wave ultrasound[12,19,20]. Unlike spectral Doppler, the sample volume in colour Doppler consists of numerous gates and blood flow within a much larger area of tissue covered by the colour box (sample volume) can be interrogated simultaneously. The Doppler frequency shift in the colour Doppler mode is processed and analysed by the auto-correlation software program into phase and frequency components, yielding direction and mean speed of the blood flow respectively. A less detailed velocity profile and only average values of the flow velocity are obtainable. Transient changes in the direction of flow during a cardiac cycle such as in triphasic velocity profile can also be demonstrated. The information is presented on the monitor as a two-dimensional transparent colour map, superimposed on a B-mode image. Since blood is fluid and takes the shape of the object that contains it, the colour map of the flowing blood gives additional information on the internal outline of the imaged vessel or cardiac chamber. By convention, blood flow towards the transducer (positive frequency shift) is coded red and away (negative frequency shift) is blue. The speed of flow is denoted by different saturation of the red and blue colours. Faster flow speed towards the transducer is assigned a brighter shade of red e.g. yellow or white and flow away is assigned a brighter shade of blue e.g. cyan or white (less saturation). Slower flow towards and away is indicated by a deeper shade of red and blue (more saturated) respectively. In parabolic laminar flow, the deeper colour shades are seen near the vessel walls and the lighter shades at the centre. The green colour is used to tag a selected specific velocity value within the vessel or cardiac chamber. The information obtained from colour Doppler is still largely qualitative and can be evaluated subjectively.

Colour codes for opposite flow directions may be seen within the same vessel (or on opposite sides of a cardiac valve) under various situations and may be classified as true or false flow reversal[12,19,20]. True flow reversal includes that of early diastole as seen in triphasic pulsatile flow; the localised

reversal of flows at a bifurcation or dilated large artery; and valvular regurgitation. The colour code for the reversed flow in a triphasic flow profile is seen as a transient change at the beginning of diastole during a cardiac cycle. The reversed flow occupies the entire area of the vessel lumen being sampled. Localised flow reversal is seen near a vessel wall simultaneously with the colour code for normal forward flow or jet, from which it is separated by a colour void (black) line or area. Valvular regurgitation is indicated when the colour code for the reverse flow appears on the opposite side of a valve as the colour for the normal forward flow. False flow reversal may be seen in a curved or tortuous vessel, or when using a curved or sector array transducer that results in the ultrasound beam meeting different sections of the same vessel at different angles. Under all these situations, the more saturated colours for opposite flow directions appear in the same vessel separated by a colour void area. In the phenomenon of aliasing associated with very high flow velocity, there is a more or less complex mix of brighter colours (less saturated) of the opposite flow directions without intervening colour void areas. The mosaic of colours may be located in the midstream or may occupy the entire cross section of the sampled chamber. (Aliasing may be difficult to differentiate from turbulence on colour Doppler alone).

2.1.8 Power Doppler imaging - Like colour Doppler, power Doppler imaging only uses pulsed wave ultrasound and a multi-gated sample volume (power box) for global interrogation of blood flow. Unlike colour Doppler the auto-correlation software in power Doppler only processes amplitude information, excluding the phase and frequency components of the Doppler shift. The Doppler amplitude signal due to blood flow in all directions is integrated to reflect the energy of flow from the sampled volume. The relationship between the amplitude of Doppler signal and the energy of blood flow is not influenced by the ultrasound beam-vessel alignment but depends on the total number or volume of moving RBCs. This information is presented in a two-dimensional, transparent colour map

superimposed on a B-mode image with only a single colour (orange) code. Higher amplitude signal or energy of blood flow (more RBCs or bigger volume) is assigned a brighter hue (less saturated colour e.g. yellow) while lower amplitude signal is indicated by a more saturated hue e.g. purple of the colour code. Integration of the amplitude of blood flow, minimal influence by the angle of alignment and superior method of blood / tissue discrimination by power Doppler make it a more sensitive technique for detection of particularly low velocity blood flow than spectral Doppler and colour Doppler are. The dynamic range of a power Doppler system can be set at a higher level without risking interference from noise. However, power Doppler is more susceptible to movement artefact leading to "flashing". Direction and speed of blood flow are not depicted since the power Doppler software does not process phase or frequency information. Further, the amplitude (flow volume) information on blood flow obtained from power Doppler currently can only be evaluated qualitatively.

2.1.9 Doppler angle - In spectral and colour Doppler, 0° is the ideal Doppler angle for obtaining accurate flow information[9,10,12]. Increasing the Doppler angle introduces errors in detecting flow and estimating flow speed and direction. Flow may be depicted occurring in both directions (red and blue) within the same vessel when the angle of insonation is sub-optimal or it changes due to curvature of the vessel. As the Doppler angle approaches 90°, the Doppler signal decreases resulting in detection of poor flow or absence of flow (flow void area that appears black). In practice, a Doppler angle of up to 60° is permissible since it is not always possible to achieve the ideal alignment between the incident ultrasound beam and the vessel in certain situations, e.g.:

a. Parallel alignment between the incident beam and the vessel may not be possible because of anatomical location, e.g. a vessel running parallel to the body surface. A wedge-shaped standoff

pad should be used, or when using a linear transducer, the colour box should be electronically steered to improve the Doppler angle.

b. A vessel may change anatomical planes along its course, may be curved or tortuous. An optimal angle may be found by manually angling the transducer.

c. With a sector or convex transducer, the angles at which the ultrasound beam meets different segments of a vessel will vary as the beam is steered through the tissue. For this reason, a linear transducer is preferred to a sector or convex transducer for Doppler imaging.

Direction ambiguity associated with sub-optimal Doppler angles is characterized by the presence of the more saturated colours (slower speed) of opposite flow directions within the same vessel separated by flow void (dark) areas or lines.

Doppler angle does not affect the estimation of amplitude. Artefacts, poor or absent flow associated with sub-optimal Doppler angles are not seen in power Doppler, making it more sensitive for flow detection since it is possible to detect flow at an angle of 90°.

2.1.10 Aliasing - In practice, the upper limit of Doppler frequency shift (speed and direction of blood flow) that can be accurately estimated in pulsed wave systems will depend on the maximum pulse repetition frequency (PRF) of the ultrasound machine[9,10,12]. When the Doppler frequency shift is equal to one half of the operating PRF (PRF/2), a critical point known as the Nyquist limit is reached beyond which estimates of the speed and direction of blood flow are inaccurate. In colour Doppler, a mixture of brighter colours for opposite flow directions appears at the centre of the blood vessel. In spectral Doppler, the tips of the velocity wave curves are cut off and displayed on the opposite side of the baseline. This phenomenon is known as aliasing. Aliasing may be corrected by selecting a higher PRF setting. If the maximum PRF setting for the machine has already been

selected, moving the baseline down or up can double the range of detectable velocities. Other methods of correction include using a lower frequency transducer, increasing the Doppler angle or scanning at a shallower depth.

2.1.11 Depth at which vessel is located - Both the incident ultrasound and echo undergo increasing levels of attenuation the longer the distance they have to travel. Subsequently, the intensity of echoes returning from deeply located vessels may become too weak for the machine to detect, making it impossible to demonstrate flow in such vessels[9,10,12]. The use of lower incident frequencies is recommended for deeply located vessels while preserving higher frequencies for superficial vessels. Another technical problem associated with pulsed wave systems when evaluating deeply located vessels is range (depth) ambiguity where presence of flow may be recorded in a position with no actual flow (colour overwrite). This is because the echo originating from a great distance may arrive at the transducer after the succeeding incident pulse has been emitted. This artefact may occur with low frequency transducers, high far gain and high PRF setting, but rarely poses a clinical problem.

2.1.12 Soft tissue motion, and movement of subject or transducer - Signals from slowly moving soft tissues and vessel walls are known as "noise"[9,10,12]. Noise signals are much stronger than Doppler signals. They affect the accuracy of estimation of flow velocity and may cause flash artefacts and colour overwrite. Motion (blood / tissue) discriminators are key components of colour and power Doppler while wall filters are equivalent components of spectral Doppler systems that are used for the reduction of noise level from flow signals. Power Doppler systems use a different method for reducing noise that allows them to operate at higher gain settings (dynamic range) than colour or spectral Doppler mode. The higher gain setting amplifies flow signals. This is the main factor

responsible for the higher sensitivity of power Doppler in detecting blood flow particularly in small, deeply located vessels and slow flows. The method of dealing with "noise" also varies between different types of machines.

2.1.13 Equipment capability - It should be remembered that spectral Doppler, colour Doppler or power Doppler mode is superimposed on the B-mode image during real-time duplex Doppler imaging. B-mode ultrasound and the Doppler modes have conflicting requirements for optimal performance.

2.1.14 Table 2.1 - Ideal-imaging requirements for B-mode and Doppler modalities

Imaging Parameter	B-mode	Spectral / colour / power Doppler
Scan angle	90°	0°
Beam type	Narrow & focused (for spatial resolution).	Wide & unfocused (For uniformity of Doppler signals).
Pulse length	Short (for spatial resolution).	Long (for penetration).
Transducer type	Higher frequencies (For spatial resolution).	Lower frequencies (for penetration). Phased or linear array (For fast beam forming).

The concurrent use of B-mode and a Doppler mode in duplex Doppler inevitably puts more demand on the capacity of the ultrasound machine, slowing down the frame rate. This calls for identification of priorities one at a time. Some machines have incorporated priority settings for grey-scale and Doppler operations.

2.1.15 Frame rate - The operating frame rates of ultrasound systems decrease in the order of B-mode, spectral, colour, and power Doppler[9,10,12]. Frame rates are significantly lower when operating colour or power Doppler mode due to the repeated sampling of each scan line (long dwell time), the use of lower transducer frequencies and PRF settings necessary for increased sensitivity to slow flow and accurate measurements. Increasing the field of view and the line density will further lower the frame rate. This means imaging slowly is necessary for small, deeply located vessels and slow flows.

2.1.16 Operator knowledge and skills - A thorough understanding, by the operator, of the underlying physical principles, technical applications and limitations as well as imaging requirements for different situations is imperative for successful spectral, colour and power Doppler application, and accurate interpretation. In addition, choice of the most appropriate acoustic window and good scanning technique are required.

2.2 ULTRASONOGRAPHIC TECHNIQUES FOR, AND DOPPLER PATTERNS OF ABDOMINAL SPLANCHNIC VESSELS IN THE DOG

2.2.1 Ultrasonographic technique for the abdominal aorta - The caudal abdominal aorta (AAo) may be imaged through the left lateral, right lateral or ventral abdominal windows[21-25]. The transducer is positioned just ventral to the lumbar transverse processes, for the left or right lateral window, and the AAo can be imaged in dorsal longitudinal and transverse planes. In the left longitudinal plane, the AAo appears as an anechoic, pulsatile tubular structure along the dorsal midline immediately ventral to the vertebral bodies[24]. Mobile echoes may be visible within the vessel lumen[23]. The walls are thin, smooth, echogenic structures that run nearly parallel to each other. The AAo is adjacent to the caudal vena cava (CVC), both running parallel to each other[22,25]. Cranial to the renal vessels, the AAo and CVC diverge, with the CVC deviating in a cranioventral direction. The AAo is located in the near field while the CVC is in the far field[22,23]. The aortic wall is slightly thicker than that of the CVC. The diameter of the AAo frequently appears to be larger than that of the CVC, probably because the diameter of the CVC is foreshortened. When mild transducer pressure is applied to the abdominal wall, there is a uniform narrowing of the tubular lumen of the vessels that is more pronounced in the CVC. The AAo can be followed caudally to its external iliac arterial branches, as it narrows in diameter[24]. It may also be followed cranially to the aortic hiatus at the level of the 13th thoracic or 1st lumbar vertebra. However, interference from ribs and gastrointestinal gas make visualisation of the AAo cranial to the renal arteries difficult, especially in deep chested dogs[24,25]. Imaging from the ventral abdominal window in a sagittal plane with the transducer placed medial to the right kidney may give a better view of the cranial AAo[25]. In the transverse plane, the AAo is a round or oval anechoic structure[21]. Compression by transducer pressure causes the vessel to adopt a more oval or elliptical shape, especially in the CVC[22]. When imaged from the right lateral

abdominal window, The AAo is located in the far field, while the CVC is in the near field. The visceral branches of the AAo that can be readily visualised by B-mode ultrasonography include the coeliac artery, cranial mesenteric artery, left renal artery, right renal artery and caudal mesenteric artery[24].

2.2.2 Doppler patterns of the normal abdominal aortic flow - The aortic blood flow is towards the transducer, when the transducer is angled cranially in a longitudinal imaging plane[24]. The AAo has a typical plug flow velocity profile with a typical high resistance pattern[24,25]. The velocity distribution or gradient is narrow. The waveform has a high, sharp systolic peak with a large, clear spectral window. Mild turbulence occurs during late systole (deceleration slope)[24]. There is a retrograde early diastolic flow, followed by a low forward late diastolic flow[24,25]. If there is a longer pause between two ventricular contractions, additional waves with lower velocities occur[25]. In humans, the waveform changes slightly from proximal to distal AAo[21]. Caudal to the renal arteries, the flow reversal in early diastole and reduction in late diastole of the aortic velocity occur to a greater degree due to the high resistance to blood flow through the muscles of the hind limbs[24].

2.2.3 Doppler patterns of abnormal abdominal aortic flow - The presence of a thrombus within the aortic lumen produces colour void on colour Doppler imaging[24,26]. If the vessel lumen is completely occluded, the thrombotic area and the vessel lumen distal to will be colour void indicating absence of blood flow. If there is stenosis of the vessel, a mosaic of red, white or yellow and blue colour hues is seen around the edges of the thrombus indicating the presence of a high velocity turbulent flow[26]. On spectral Doppler, flow cranial to an occluded Ao appears as a low frequency, low velocity systolic spike sometimes referred to as the “occlusive thumb”. If there is stenosis, a high velocity turbulent pattern is seen distally[24] or a low velocity flow is seen along the margin of the thrombus[26]. In a recanalising thrombus or one in which the edges are retracting, tiny channels of

blood flow can be detected by the Doppler technique. Doppler ultrasound can be used to evaluate and monitor resolution of thrombus with streptokinase administration or other anticoagulant therapy[27].

2.2.4 Ultrasonographic techniques of the coeliac and cranial mesenteric arteries - The B-mode ultrasound techniques for imaging the coeliac artery (CA) and cranial mesenteric artery (CMA) in the dog have been described. Both vessels can be seen in the same imaging plane, with the CA located a few millimetres cranial to the CMA[23,24]. The vessels are seen in their long axis coursing towards the transducer from the ventral surface of the aorta, when a ventral mid abdominal window in the sagittal position is used[23]. If the animal is in dorsal recumbency, the CA and CMA form a V-shape in the sagittal plane. When the dog is in right lateral recumbency, the vessels lie parallel in contact with each other[25]. If the transducer face is directed towards the lateral aspect of the aorta, the origins of the CA and CMA may be seen in cross section as paired anechoic circles[24]. Alternatively from a dorsal plane on the right side, cross sections of the vessels may be identified between the long axis of the CVC and aorta[24]. The transducer can be rotated to align with the long axis of the vessels that can be followed to their origin or destination[24]. The CMA can be followed in cross section as it turns ventrally and caudally, and then in an oblique longitudinal plane as it travels caudally to the root of the mesentery[24]. The mesenteric branch of the portal vein is found in close proximity of the CMA in the root of the mesentery, and adjacent, long jejunal lymph nodes can be seen flanking the artery[24]. The average size of the CA is about 4 mm in diameter, it makes an acute cranial curve within the first centimetre after leaving the aorta and trifurcates approximately 2 cm from its origin[23,24]. It is difficult to image all the three branches in a single plane[24], although each of them can be followed to the visceral organs they supply, in a cooperative, relaxed patient with good resolution Doppler equipment[23]. However, appreciable amounts of gastrointestinal gas, and the small

size or tortuous course of these vessels may preclude their visualisation[23,24]. Withholding food and use of ultrasonographic contrast agent to enhance the Doppler signals may improve evaluation of these vessels[28].

2.2.5 Doppler patterns of the normal coeliac and cranial mesenteric arterial flow - On colour Doppler, the blood flow of both the CA and CMA is directed towards the transducer[25]. The Doppler spectra of both vessels is characterised by a broad systolic peak with a small 'spectral window' or nearly 'full envelope'. Blood flows in the forward direction throughout the cardiac cycle, with a gradually diminishing velocity towards end diastole. This is classified as a blunted parabolic velocity profile and intermediate resistance flow pattern[25]. The outline of the Doppler spectrum of both CA and CMA in diastole has an undulating contour. In some dogs, the CA shows a double systolic peak, with the first peak being higher than the second[25]. The blood flow of the CMA may be turbulent at the origin from the aorta.

Physiological variation of blood flow of the CA and CMA with prandial state has been described in the dog[29]. There is a high resistance flow pattern in a fasted dog and a low resistance postprandially as the intestinal vascular bed dilates[24]. Kircher *et al*[29] found that arterial resistance of the CA in fasted dogs was significantly lower with mean RI and PI values of 0.763 ±0.025 and 1.962 ± 0.216 respectively as compared to 0.803 ±0.029 and 2.290 ±0.311 of the CMA. The postprandial RI and PI values decreased significantly in both vessels, the RI reducing by 12-15% and the PI by 25-29%. Maximum reduction in arterial resistance occurred 40 minutes after feeding in the CA and 60 minutes in the CMA. Apart from the high fat diets that caused maximum reduction in RI and PI values of the CMA 20 minutes after feeding before returning to normal at 90 minutes, no significant differences between the effects of diets of different compositions on splanchnic blood flow were found[29].

2.2.6 Doppler patterns of abnormal coeliac and cranial mesenteric arterial flow - Reference to any abnormality in the Doppler patterns of the CA or CMA could not be found in the veterinary literature.

2.2.7 Ultrasonographic techniques of the common hepatic artery - Frequently, the common hepatic artery can only be imaged with the colour Doppler technique[25]. It courses cranially parallel to, and between the caudal vena cava and the MPV from its origin at the coeliac trunk. Blood flow of the common hepatic artery demonstrated on colour Doppler from a ventral abdominal window is away from the transducer[24].

2.2.8 Doppler patterns of the normal common hepatic arterial flow - The normal Doppler flow pattern of the common hepatic artery is characterised by broad systolic peaks without spectral window (i.e. 'full envelope'), typical of parabolic velocity profile and low resistance flow pattern[25]. There is a continuous, gradually decreasing but high diastolic flow velocity[25]. In a quantitative spectral Doppler study of the common hepatic artery, the mean PSV in fasted, normal Beagle was found to be 1.5 m/s (range 1.1-2.3 m/s) and RI was 0.68 (range 0.62-0.74)[30]. No difference was found in PSV and RI values of the common hepatic artery measured at two or 24 hours postprandially. However, the mean PSV (1.0 m/s) and RI (0.59) values in Deerhound and Irish wolfhound puppies were found to be significantly lower than that of adult Beagles[30]. It was not clear if this difference was due to age or breed. Dogs with congenital arterioportal fistula had a higher mean PSV, but lower mean RI value than those of normal puppies. The investigators did not find any difference in the blood flow of the common hepatic artery between normal dogs and those with portal vein thrombosis or those with acquired hepatic insufficiency[30].

2.2.9 Doppler patterns of abnormal common hepatic arterial flow - An abnormality in the Doppler patterns of the common hepatic artery has not been reported in the dog.

2.2.10 Ultrasonographic technique for the caudal vena cava - The technique for B-mode ultrasonography of the abdominal CVC is the same as described for the AAo in paragraph 2.2.1. The B-mode ultrasonographic characteristics of the CVC and its relationship with the AAo were also discussed in the same paragraph. The CVC is seen in the near field when scanning through the right lateral abdominal window. It is more compressible with transducer pressure than the AAo[22], and is straight as compared to the main portal vein (MPV), with which it also runs a parallel course[25]. The MPV is wavier and located ventral to the CVC. The CVC can be followed caudally and cranially. In most dogs, however, intercostal[24] or right paramedian[25] positioning of the transducer is necessary to visualise the cranial portion of the abdominal CVC as it enters the liver.

2.2.11 Doppler patterns of the normal caudal vena cava - Blood flow in the CVC is away from the transducer when imaging in the longitudinal plane, with the transducer angled dorsocranially. The flow is coded blue colour Doppler and indicated by tracing below the baseline on spectral Doppler. Dramatic variation in waveform of the cranial CVC occurs in relation to cardiac cycles[31], as well as intrathoracic and intra-abdominal pressure changes associated with respiratory cycles[25]. It gives the waveform a triphasic pattern. The first forward flow coincides with atrial diastole as blood flows into the right heart[24]. The second peak of forward flow is caused by ventricular diastole, and the third wave that may be a reverse flow occurs during atrial systole. In addition, every inspiration causes a forward flow wave with high velocity[25]. Less pronounced variation in the waveform of the caudal portion of the CVC and its tributaries is seen.

2.2.12 Doppler patterns of abnormal caudal vena cava flow - Abnormalities in the flow pattern of the CVC are indicators of cardiovascular or hepatic disease. Interference with the blood flow of the CVC causes various changes in the Doppler pattern depending on the nature and degree of the interference. Central venous hypertension may be due to right heart failure; pulmonary hypertension; pericardial effusion with tamponade; constrictive pericarditis; right atrial tumour or disorders of the tricuspid valve[21,32,33]. The blood flow velocity may be decreased with greater flow reversal during atrial systole[24], or there may be a complete flow reversal. Stenosis or occlusion of the CVC may be due to thrombosis[31,34,35], membranous web[36,37], kinking[38], heartworm disease or compression by adjacent masses such as tumours[24]. Complete obstruction may lead to absence of blood flow at point of obstruction and reversed or bi-directional flow caudal to it[24 37] on colour or spectral Doppler. The flow pattern may be pulsatile[37]. In a re-canalising thrombus, the channels may be visible on colour Doppler[21].

2.2.13 Ultrasonographic technique for the splenic artery and vein - The course of the splenic artery is variable, following the position of the mobile spleen[24]. The splenic artery may be imaged through a ventral mid abdominal window as it branches off from the CA, and may be followed to the spleen in a cooperative, relaxed patient with good resolution Doppler equipment, and in the absence of interference from gastrointestinal gas[23]. However, imaging the splenic artery continuously from the coeliac trunk to the spleen is rarely possible due to its tortuous course and interference from gastrointestinal gas[25]. Only colour Doppler imaging can demonstrate hilar and parenchymal splenic arteries, adjacent to the splenic veins[25]. The technique for imaging the intra-splenic, hilar and main splenic veins is similar to that described for the splenic artery although this has not been mentioned in the literature.

2.2.14 Doppler patterns of the normal splenic arterial and venous flow - From the ventral abdominal window on colour Doppler, blood flow of the main, hilar and parenchymal splenic arteries is towards the transducer[24]. The Doppler spectrum of both main and parenchymal splenic artery is typically of low resistance (broad systolic peaks and continuous high diastolic flow) and a parabolic flow velocity profile (systolic peaks without spectral window). An extra systolic peak is seen in the waveform of the main splenic artery in some dogs[25]. The RI of the parenchymal splenic artery was reported to be 0.39[24].

Doppler spectrum of a splenic vein imaged from the ventral abdominal window on spectral Doppler shows flow away from the transducer, with slightly undulating, continuous, low velocity forward flow[24]. The velocity changes are due to the respiratory pressure changes, similar to that of the MPV, into which the splenic vein drains[25].

2.2.15 Doppler patterns of abnormal splenic arterial and venous flow - In a review of fifteen cases of canine splenic torsion confirmed during surgery or at postmortem, Saunders *et al*[39] found splenomegaly in all dogs examined by B-mode ultrasonography. Echogenicity of the splenic parenchyma, however, had three variations: normal, diffusely hypoechoic and mottled with hypoechoic regions. Nine of the dogs also had multiple, linear hyperechoic foci or coarse/lacy pattern. The reviewers noted that colour Doppler and spectral Doppler imaging techniques did not detect blood flow at the hilar splenic vein in all 15 dogs. They concluded that Doppler ultrasonography might be crucial in the diagnosis of splenic torsion. Reference to any abnormality in the Doppler patterns of the splenic artery could not be found in the veterinary literature.

2.2.16 Ultrasonographic technique for the renal artery - The left renal artery (LRA) and right renal artery (RRA) may be imaged from the left or right flank using dorsal, transverse and oblique scan planes[23,24]. The dorsal plane is obtained by placing the transducer along the longitudinal axis just ventral to the transverse processes of the lumbar vertebrae[24]. The transducer is angled dorsally to locate the abdominal aorta. Slight rotational adjustments will locate the long axis of the aorta, which can then be followed cranially or caudally by sliding the transducer. The LRA or RRA can be located by orientating the transducer face to the left or right side of the aorta respectively, just caudal to the CMA[24]. Alternatively, the renal artery can be imaged from the hilus of the kidney and followed to its origin from the aorta[25]. The LRA leaves the lateral aspect of the aorta and runs in a caudolateral direction, makes an abrupt 'U-turn' to travel cranially before returning to the lateral, and ventral direction to enter the left renal hilus[23,24]. Multiple LRAs are occasionally identified, and is more common with the LRA than with the right[23]. The RRA is located slightly cranial to the LRA. It travels laterally across and dorsal to the CVC, and then moves in a cranial, ventral and lateral direction into the right renal hilus[23,24]. At the renal hilus, each renal artery divides into a dorsal and ventral branch, each of which subdivides into four to six interlobar arteries (ILA)[23].

2.2.17 Doppler patterns of the normal renal arterial flow - The dorsal longitudinal position of the transducer in the paralumbar region provides an excellent angle for Doppler evaluation of the renal, interlobar, and arcuate arteries[24]. On colour Doppler, these vessels are readily visible[24]. The renal artery has a typical parabolic flow velocity profile (broad peak, no spectral window in systole) with a gradual decrease in flow throughout diastole[25,40]. An extra systolic peak is sometimes present[25]. Diastolic flow velocity is high, with an initial peak, and continually forward. It decreases gradually, reflecting the low resistance in the renal vascular bed[25,34]. A study with a single 24 kg dog reported

the volume of blood flow through the RRA and LRA, measured by Doppler technique, to be 310 and 360 ml/min respectively as compared to 300 and 340 ml/min measured by electromagnetic flowmeter[41].

2.2.18 Doppler patterns of abnormal renal arterial flow - Reference to any abnormality in the Doppler patterns of the renal artery could not be found in the veterinary literature.

2.2.19 Ultrasonographic technique for the renal parenchymal vessels - The renal interlobar arteries (ILAs) radiate from the renal pelvis in a uniformly spaced fashion through the medulla, with a straight course, to the corticomedullary junction[23]. Here, ILAs branch into arcuate arteries, which are oriented perpendicular to the ILAs, and follow the contour of the corticomedullary junction. Transverse images of arcuate arteries are often identified on B-mode ultrasonography as round, hyperechoic, and sometimes shadowing structures, that colour Doppler confirms to be vessels[23]. Finn-Bodner and Hudson[24] noted that colour Doppler could image blood flow of the interlobar veins on longitudinal dorsal plane of the kidney.

2.2.20 Doppler patterns of normal renal parenchymal blood flow - Colour Doppler readily demonstrates the blood flow of ILAs[24,42]. Interlobular arteries, originating from arcuate arteries, are also visible within the cortex on colour Doppler imaging modality[25]. The RI of an ILA or arcuate artery of dogs (0.61 ±0.05)[43-45] is similar to those of cats[46] and people[47]. The ability of colour Doppler to demonstrate the interlobar vein flow has been mentioned[24].

2.2.21 Doppler patterns of abnormal renal parenchymal flow in humans and dogs - In a study with human patients, high frequency shifts ("tumour signals"), exceeding that from the ipsilateral

renal artery or greater than 2.5 kHz at 3.0 MHz insonating frequency, were reported from the margins of parenchymal renal masses in 75-100% of primary and metastatic malignant renal tumours as compared to none obtained from benign masses[48]. It was postulated that the Doppler technique might prove useful in differentiating malignant from benign masses.

Reduction or absence of blood flow in an arterial segment, or a few vessels has been reported in association with acute renal infarct in human patients, although a normal Doppler finding does not exclude the diagnosis[49]. A characteristic plug flow velocity profile (narrow systolic peak) and high resistance flow pattern (sharp reversal of diastolic flow, often with a biphasic reversed M pattern) of intra-renal arteries has also been reported in human patients with renal vein thrombosis[50,51].

Increased renal vascular resistance to flow reduces the diastolic flow to a greater extent than systolic flow, thereby leading to an increase in the value of the resistive index[35]. An RI value equal to, or less than 0.70 is considered to be normal while a value greater than 0.70 is considered to be abnormal in man, dog and cat[43-47]. Increased RI value has been reported in acute renal failure in children[52] and in dogs[42,44], as well as in acute tubular necrosis[51,53-55]. Doppler evaluation is considered to be most helpful in differentiating acute tubular necrosis from pre-renal renal failure. It also is of prognostic value in children since surviving children had less increase in the RI value. In some cases of acute tubular necrosis, such as that due to aminoglycoside toxicity in dogs, the RI may not be elevated[56]. In human patients, elevation of the RI value in obstructive pelvic dilation, in conjunction with administration of furosemide and saline, is considered to be useful for differentiating obstructive from non-obstructive pelvic dilation in which the RI is normal[57-62]. Initial observations have shown that elevation of the RI value also occurs in dogs with obstructive pelvic dilatation[63], although this is not a consistent occurrence[45,64]. Increased RI values of the ILA and AA have also been observed in

association with renal allografts in dogs[54,65,66] but not with autografts in cats[67]. The increased RI in dogs was thought to be due to acute rejection of canine allografts[54].

No reference has been made to any abnormality of the interlobar vein flow in the veterinary literature.

2.2.22 Ultrasonographic technique for the renal vein - The right and left renal veins can be imaged by similar techniques as those for the renal arteries[23,24]. The renal veins parallel the course and location, but are generally wider than their corresponding arteries, running in an oblique cranial and dorsal direction from the corresponding kidneys to the CVC[23-25]. The left renal vein is longer than the corresponding artery and its counterpart on the right as it crosses the ventral surface of the aorta and proceeds to the right of the midline to enter the CVC. The right adrenal gland is located just cranial to the entry point of the right renal vein into the CVC. Valves of the renal veins have not been identified with ultrasonography[24].

2.2.23 Doppler patterns of the normal renal vein flow - On dorsal plane, colour Doppler image of the renal vein is coded blue or blood flow is directed away from the transducer[24,25]. The Doppler spectrum changes slightly in association with the right atrial and intra-abdominal pressure changes[25]. Each heartbeat is followed by an increased forward flow. If ventricular contractions are close enough, the forthcoming wave on spectral Doppler tracing is superimposed on the previous wave, producing faster flow. A longer pause between ventricular contractions, however, leads to a gradual decrease in the velocity of renal venous blood flow[25].

2.2.24 Doppler patterns of abnormal renal vein flow - Reference to any abnormality in the Doppler patterns of the renal vein could not be found in the veterinary literature.

2.2.25 Ultrasonographic technique for the main portal vein - Imaging of the MPV may be accomplished best with the dog on dorsal or a slightly oblique dorsal recumbency, in an oblique sagittal plane[24,25]. The cranial part of the transducer is placed on the linea alba and the caudal part turned slightly to the right[25]. The portal vein can be followed cranially as it traverses the cranial abdomen obliquely, coursing dorsally, cranially, and to the right toward the porta hepatis in close proximity to the hepatic artery[24]. Visualisation of the MPV, as it travels dorsally to the stomach, is frequently impeded by gastric gas[24]. The MPV can be re-visualised cranial to the stomach as the vessel enters the porta hepatis to the right of the midline. At this position, visualisation is achieved by placing the transducer in a right paramedian longitudinal plane immediately caudal to the xiphisternum and angling dorsocranially. The CVC and MPV are adjacent and parallel to each other at the porta hepatis. The MPV is located slightly ventral and to the left of the CVC[24]. An alternative is to use the right 8-12th intercostal spaces midway between the sternum and spine, in transverse and dorsal longitudinal planes to visualise the porta hepatis and MPV in short and long axis respectively[68-70]. The MPV turns dorsally just before its bifurcation, coming into contact with the CVC[25,71] and divides into right and left portal veins, at the porta hepatis, through which its branches enter and can be followed into the hepatic parenchyma[24,71].

2.2.26 Doppler patterns of normal main portal vein flow - A slightly phasic Doppler spectrum associated with respiration has been reported for the MPV[25,69,72]. There is, however, disagreement on whether the observed variation in velocity represents increased and decreased flow[25,69] or is an artefact[72]. According to Lamb[72], only minor variations in the maximum velocity of the MPV was seen in some dogs when a large sample volume is used for obtaining Doppler spectra, otherwise the velocity was constant in most dogs. These workers attributed the observed variations in the portal vein flow velocity to displacement of a small sample volume from the centre of the vessel lumen

during respiratory excursions. Published reports indicate the direction of blood flow in the MPV to be towards the liver (hepatopetal) or away from the transducer[25,70,72]. The only available reference to peak velocity for portal blood flow reported that its mean value was18.11 cm/s ±7.6[72]. Mean time-averaged mean velocity values obtained by different methods were recorded as 15.8 cm/s ±1.8; 15.1 cm/s ±1.4; and 14.7 cm/s ±2.5[72], and mean portal blood flow were recorded as 49.8 ml/min/kg ±13.5[70]; 31 ml/min/kg ±9[69]; 40.9 ml/min/kg ±9.6; 41.1 ml/min/kg ±8.0; and 43.4 ml/min/kg ±13.0[72]. The mean congestion index for normal portal blood flow was 0.042 ±0.01[69,72]. Lamb[72] recommends use of the uniform insonation method for determination of blood flow velocity of the portal vein, even though results obtained by this method did not differ from that of peak velocity method, because it was easier to use, required a shorter examination time, and produced a higher amplitude Doppler signal.

Physiological variations in MPV blood flow in association with prandial states have been reported in the dog [73]. Exercise and upright position are known to reduce portal blood flow in people[74].

2.2.27 Doppler patterns of abnormal main portal vein flow - Abnormalities in Doppler patterns of MPV blood flow have been observed in portal hypertension[32,69,75], congenital portosystemic shunt[76,77], congenital arterioportal fistula[78,79], non-obstructive portal vein thrombosis[75], hepatic fibrosis and undiagnosed conditions[76] in small animals.

In portal hypertension, reduced portal blood flow was reported due to obstructive portal vein thrombosis [75], and experimentally induced hepatic cirrhosis[69] in the dog. In each of two cases of obstructive portal vein thrombosis, the thrombus was detected by B-mode ultrasonography, located within the portal vein at the porta hepatis[75]. The thrombus appeared as a localised flow void on

colour Doppler imaging[32]. A tumour thrombus should be suspected if blood flow is detected within the thrombus on colour Doppler[32]. The presence of portal hypertension in one clinical case of portal vein thrombosis was confirmed by finding a portal venous pressure of 50 cm of water measured by placing a catheter in the mesenteric vein[75]. In the second case, portal hypertension was deduced from evidence of ultrasonographic findings of splenomegaly, dilated intrasplenic veins and portal tributaries, and reduced size of intrahepatic portal and hepatic veins[75]. In both dogs, mean portal blood flow velocity (time-averaged mean velocity) was lower at 10 and 11 cm/s, congestion index was higher at 0.11 and 0.2, and portal vein cross sectional area increased to 1.1 and 2.2 cm^2 respectively[75]. There was decreased signal amplitude of the Doppler spectrum. In experimentally induced hepatic cirrhosis, the presence of portal hypertension was concluded on the basis of finding severe cirrhosis with extensive acquired extrahepatic portosystemic shunts at necropsy[69]. Mean portal blood flow velocity and portal blood flow were significantly lower at 9.2 ± 1.70 cm/s and 17.2 ± 4.9 ml/min/kg respectively, and congestion index was significantly higher at 0.062 ± 0.018. Reduced portal blood flow velocity has also been reported in naturally occurring hepatic fibrosis in dogs[76].

Colour Doppler detected the abnormal presence and direction of blood flow in 92% of 38 dogs diagnosed by portography with intrahepatic and extrahepatic congenital portocaval shunts[76]. Turbulent blood flow was seen in the CVC at the site of entry of the shunting vessel in 42% of the cases. In one case, blood flow direction was reversed. Increased and or variable blood flow velocity of the MPV was found on spectral Doppler in 72% of the congenital portosystemic shunt. The increased portal flow velocity ranged from 20-35 cm/s[76]. Similar Doppler abnormalities of the MPV blood flow were reported in cats with congenital portosystemic shunt[77]. Increased or variable portal blood flow velocity has also been reported in dogs with non-obstructive portal vein thrombosis[75], and

undiagnosed hepatic disease[76]. Other investigators also reported turbulent flow in the CVC at the entry point of the shunting vessel[80].

Colour Doppler or spectral Doppler detected the abnormal presence and direction of blood flow in cases of congenital arterioportal fistula diagnosed by coeliac arteriography or postmortem in dogs[78,79]. Colour Doppler identified an enlarged, tortuous right medial portal vein and hepatic artery[79]. The direction of blood flow of the right medial portal vein and MPV was reversed (hepatofugal). On spectral Doppler of both the right medial portal vein and MPV, there was a pulsatile, low resistance parabolic velocity profile with a systolic peak, similar to that of the common hepatic artery. The peak systolic velocity of the MPV blood flow was higher at 60 cm/s[79]. In another study of congenital arterioportal fistula in two dogs, a mean PSV of 3.8 m/s ±1.9 and RI of 0.50 ±0.04 were reported[30].

2.2.28 Ultrasonographic technique for the intra-hepatic vessels - The hepatic veins and intrahepatic portal veins can be imaged with the dog in dorsal recumbency, and transducer positioned at the xiphisternum in transverse and sagittal planes. The transducer must be angled cranially and dorsally. Rotating and angling the transducer in this position, and sometimes obliquely to the right of the midline allows visualisation of the left lateral, left medial, quadrate, and right medial of both hepatic and portal venous systems, though each in a different plane[81]. The right lateral and caudate veins can be identified by examining from a right lateral position between the 9-11th intercostal spaces, halfway along the ribs in a longitudinal plane[81]. Food and gas within the stomach may interfere with visualisation of the vessels. The branch points of portal veins from the MPV are located more caudoventrally when compared with those of the hepatic veins with the CVC[71]. Portal

veins are surrounded by hyperechoic connective tissue whereas hepatic veins, in general are not[25,31,81,82].

2.2.29 Doppler patterns of the normal intra-hepatic blood flow - Normal hepatic parenchyma may not produce any tracing on spectral Doppler, but it is not unusual to obtain frequency shifts of up to 1.0 kHz from normal parenchyma, or benign hepatic parenchymal lesions when an insonating frequency of 5.0 MHz is used[32]. The intrahepatic branches of the hepatic artery generally are difficult to see on colour Doppler in healthy dogs, because of their small size[25]. Colour Doppler of intrahepatic portal veins imaged in transverse plane from the xiphisternal position indicates flow towards the transducer. However, flow of the right portal vein, after turning caudal from porta hepatis seen from a transverse oblique plane is away from the transducer[24]. On spectral Doppler there is continuous forward low velocity flow that is slightly undulating[24]. Temporary breaks are seen in the Doppler spectrum as respiratory diaphragmatic motion moves the sample volume out of the vessel lumen[24]. The Doppler spectra of hepatic veins entering the CVC show flow away from the transducer, and are similar to the CVC flow with three phases corresponding to atrial pressure. Fast forward flow is seen during atrial diastole. The flow then slows as the atrium fills and pressure builds. Forward flow increases again during ventricular diastole as the tricuspid valve opens. The flow then nearly stops, or may reverse slightly during atrial systole[24,32]. However, this pattern may be more complex as varying respiratory and intra-abdominal pressures may also have influence in addition to the cardiac cycles[32]. During inspiration, there is increased flow toward the heart because of decreased intrathoracic pressure and increased intra-abdominal pressure. These effects are reversed during expiration. Doppler spectra of the hepatic veins and CVC should therefore be obtained at normal end expiration in a quiet animal whenever possible.

2.2.30 Doppler patterns of abnormal intra-hepatic blood flow - Abnormalities in Doppler characteristics of hepatic blood flow have been observed in portal hypertension[32,69,75], congenital portosystemic shunt[76,77], congenital arterioportal fistula[78,79] and parenchymal pathology[32] in small animals.

In the evaluation of focal and multifocal hepatic neoplasia, continuous or pulsatile, high frequency shifts equal to or greater than 5 kHz, compatible with neovascularity and high velocity arteriovenous shunts have been associated with hepatocellular carcinomas and metastatic adrenal tumours in the dog[32]. Benign or non-highly vascular tumours have not shown similar characteristics.

In portal hypertension due to right-sided heart failure, or obstruction of the CVC at or cranial to the diaphragm, turbulent, reduced, absent or reversed blood flow may be observed in the CVC or hepatic veins on colour Doppler and spectral Doppler [32]. There is increased pulsatility in the hepatic veins, which, in human patients, can also be transmitted to the portal vein[83]. Similar changes may also be seen in healthy, well-hydrated individuals because the large blood volume distends the venous systems[31].

2.3 ANAEMIA AND CANINE BABESIOSIS

2.3.1 Anaemia - Is defined as reduced RBC mass, RBC count, packed cell volume (PCV), or haemoglobin concentration below the reference point for a given animal species[84-86]. Anaemia is regenerative if the bone marrow is responding appropriately to the reduced PCV, and non-regenerative if the marrow does not appear to be responding adequately. Regenerative anaemia is caused by blood loss either through haemorrhage or intravascular haemolysis. Non-regenerative anaemia is due to suppression of blood formation, especially the bone marrow, and is also seen within the first 48 hours of acute blood loss or peracute haemolysis[84].

2.3.2 Anaemia and blood flow - The viscosity of blood mainly depends on the concentration of RBCs[85]. In acute, severe anaemia, the blood viscosity may drop by as much as 50% of the normal value. This decreases the resistance to blood flow in the peripheral vessels so that far greater than normal quantities of blood return to the heart. Further more, hypoxia due to diminished transport of oxygen by the blood causes the tissue vessels to dilate, further decreasing viscosity and peripheral resistance, and allowing further increase in venous return and increase in cardiac output.

In chronic, progressive anaemia with moderate blood loss, one of the body's compensatory mechanisms is to lower oxygen-haemoglobin affinity to enhance tissue delivery of oxygen. Another is to effect changes in tissue perfusion such that blood is preferentially shunted to the most vital organs, and to increase the cardiac output[86].

2.3.3 Canine babesiosis - Canine babesiosis (CB) is a tick-transmitted infection of dogs caused by pathogenic protozoan piroplasm parasites, *Babesia canis* and *Babesia gibsoni*, that infect RBCs,

and is characterised by anaemia[87-91]. Three subspecies of *Babesia canis* have been identified namely, *B. canis canis*, *B. canis vogeli,* and *B. canis rossi*, the most virulent of the three subspecies[92-96]. In South Africa, infection is due to *B. canis rossi*[93-97]. Canine babesiosis is known to manifest a wide range of clinical forms, and varying degrees of severity from mild to peracute, fatal disease[98,99]. The three subspecies of *B. canis* appear to induce clinically distinct diseases[94]. In addition, various clinical manifestations due to infection by *B. c. rossi* subspecies alone have been recognised[96,99]. These varieties may have introduced a measure of confusion into the literature, and it is frequently uncertain which of the three subspecies was referred to in the non-South African literature. The disease has thus been classified in various ways. The disease due to *B. c. rossi* infection is known to manifest in uncomplicated and complicated forms[96,99]. In another approach, the clinical manifestations of animal babesioses were grouped into the hypotensive shock and haemolytic anaemia syndromes[92,100]. Jacobson *et al*[101], however, observed that there might be an overlap between these two syndromes. Peracute, acute, subacute or chronic forms of animal babesiosis have also been referred to, apparently based on clinical manifestations, alterations in the haemogram or on the character of organ pathology[102,103]. Brief accounts of the various classifications follow: thereafter the present study will use the South African system of classification into uncomplicated and complicated forms, based on the clinical manifestations.

2.3.4 Uncomplicated canine babesiosis - The symptoms of classical CB, also frequently referred to as the uncomplicated disease, are anorexia, lethargy, fever, pale mucous membranes, waterhammer pulse and splenomegaly[87,98,99,104]. Uncomplicated CB is further recognised as mild (Hct ≥ 20%) or severe (Hct < 20%) disease according to the degree of anaemia that is present[101]. The disease is associated with regenerative anaemia in the infected dog[87,92,103]. The parasites can be demonstrated within RBCs in the peripheral blood smear, which is the standard diagnostic test for

CB[87,103]. When this proves difficult, especially in atypical or chronic forms of the disease, serological tests such as the indirect fluorescent antibody test may be employed[93]. Diminazene aceturate, imidocarb and trypan blue are recognised, and recommended chemotherapeutic agents against CB[105], and dogs, treated as outpatients, recover uneventfully.

2.3.5 Complicated canine babesiosis - Complicated or atypical CB may be due to concurrent infection with *Ehrlichia canis*[91], or due to systemic inflammatory response syndrome (SIRS) that frequently develops into severe illness[96]. The SIRS may occur alone, although it is more frequently associated with single or multiple organ damage / dysfunction (MODS)[106]. Canine babesiosis complicated by organ dysfunction may present with one or more syndromes due to acute renal failure, hepatopathy (icterus), haemoconcentration (so called "red biliary"), immune mediated haemolytic anaemia, pulmonary oedema / acute respiratory distress syndrome, disseminated intravascular coagulopathy, rhabdomyolysis, or cerebral involvement[98,99,107,108].

A review of records of the Onderstepoort Veterinary Academic Hospital in Pretoria, South Africa, reported that 31% of CB patients developed severe illness and required hospitalisation[96]. Out of these, 50% had severe anaemia while the remaining cases were non-anaemic or had moderate anaemia[96].

The complicated forms of CB are thought to be similar, with regard to their disease mechanism and pathology, to bovine babesiosis due to *Babesia bovis*, human babesiosis, human *Plasmodium falciparum* malaria, sepsis in dogs and humans, trypanosomosis and many other conditions characterised by SIRS and MODS[96,98,106,107,109-112]. In each of these diseases, a hypotensive syndrome develops as a result of the inflammatory response[113].

2.3.6 Hypotensive shock syndrome in canine babesiosis - This is caused by the most pathogenic species, and *Babesia canis rossi* has been identified as one of those commonly causing this syndrome[92,101]. Clinically, a good correlation was found between reduced systemic arterial blood pressure (hypotension) and a state of physical collapse in severe cases of CB[101]. Both hypotension and localised hypercoagulable state within the microvasculature favour sludging (sequestration) of RBCs, all three occurring in the acute phase of the disease[114]. In a study of experimental bovine babesiosis, it was observed that blood pressure began to drop well before the reduction in Hct level or the occurrence of hypotensive shock[115]. The release of cytokines by monocytes, lymphocytes and endothelial cells in response to parasitic infection is thought to play an important role in bovine babesiosis, in the development of hypotension, the sequestration of RBCs within capillaries, or the loss of fluid into the interstitial tissue, potentially leading to shock[116-118]. Cytokines cause vasodilation and increased vascular permeability. The fall in Hct during this phase of the disease is therefore thought to be due to sequestration of blood within organ capillaries, and the dilution of circulating blood by influx of interstitial fluid in response to the hypotension rather than due to haemolysis[94,118]. Hypotension, and the sequestration of blood within capillaries result in poor tissue perfusion and tissue hypoxia[92]. The hypoxia may be responsible for lactic acidosis seen early in the course of this form of the disease[119], and may lead to extensive tissue damage[92].

2.3.7 Haemolytic anaemia syndrome in canine babesiosis - The haemolytic anaemia syndrome is said to result from infection by less pathogenic *Babesia* species or strains, and is characterised by pyrexia and haemolysis, but rarely by tissue damage[92]. Parasitised RBCs are primarily destroyed by the parasites themselves or by phagocytosis[90,92]. However, the occurrence of immune-mediated haemolysis as a complication of CB leading to severe anaemia, hypoxia and

tissue damage has been widely recognised[92,98,103,110,120]. Intravascular haemolysis may reduce the number of RBCs by more than 50% and may lead to haemoglobinaemia and haemoglobinuria[103,121,122]. Destroyed RBCs are subsequently removed by the reticuloendothelial system[123,124].

2.3.8 Canine babesiosis and hepatic pathology - Hepatomegaly in acute CB is thought to be primarily due to increased blood volume in the organ (venous stasis)[103,114]. Hyperplasia and hypertrophy of the Kupffer cells, that are a part of the reticuloendothelial system lining the hepatic sinusoids, may impede blood flow and account to some extent for the congestion of the sinusoids[103]. Hypotension and a hypercoagulable state may also play important roles in sequestration RBCs within hepatic sinusoids[114]. The resulting reduction in blood flow in hepatic sinusoids causes anoxia and degeneration or necrosis of hepatocytes leading to increased serum levels of transaminase enzymes[103,125-128]. Later, the bile canaliculi become distended with bile[103]. In the subacute disease, Kupffer cells are less prominent or numerous, and hepatic necrosis rarely occurs[103]. In the more chronic forms of the disease, the most prominent change in the liver is dilatation of the sinusoids[103]. The liver changes are similar to any condition causing severe anaemia, and may resemble those seen in canine ehrlichiosis[129]. The presence of extensive foci of extramedullary haematopoiesis in the liver has been reported in *B. gibsoni* infection[130].

2.3.9 Canine babesiosis and splenic pathology - Severe enlargement of the spleen in acute CB is primarily due to increased blood content as a result of venous stasis that distends the sinusoids of the red pulp[103,110,114]. Congestion of capillary beds with infected and non-infected RBCs in the spleen (and liver, lungs, kidneys and brain) also referred to as sequestration, sludging or haemoconcentration are found at postmortem examinations[110,121,122]. Histopathological observations

also indicate a marked response by the reticuloendothelial system[103]. Histiocytes lining the sinuses of the spleen (and lymph nodes, and sinusoids of the liver) undergo hypertrophic and hyperplastic changes, that impede blood flow, and is thought to be a major contributor to the splenomegaly of babesial infections[103]. Perivascular infiltrations with lymphocytes and monocytes have also been observed histopathologically[103]. In the chronic disease due to B. gibsoni, extramedullary haematopoiesis is often seen in the spleen and lymph nodes[130].

2.3.10 Canine babesiosis and renal pathology - Capillaries of both canine and bovine renal parenchyma, more commonly near the corticomedullary junction, become congested with parasitised and non-parasitised RBCs in acute CB, although canine kidneys appear to be less severely affected[103,110]. The renal tubular epithelial cells swell, and may become necrotic due to anoxic damage[103]. Haemoglobin casts are commonly found and may sometimes plug the collecting tubules[110]. Clinical evidence of kidney damage includes the appearance of granular and hyaline tubular casts in the urine, proteinuria, and elevated blood urea nitrogen levels[110,131,132]. Oliguria or anuria is seen in cases that develop acute renal failure[110]. In the chronic disease, kidney lesions consist of varying degrees of tubular degeneration, and mild to moderate mononuclear cell infiltrates, similar to that seen in chronic interstitial nephritis[103].

2.4 REFERENCES

1. Satomura S. Study of flow patterns in peripheral arteries by ultrasonics. *Journal of Acoustic Society of Japan*. 1959;15:151-158.
2. Bommer WJ, Miller L. Real-time two-dimensional colour-flow Doppler: enhanced Doppler flow imaging in the diagnosis of cardiovascular disease. *American Journal of Cardiology*. 1982;49:944.
3. Miyatake K, Okamoto M, Kinoshita N, Izumi S, Owa M, Takao S, Sakakibara S, Nimura Y. Clinical applications of a new type of real-time two-dimensional Doppler flow imaging system. *American Journal of Cardiology*. 1984;54:857.
4. Merritt CRB. Doppler colour flow imaging. *Journal of Clinical Ultrasound*. 1987;15:591.
5. Rubin JM, Adler RS. Power Doppler expands standard colour capability. *Diagnostic Imaging*. 1993;12:66-69.
6. Rubin JM, Bude RO, Carson PL, Bree RL, Alder RS. Power Doppler ultrasound: a potentially useful alternative to mean frequency-based colour Doppler ultrasound. *Radiology*. 1994;190:853-856.
7. Bude RO, Rubin JM, Alder RS. Power verses conventional colour Doppler sonography: comparison in the depiction of normal intrarenal vasculature. *Radiology*. 1994;192:777-780.
8. Barber FE, Baker DW, Nation AWC, Strandness JDE, Reid JM. Ultrasonic duplex echo Doppler scanner. In: *IEEE Transactions on Biomedical Engineering.* 1974:109-113.
9. Kremkau FW. *Diagnostic Ultrasound: Principles and Instruments*. Fourth ed. Philadelphia: WB Saunders Company; 1993.
10. Wells PNT. Basic principles and Doppler physics. In: Taylor KJW, Burns PN, Wells PNT, eds. *Clinical Applications of Doppler Ultrasound*. New York: Raven Press; 1995:1-17.

11. Haerten RL. Physical and technical principles. In: Haerten RL, Muck-Weymann ME, eds. *Principles of Doppler and Colour Doppler Imaging: An Introduction to the Fundamentals*. Second ed. Erlangen: Siemens Aktiengesellschaft; 1994:13-28.

12. Klews PM. Physics and technology of colour Duplex sonography. In: Wolf KJ, Fobbe F, eds. *Colour Duplex Sonography: Principles and Clinical Applications*. New York: Thieme Medical Publishers, Inc.; 1995:245-294.

13. Burns PN. Interpreting and analysing the Doppler examination. In: Taylor KJW, Burns PN, Wells PNT, eds. *Clinical Applications of Doppler Ultrasound*. Second ed. New York: Raven Press; 1995:55-98.

14. Muck-Weymann ME. Evaluation of the Doppler spectrum. In: Haerten RL, Muck-Weymann ME, eds. *Principles of Doppler and Colour Doppler Imaging: An Introduction to the Fundamentals*. Second ed. Erlangen: Siemens Aktiengesellschaft; 1994:45-52.

15. Gill RW. Pulsed Doppler with B-mode imaging for quantitative blood flow measurement. *Ultrasound in Medicine and Biology*. 1979;5:223-235.

16. Gill RW. Accuracy calculations for ultrasonic pulsed Doppler blood flow measurements. *Australasian Physical & Engineering Sciences in Medicine*. 1982;5:51-57.

17. Moriyasu F, Ban N, Nishida O, Nakamura T, Miyake T, Uchino H, Kanematsu Y, Koizumi S. Clinical application of an ultrasonic duplex system in the quantitative measurement of portal blood flow. *Journal of Clinical Ultrasound*. 1986;14:579-588.

18. Moriyasu F, Nishida O, Ban N, Nakamura T, Sakai M, Miyake T, Uchino H. "Congestion index" of the portal vein. *American Journal of Roentgenology*. 1986;146:735-739.

19. Kremkau FW. Principles and instrumentation. In: Merritt CRB, ed. *Doppler Colour Imaging*. New York: Churchill Livingstone; 1992:7-60.

20. Klews PM. Introduction to colour duplex sonography. In: Wolf KJ, Fobbe F, eds. *Colour Duplex Sonography: Principles and Clinical Applications*. New York: Thieme Medical Publishers; 1995:1-13.

21. Sauerbrei EE, Nguyen KT, Nolan RL. The retroperitoneal blood vessels. In: *Abdominal Sonography*. New York: Raven Press; 1992:207-230.

22. Spaulding KA. Helpful hints in identifying the caudal abdominal aorta and caudal vena cava. *Veterinary Radiology & Ultrasound*. 1992;33:90-92.

23. Spaulding KA. A review of sonographic identification of abdominal blood vessels and juxta vascular organs. *Veterinary Radiology & Ultrasound*. 1997;38:4-23.

24. Finn-Bodner ST, Hudson JA. Abdominal vascular sonography. *Veterinary Clinics of North America. Small Animal Practice*. 1998;28:887-942.

25. Szatmari V, Sotonyi P, Voros K. Normal duplex Doppler waveforms of major abdominal blood vessels in dogs: A review. *Veterinary Radiology & Ultrasound*. 2001;42:93-107.

26. Mattoon JS, Nyland TG. Abdominal fluid, lymph nodes, masses, peritoneal cavity, and great vessel thrombosis. In: Nyland TG, Mattoon JS, eds. *Small Animal Diagnostic Ultrasound*. Second ed. Philadelphia: W.B. Saunders Co.; 2002:82-91.

27. Ramsey CC, Burney DP, MacIntire DK, Finn-Bodner ST. Use of streptokinase in four dogs with thrombosis. *Journal of American Veterinary Medical Association*. 1990;209:780-785.

28. Schmid V, Lang J. Intravascular ultrasound contrast media. *Veterinary Radiology & Ultrasound*. 1995;36:307-314.

29. Kircher P, Lang J, Blum J, Gaschen F, Doherr M, Sieber C, Gaschen L. Influence of food composition on splanchnic blood flow during digestion in unsedated normal dogs: a Doppler study. *Veterinary Journal*. 2003;166:265-272.

30. Lamb CR, Burton CA, Carlisle CH. Doppler measurement of hepatic arterial flow in dogs: technique and preliminary findings. *Veterinary Radiology & Ultrasound*. 1999;40:77-81.

31. Sauerbrei EE, Nguyen KT, Nolan RL. The liver. In: *Abdominal Sonography*. New York: Raven Press; 1992:73-110.

32. Nyland TG, Mattoon JS, Herrgesell EJ, Wisner ER. Liver. In: Nyland TG, Mattoon JS, eds. *Small Animal Diagnostic Ultrasound*. Second ed. Philadelphia: W.B.Saunders Company; 2002:93-127.

33. Selcer BA. The liver and gallbladder. In: Cartee RE, ed. *Practical Veterinary Ultrasound*. Philadelphia: Williams & Wilkins; 1995:88-106.

34. Fruechte D, Zwiebel WJ. Anatomy and normal Doppler signatures of abdominal vessels. In: Zwiebel WJ, ed. *Introduction to Vascular Ultrasonography*. Third ed. Philadelphia: W.B. Saunders Company; 1992:335-350.

35. Nyland TG, Mattoon JS, Herrgesell EJ, Wisner ER. Urinary tract. In: Nyland TG, Mattoon JS, eds. *Small Animal Diagnostic Ultrasound*. Second ed. Philadelphia: W.B. Saunders Company; 2002:158-195.

36. Tobias AH, Thomas WD, Kittleson MD, Komtebedde J. Cor triatrium dexter in two dogs. *Journal of the American Animal Hospital Association*. 1989;25:277-283.

37. Szatmari V, Sotonyi P, Voros K. Doppler ultrasound detection of retrograde pulsatile flow in the caudal vena cava of a puppy with cor triatriatum dexter. *Veterinary Record*. 2000;147:68-72.

38. Cornelius L, Mahaffey M. Kinking of the intrathoracic caudal vena cava in five dogs. *Journal of Small Animal Practice*. 1985;26:67-80.

39. Saunders HM, Neath PJ, Brockman DJ. B-mode and Doppler ultrasound imaging of the spleen with canine splenic torsion: a retrospective evaluation. *Veterinary Radiology & Ultrasound*. 1998;39:349-353.

40. Sauerbrei EE, Nguyen KT, Nolan RL. The kidney. In: *Abdominal Sonography*. New York: Raven Press; 1992:207-230.

41. Reid MH, Mackay RS, Lantz MT. Noninvasive blood flow measurements by Doppler ultrasound with applications to renal arterial flow determination. *Investigative Radiology*. 1980;15:323-331.

42. Daley CA, Finn-Bodner ST, Lenz SD. Contrast-induced renal failure documented by colour Doppler imaging in a dog. *Journal of the American Animal Hospital Association*. 1994;30:33-37.

43. LaFortune M, Patriquin H, Demeule E, Trinh BC, Dufresne MP, Legault L, Raymond J. Renal artery stenosis: Slowed systole in the downstream circulation - experimental study in dogs. *Radiology*. 1992;184:475-478.

44. Morrow KL, Salman MD, Lappin MR, Wrigley RH. Comparison of the resistive index to clinical parameters in dogs with renal disease. *Veterinary Radiology & Ultrasound*. 1996;37:193-199.

45. Nyland TG, Fisher BS, Doverspike M, Hornof WJ, Olander HJ. Diagnosis of urinary tract obstruction in dogs using duplex Doppler ultrasonography. *Veterinary Radiology & Ultrasound*. 1993;34:348-352.

46. Rivers BJ, Walter PA, O'Brien TD. Duplex Doppler estimation of Pourcelot resistive index in arcuate arteries of sedated normal cats. *Journal of Veterinary Internal Medicine*. 1996;10:28-33.

47. Platt JF. Duplex Doppler evaluation of native kidney dysfunction: obstructive and nonobstructive disease. *American Journal of Roentgenology*. 1992;58:1035-1042.

48. Ramos IM, Taylor KJ, Kier R. Tumour vascular signals in renal masses: detection with Doppler ultrasound. *Radiology*. 1988;168:633-637.

49. Erwin BC, Carroll BA, Walter JF, Sommer FG. Renal infarction appearing as an echogenic mass. *American Journal of Roentgenology*. 1982;138:759-761.

50. Parvey HR, Eisenberg RL. Image-directed Doppler sonography of the intrarenal arteries in acute renal vein thrombosis. *Journal of Clinical Ultrasound*. 1990;18:512-516.

51. Platt JF, Ellis JH, Rubin JM, DiPietro MA, Sedman AB. Intrarenal arterial Doppler sonography in patients with nonobstructive disease. *American Journal of Roentgenology*. 1990;154:1223-1227.

52. Wong SN, Lo RNS, Yu ECL. Renal blood flow pattern by noninvasive Doppler ultrasound in normal children and acute renal failure patients. *Journal of Ultrasound Medicine*. 1989;8:135-141.

53. Platt JF, Rubin JM, Ellis JH. Acute renal failure: Possible role of duplex Doppler US in distinction between acute prerenal failure and acute tubular necrosis. *Radiology*. 1991;179:419-423.

54. Pozniak MA, Kelcz F, D'Alessandro A. Sonography of renal transplants in dogs: The effect of acute tubular necrosis, cyclosporine nephrotoxicity, and acute rejection on resistive index and renal length. *American Journal of Roentgenology*. 1992;158:791-797.

55. Rivers BJ, Walter PA, Polzin DJ, King VL. Duplex Doppler estimation of intrarenal Pourcelot resistive index in dogs and cats with renal disease. *Journal of Veterinary Internal Medicine*. 1997;11:250-260.

56. Rivers BJ, Walter PA, Letourneau JG, Finlay DE, Ritenour ER, King VL, O'Brien TD, Polzin DJ. Estimation of arcuate artery resistive index as a diagnostic tool for aminoglycoside-induced acute renal failure in dogs. *American Journal of Veterinary Research*. 1996;57:1536-1544.

57. Bude RO, DiPietro MA, Platt JF, Rubin JM. Effect of furosemide and intravenous normal saline fluid load upon the renal resistive index in nonobstructed kidneys in children. *Journal of Urology*. 1994;151:438-441.

58. Renowden SA, Cochlin DL. The potential use of diuresis Doppler sonography in PUJ obstruction. *Clinical Radiology*. 1992;46:94-96.

59. Renowden SA, Cochlin DL. The effect of intravenous furosemide on the Doppler waveform in normal kidneys. *Journal of Ultrasound Medicine*. 1992;11:65-68.

60. Shokeir AA, Nijman RJ, el-Azab M, Provoost AP. Partial ureteral obstruction: Effect of intravenous normal saline and furosemide upon the renal resistive index. *Journal of Urology*. 1997;157:1074-1077.

61. Gottlieb RH, Luhmann K, Oates RP. Duplex ultrasound evaluation of normal native kidneys and native kidneys with urinary tract obstruction. *Journal of Ultrasound in Medicine*. 1989;8:609-611.

62. Platt JF, Rubin JM, Ellis JH. Duplex Doppler ultrasound of the kidney: differentiation of the obstructive from nonobstructive dilatation. *Radiology*. 1989;171:515-517.

63. Ulrich JC, York JP, Koff SA. The renal vascular response to acutely elevated intrapelvic pressure: Resistive index measurements in experimental urinary obstruction. *Journal of Urology*. 1995;154:1202-1204.

64. Dodd GD, Kaufman PN, Bracken RB. Renal arterial duplex Doppler ultrasound in dogs with urinary obstruction. *Journal of Urology*. 1991;145:644-646.

65. Berland LL, Lawson TL, Adams MB. Evaluation of canine renal transplants with pulsed Doppler duplex sonography. *Journal of Surgical Research*. 1985;39:433-438.

66. Takahashi S, Narumi Y, Takahara S, Suzuki S, Kyo M, Cruz M, Takamura M, Kokado Y, Ichimaru N, Toki K, Nakamura H, Okuyama A. Acute renal allograft rejection in the canine: Evaluation with serial duplex Doppler ultrasonography. *Transplant Proceedings*. 1999;31:1731-1734.

67. Newell SM, Ellison GW, Graham JP, Ginn PE, Lanz OI, Harrison JM, Smith JS, Van Guilder JM. Scintigraphic, sonographic, and histologic evaluation of renal autotransplantation in cats. *American Journal of Veterinary Research*. 1999;60:775-779.

68. Jian-Xin WU, Carlisle CH. Ultrasonographic examination of the liver based on recognition of hepatic and portal veins. *Veterinary Radiology & Ultrasound*. 1995;36:234-239.

69. Nyland TG, Fisher PE. Evaluation of experimentally induced canine hepatic cirrhosis using duplex Doppler ultrasound. *Veterinary Radiology*. 1990;31:189-194.

70. Kantrowitz BM, Nyland TG, Fisher P. Estimation of portal blood flow using duplex real-time and Doppler ultrasound imaging in the dog. *Veterinary Radiology & Ultrasound*. 1989;30:222-226.

71. Carlisle CH, Wu JX, Heath TJ. Anatomy of the portal and hepatic veins of the dog: a basis for systemic evaluation of the liver by ultrasonography. *Veterinary Radiology & Ultrasound*. 1995;36:227-233.

72. Lamb CR, Mahoney PN. Comparison of three methods for calculating portal blood flow velocity in dogs using duplex Doppler ultrasonography. *Veterinary Radiology & Ultrasound*. 1994;35:190-194.

73. Strombeck DR, Guilford WG. *Small Animal Gastroenterology*. Second ed. London: Wolfe; 1991.

74. Ohnishi K, Saito M, Nakayama T, Iida S, Nomura F, Koen H, Okuda K. Portal venous haemodynamics in chronic liver disease: Effects of posture change and exercise. *Radiology*. 1985;155:757-761.

75. Lamb CR, Wrigley RH, Simpson KW. Ultrasonographic diagnosis of portal vein thrombosis in four dogs. *Veterinary Radiology & Ultrasound*. 1996;37:121-129.

76. Lamb CR. Ultrasonographic diagnosis of congenital portosystemic shunts in dogs: Results of a prospective study. *Veterinary Radiology & Ultrasound*. 1996;37:281-288.

77. Lamb CR, Forster-van Hirjfte MA, White RN, McEvoy FJ, Rutgers HC. Ultrasonographic diagnosis of congenital portosystemic shunt in 14 cats. *Journal of Small Animal Practice*. 1996;37:205-209.

78. Bailey MQ, Willard MD, McLoughlin MA, Gaber C, Hauptman J. Ultrasonographic findings associated with congenital hepatic arteriovenous fistula in three dogs. *Journal of the American Veterinary Medical Association*. 1988;192:1099-1101.

79. Szatmari V, Nemeth T, Kotai I, Voros K, Sotonyi P. Doppler ultrasonographic diagnosis and anatomy of congenital intrahepatic arterioportal fistula in a puppy. *Veterinary Radiology & Ultrasound*. 2000;41:284-286.

80. Holt DE, Schelling CG, Saunders HM, Orsher RJ. Correlation of ultrasonographic findings with surgical, portographic and necropsy findings in dogs and cats with portosystemic shunts: 63 cases (1987-1993). *Journal of the American Veterinary Medical Association*. 1995;207:1190-1193.

81. Wu J-X, Carlisle CH. Ultrasonographic examination of the canine liver based on recognition of hepatic and portal veins. *Veterinary Radiology & Ultrasound*. 1995;36:234-239.

82. Wachsberg RH, Angyal EA, Klein MK, Kuo H-R, Lambert WC. Echogenicity of hepatic versus portal vein walls revisted with histologic correlation. *Journal of Ultrasound Medicine*. 1997;16:807-810.

83. Gorka TS, Gorka W. Doppler sonographic diagnosis of severe portal vein pulsatility in constrictive pericarditis: Flow normalisation after pericardiectomy. *Journal of Clinical Ultrasound*. 1999;27:84-88.

84. Nelson RW, Couto CG. Anaemia. In: Nelson RW, Couto CG, eds. *Small Animal Internal Medicine*. Second ed. St. Louis: Mosby; 1998:1160-1173.

85. Guyton AC, Hall JE. Red blood cells, anaemia, and polycythemia. In: Guyton AC, Hall JE, eds. *Textbook of Medical Physiology*. Tenth ed. Philadelphia: W.B. Saunders Company; 2000:382-391.

86. Rogers KS. Anaemia. In: Ettinger SJ, Feldman EC, eds. *Textbook of Veterinary Internal Medicine: Diseases of the Dog and Cat*. Fifth ed. Philadelphia: W.B. Saunders Company; 2000:198-203.

87. Malherbe WD. The manifestations and diagnosis of Babesia infections. *Annals of New York Academy of Science*. 1956;64:128-146.

88. Purnell RE. Babesiosis in various hosts. In: Ristic M, Kreier JP, eds. *Babesiosis*. New York: Academic Press; 1981:25-63.

89. McCosker PJ. The global importance of babesiosis. In: Ristic M, Kreier JP, eds. *Babesiosis*. New York: Academic Press; 1981:1-24.

90. Ewing SA. Methods of reproduction of Babesia canis in erythrocytes. *American Journal of Veterinary Research*. 1965;26:727-733.

91. Ewing SA, Buckner RG. Manifestation of babesiosis, ehrlichiosis, and combined infections in the dog. *American Journal of Veterinary Research*. 1965;26:815-828.

92. Taboada J, Merchant SR. Babesiosis of companion animals and man. *Veterinary Clinics of North America. Small Animal Practice*. 1991;21:103-123.

93. Uilenberg G, Franssen FF, Perie NM, Spanjer AA. Three groups of Babesia canis distinguished, and a proposal for nomenclature. *Veterinary Quarterly*. 1989;11:33-40.

94. Schetters TP, Moubri K, Precigout E, Kleuskens J, Scholtes NC, Gorenflot A. Different Babesia canis isolates, different diseases. *Parasitology*. 1997;115:485-493.

95. Carret C, Walas F, Carcy B, Grande N, Precigout E, Moubri K, Schetters TP, Gorenflot A. *Babesia canis canis, Babesia canis vogeli, Babesia canis rossi*: Differentiation of the three subspecies by a restriction fragment length polymorphism analysis on amplified small subunit ribosomal RNA genes. *Journal of Eukaryotic Microbiology*. 1999;46:298-303.

96. Reyers F, Leisewitz AL, Lobetti RG, Milner RJ, Jacobson LS, van Zyl M. Canine babesiosis in South Africa: more than one disease. Does this serve as a model for falciparum malaria? *Annals of Tropical Medicine and Parasitology*. 1998;92:503-511.

97. Lewis BD, Penzhorn BL, Lopez-Rebollar LM, De Waal DT. Isolation of a South African vector-specific strain of *Babesia canis*. *Veterinary Parasitology*. 1996;63:9-16.

98. Malherbe WD, Parkin BS. Atypical symptomatology in Babesia canis infection. *Journal of the South African Veterinary Medical Association*. 1951;22:25-36.

99. Jacobson L, Clark IA. The pathophysiology of canine babesiosis: New approaches to an old puzzle. *Journal of the South African Veterinary Association*. 1994;65:134-145.

100. Freeman MJ, Kirby BM, Panciera DL, Henik RA, Rosin E, Sullivan LJ. Hypotensive shock syndrome associated with acute Babesia canis infection in a dog. *Journal of American Veterinary Medical Association*. 1994;204:94-96.

101. Jacobson LS, Lobetti RG, Vaughan-Scott T. Blood pressure changes in dogs with babesiosis. *Journal of the South African Veterinary Association*. 2000;71:14-20.

102. Irwin PJ, Hutchinson GW. Clinical and pathological findings of *Babesia* infections in dogs. *Australian Veterinary Journal*. 1991;68:204-209.

103. Hildebrandt PK. The organ and vascular pathology of babesiosis. In: Ristic M, Kreier JP, eds. *Babesiosis*. New York: Academic Press, Inc; 1981:459-473.

104. Lobetti RG. Canine babesiosis. *Parasitology*. 1998;20:418-430.

105. Moore DJ. Therapeutic implications of Babesia canis infection in dogs. *Journal of the South African Veterinary Association*. 1979;50:346-352.

106. Welzl C, Leisewitz AL, Jacobson LS, Vaughan-Scott T, Myburgh E. Systemic inflammatory response syndrome and multiple-organ damage / dysfunction in complicated canine babesiosis. *Journal of the South African Veterinary Association*. 2001;72:158-162.

107. Botha H. The cerebral form of babesiosis in dogs. *Journal of the South African Veterinary Medical Association*. 1964;35:27-28.

108. Basson PA, Pienaar JG. Canine babesiosis: a report on the pathology of three cases with special reference to the cerebral form. *Journal of the South African Veterinary Association*. 1965;36:333-341.

109. Wright IG. The kallikrein system and its role in the hypotensive shock syndrome of animals infected with the haemoprotozoan parasites Babesia, Plasmodia and Trypanosoma. *General Pharmacology*. 1979;10:319-325.

110. Maegraith B, Gilles HM, Devakul K. Pathological processes in *Babesia canis* infections. *Zeitschrift fur Tropenmedizin und Parasitologie*. 1957;8:485-514.

111. Brady CA, Otto CM. Systemic inflammatory response syndrome, sepsis, and multiple organ dysfunction. *Veterinary Clinics of North America. Small Animal Practice*. 2001;31:1147-1162.

112. Clark IA, Jacobson LS. Do babesiosis and malaria share a common disease process? *Annals of Tropical Medicine and Parasitology*. 1998;92:483-488.

113. Clark IA, Rockett KA, Cowden WB. Proposed link between cytokines, nitric oxide and human cerebral malaria. *Parasitology Today*. 1991;7:205-207.

114. Schetters TPM, Kleuskens J, Scholtes NC, Gorenflot AF. Parasite localisation and dissemination in the *Babesia*-infected host. *Annals of Tropical Medicine and Parasitology*. 1998;92:513-519.

115. Wright IG, Kerr JD. Hypotension in acute *Babesia bovis* (*B. argentina*) infections of splenectomised calves. *Journal of Comparative Pathology*. 1977;87:531-537.

116. Mahoney DF. *Babesia* of domestic animals. In: Kreier JP, ed. *Parasitic Protozoa*. New York: Academic Press; 1977:1-52.

117. Wright IG. Kinin, kininogen, and kininase levels during acute *Babesia bovis* infection of cattle. *British Journal of Pharmacology*. 1977;61:567-572.

118. Wright IG, Mahoney DF. The activation of kallikrein in acute *Babesia argentina* infections of splenectomised calves. *Zeitschrift fur Parasitenkd*. 1974;43:271-278.

119. Button C. Metabolic and electrolyte disturbances in acute canine babesiosis. *Journal of the South African Veterinary Association*. 1979;175:475-479.

120. Farwell GE, LeGrand EK, Cobb CC. Clinical observations on *Babesia gibsoni* and *Babesia canis* infections in dogs. *Journal of the American Veterinary Medical Association*. 1982;180:507-511.

121. Abdullahi SU, Mohammed AA, Trimnelly AR, Sannusi A, Alafiatayo R. Clinical and haematological findings in 70 naturally occurring cases of Canine babesiosis. *Journal of Small Animal Practice*. 1990;31:145-147.

122. Shortt HE. *Babesia canis*: The lifecycle and laboratory maintenance in its arthropod and mammalian hosts. *International Journal for Parasitology*. 1973;3:119-148.

123. Simpson CF. Electron microscopic comparison of *Babesia* spp. and hepatic changes in ponies and mice. *American Journal of Veterinary Research*. 1970;31:1763-1768.

124. Simpson CF. Phagocytosis of *Babesia canis* by neutrophils in peripheral circulation. *American Journal of Veterinary Research*. 1974;35:701-704.

125. Malherbe WD. Clinicopathological studies of *Babesia canis* infection in dogs. I. The influence of the infection on bromosulphthalein retention in the blood. *Journal of the South African Veterinary Medical Association*. 1965;36:25-30.

126. Malherbe WD. Clinicopathological studies of *Babesia canis* infection in dogs. II. The influence of the infection on plasma transaminase activity. *Journal of the South African Veterinary Medical Association*. 1965;36:173-176.

127. Malherbe WD. Clinicopathological studies of *Babesia canis* infection in dogs. III. The influence of the infection on plasma alkaline phosphatase activity. *Journal of the South African Veterinary Medical Association*. 1965;36:179-182.

128. Malherbe WD. Clinicopathological studies of *Babesia canis* infection in dogs. IV. The effect on bilirubin metabolism. *Journal of the South African Veterinary Medical Association*. 1965;36:569-573.

129. Hildebrandt PK, Huxsoll DL, Walker JS, Nims RM, Taylor R, Andrews M. Pathology of canine ehrlichiosis (tropical canine pancytopenia). *American Journal of Veterinary Research*. 1973;34:1309-1320.

130. Botros BAM, Moch RW, Barsoum IS. Some observations on experimentally induced infections of dogs with *Babesia gibsoni*. *American Journal of Veterinary Research*. 1975;36:293-296.

131. Malherbe WD. Clinicopathological studies of *Babesia canis* infection in dogs. V. The influence of the infection on kidney function. *Journal of the South African Veterinary Medical Association*. 1966;37:261-264.

132. Lobetti RG, Jacobson LS. Renal involvement in dogs with babesiosis. *Journal of the South African Veterinary Association*. 2001;72:23-28.

CHAPTER 3

INFLUENCE OF NORMOVOLEMIC ANEMIA ON DOPPLER CHARACTERISTICS OF THE ABDOMINAL AORTA AND SPLANCHNIC VESSELS IN BEAGLES

Lee M. Koma, BVM, MPhil; Tim C. Spotswood, BVSc; Robert M. Kirberger, BVSc, MMedVet; Piet J. Becker, MSc, PhD

As published in the American Journal of Veterinary Research, 2005;66:187-195

3.1 ABSTRACT

3.1.1 Objective—To ultrasonographically evaluate the haemodynamics in the abdominal aorta (AAo) and splanchnic vessels in dogs with experimentally induced normovolemic anemia.

3.1.2 Animals—11 healthy Beagles.

3.1.3 Procedure—The AAo, cranial mesenteric artery (CMA), celiac artery (CA), hilar splenic artery (HSA), and main portal vein (MPV) were evaluated in conscious dogs immediately before and after experimental induction of severe normovolemic anemia (Hct, 16%), and during recovery from moderate and mild anemia (Hct, 26% and 34%, respectively). Peak systolic velocity (PSV) or peak velocity (PV), time-averaged mean velocity (TAV_{mean}), pulsatility index (PI), resistive index (RI), blood flow, congestion index (CI) and heart rate (HR) were recorded. Results were compared for anemic and control states.

3.1.4 Results—Severe anemia caused significant increases in HR (25-70%); PSV (AAo, 45.8%; CMA, 56.1%; CA, 41.9%); PV (MPV, 84.2 %); and TAV_{mean} (AAo, 69.4%, CMA, 64.3%; CA, 29.7%; MPV, 76.9%); and significant decreases in PI (AAo, 26.1%; HSA, 19.3%) and CI (MPV, 45.2%). There was no significant change in PI of the CMA or CA; portal blood flow; or RI of any artery. Significantly higher TAV_{mean} persisted in all vessels during moderate anemia, but higher PSV persisted only in the CMA; PI (CMA, CA) and RI (CA) decreased significantly; and portal blood flow increased significantly. Significant increase in TAV_{mean} (AAo, CMA) persisted during mild anemia, and both PI (AAo, CMA, HSA) and RI (CMA) were significantly lower.

3.1.5 Conclusions and Clinical Relevance—Doppler ultrasonography revealed hyperdynamic circulation in the AAo and splanchnic vessels in dogs with experimentally induced normovolemic anemia. (*Am J Vet Res* 2005;66:187–195)

3.2 INTRODUCTION

Studies in dogs,[1-3] and rats[4] conducted by use of invasive techniques have documented a hyperdynamic cardiovascular response to severe anemia characterized by increased cardiac output, reduced systemic vascular resistance, and increased blood flow (hyperemia) to various organs, including the abdominal splanchnic vascular bed. Variation in hemodynamic response is attributable to differing degrees of anemia, and there is variation in the hemodynamic response among vital organs such as the heart and brain and nonvital organs such as the kidneys, liver, spleen, or gastrointestinal tract.[2,5]

In severely anemic human fetuses with RBC alloimmunization, noninvasive duplex Doppler ultrasonography (DUS) has been used to document increases in hemodynamic variables such as blood flow,[6] time-averaged mean velocity (TAV_{mean}),[7] and peak systolic velocity (PSV)[8] within various blood vessels, thereby supporting findings in studies conducted in other animals. Peak systolic velocity of the middle cerebral artery[9,10] or main splenic artery[11] and TAV_{mean} of the middle cerebral artery[12] are good DUS indices and have been proposed as clinical tests for use in the prediction, detection, and management of severe anemia in human fetuses. In nonhuman animals, a significant increase in cerebral blood flow has been reported in an anemic newborn lamb.[13] To our knowledge, a hyperdynamic state in the abdominal splanchnic circulation in dogs with severe anemia has not been documented by use of noninvasive DUS. Reduction of splanchnic vascular resistance in hyperdynamic states has also not been determined by use of noninvasive techniques in humans or other animal species.

At Onderstepoort Veterinary Academic Hospital, University of Pretoria, it is proposed to use DUS to detect hemodynamic changes that may be associated with complicated canine babesiosis. Serious clinical consequences and therapeutic challenges are encountered in dogs with complicated babesiosis.[14] Anemia is a common characteristic of the disease.[14] Pathologic mechanisms underlying these complications are poorly understood but believed to be similar to that of cattle with complicated babesiosis or humans with complicated falciparum malaria.[15-18] The mechanisms for these complications are believed to involve systemic inflammatory responses characterized by impaired perfusion and subsequently damage to 1 or multiple organs.[18] Sequestration of RBCs within microvessels is most commonly blamed for impaired tissue perfusion and hypoxia, and congestion of capillary beds in various organs has commonly been reported during postmortem examinations.[17] Hypotension has also been reported in both experimentally[16] and naturally[19] infected animals. Knowledge and ability to noninvasively detect hemodynamic changes associated with anemia in organs such as the liver, spleen, and kidneys that are commonly involved in complicated babesiosis in dogs may permit correct interpretation of DUS results in affected dogs, improve the understanding of pathophysiologic mechanisms, and be useful in predicting possible complications and monitoring clinical progress of dogs with babesiosis and related diseases, such as falciparum malaria.

Noninvasive DUS has been used in dogs to detect changes in abdominal splanchnic hemodynamic physiologic and pathophysiologic processes.[20-26] Peak systolic velocity, end-diastolic velocity, mean velocity, pulsatility index (PI), resistive index (RI), blood flow, or the congestion index (CI) have been used to document hemodynamic changes associated with digestive function[25,26] or chronic hepatic disorders.[21,23,24]

The purpose of the study reported here was to evaluate by use of noninvasive DUS blood flow or blood flow velocities (peak and mean) and vascular resistance in the abdominal aorta and splanchnic vessels of dogs with experimentally induced normovolemic anemia.

3.3 MATERIALS AND METHODS

3.3.1 Animals—Eleven beagles comprising 1 sexually intact male, 3 neutered males, and 7 sexually intact nonpregnant females were used in the study. Mean ± SD body weight was 12.0 ± 1.8 kg. Mean age of 4 males and 5 females was 2.63 ± 0.05 years; the exact age of 2 females could not be established. All Beagles were in good physical condition and appeared to be healthy. The dogs were part of the Onderstepoort Veterinary Academic Research Unit, Faculty of Veterinary Science, University of Pretoria. During the study, dogs were transferred and housed in large kennels at the Onderstepoort Veterinary Academic Hospital. In the first week of the study, 1 dog was entered into the study. Two dogs were entered into the study each subsequent week. At the hospital, dogs were fed a commercial food high in protein and caloric content. The Animal Use and Care Committee of the Faculty of Veterinary Science, University of Pretoria, approved this study.

3.3.2 Experimental design—The study was conducted such that each dog served as its own control animal (hemodynamics of physiologic and anemic states were compared within each dog). Duplex Doppler variables for the abdominal aorta (AAo) and abdominal splanchnic vessels were measured immediately before and after induction of severe normovolemic anemia (Hct 15 to 17%). Dogs were allowed to recover from anemia, and measurements were repeated during periods of moderate (Hct, 25% to 27%) and mild (Hct, 31% to 37%) anemia. Duplex Doppler evaluation of

abdominal splanchnic hemodynamics was performed immediately after an echocardiographic examination, which was conducted as part of another study that examined the effects of normovolemic anemia on left ventricular function. The echocardiographic examination was completed within 45 to 60 minutes, and the abdominal splanchnic Doppler examination required between 90 and 120 minutes, depending on patient cooperation. Regularly scheduled breaks of 5 to 10 minutes were permitted during each examination. At the end of the study, all dogs had recovered sufficiently from the induced anemia and were returned to the veterinary research facility.

3.3.3 Induction of anemia—Approximately 20% of the circulating blood volume was removed 1 to 3 times/d during a 3- or 5-day period to induce severe anemia (Hct 15 to 17%). The bleeding procedure was a modification of the method described in another study.[27] Plasma from the blood that was removed was added to a lactated Ringer's solution (an amount calculated to replace the volume of removed RBCs) and infused into the dog in an attempt to maintain a normal circulating blood volume; however, no measurements were performed to confirm normovolemia. Doppler measurements of dogs in the severely anemic state commenced no sooner than 16 hours after completion of the volume replacement.

3.3.4 Ultrasonographic examinations—All examinations were performed by 1 investigator (LMK). Food was withheld from dogs for 12 hours prior to ultrasonography. Dogs were not sedated or anesthetized for the examinations. The ventral and left lateral portions of the abdomen and right lateral portion of the thorax from the 6th to 13th ribs were clipped, cleaned, and covered with acoustic gel. For general abdominal imaging, dogs were positioned in dorsal recumbency. Images of the spleen in parasagittal, transverse, and oblique planes were obtained in the left cranial quadrant of the abdomen, and images of the left kidney in dorsal, transverse, and oblique planes were

obtained slightly caudal to the position of the spleen. Dogs were then positioned in right lateral recumbency to enable us to obtain images of the AAo, cranial mesenteric artery (CMA), and celiac artery (CA) in the parasagittal or dorsal plane. Dogs were then positioned in left lateral recumbency to enable us to obtain images of the main portal vein (MPV) in dorsal, transverse, and oblique planes caudal to the liver via the right 9th to 12th intercostal spaces.

All examinations were performed by use of an ultrasound machine[a] with a convex-array, linear-array, or phased-array transducer. The B-mode examination of the general abdominal cavity, organs, and AAo was conducted by use of a 5.0-MHz convex-array transducer; identification and evaluation of the CMA, CA, and hilar splenic artery (HSA) was performed by use of a 7.5-MHz linear-array transducer, although we sometimes used a convex-array transducer. The MPV was identified by use of a 6.0-MHz phased-array transducer. All machine settings, including overall gain, depth compensation gain, edge enhancement, focus, and line density, were adjusted during each examination to obtain optimal image quality.

Doppler examinations of the AAo and MPV were performed at a Doppler frequency of 3.5 MHz. The sample window was obtained anywhere along the length of the AAo cranial to the origin of the left renal artery. Sample window for the MPV was obtained at the best location within the vessel, which was typically immediately caudal to the liver, a point at which a long axis vessel-beam intercept angle of 60° could be obtained by use of the intercostal space. Evaluation of the CMA, CA, and HSA were performed at a Doppler frequency of 5.2 MHz, although we also used a frequency of 3.5 MHz for the CMA and CA. The sample window for the CMA or CA was obtained within each vessel approximately 5 mm from the vessel's origin from the aorta. For the HSA, the sample window was obtained approximately 5 mm from the splenic hilus, within or outside the parenchyma. Use of a 7.5-

MHz frequency for B-mode examinations and color Doppler ultrasonography facilitated the determinations for the sample windows.

In the AAo and MPV, the one cursor of the Doppler gate was placed close to an inner surface of the vessel wall and the second on the opposite surface as a modification of the technique of uniform insonation.[28] This maintained the size of the sample window within at least two thirds of the vessel diameter and avoided wall artifacts or spectral contamination from adjacent vessels. In the CMA, CA or HSA, the cursors were oriented transversely across the vessel diameter as it coursed toward the transducer. In all vessels, except for the HSA, vessel-beam alignment was subjected to an angle-correction procedure before the spectral tracing was recorded. Angle correction was assisted by manual adjustment of the transducer and the electronic steering capacity of the linear-array transducer. The vessel-beam angle was recorded. Machine settings were optimized for high-sensitivity imaging in the Doppler mode. In 1 animal, heart rate (HR) could not be determined during the control period because the dog was intolerant to the placement of ECG pads. In addition, the HR, together with Doppler measurements of the CA and HSA were not obtained in 1 dog each, and of the MPV were not obtained in 4 dogs for various reasons discussed later.

3.3.5 Data analysis—Abdominal organs were subjectively evaluated by use of B-mode ultrasonography. Measurement of the thickest area of the spleen was used to estimate its size. Echogenicity of the spleen, liver, and kidneys was subjectively compared with each other. Diameter of the largest branch of the splenic vein in the body of the spleen was measured at the splenic hilus (long-axis view) and the cross-sectional area calculated. The largest cross-sectional area of the MPV was obtained by cine looping an image (short-axis view) and measuring it by use of the elliptical program of the onboard computer. This minimized errors attributable to variation in the cross-

sectional area with time caused by respiration. Doppler spectra of each vessel were evaluated for flow patterns with the use of a concurrent ECG. The instantaneous HR for each Doppler cycle was computed from the preceding R–R interval on the ECG. Because an R–R interval is the number of milliseconds that elapses during 1 cardiac cycle, the total number of cardiac cycles (ie, HR) that would be completed within 1 minute (ie, 60,000 ms) on the basis of this interval was computed as HR = 60,000/R–R interval.

During each experiment, measurements were obtained from spectral cycles whose preceding R–R intervals were approximately equal, excluding obvious sinus arrhythmias. Values recorded for HR, PI, RI, PSV, and TAV_{mean} and MPV peak velocity (PV), TAV_{mean}, blood flow, and CI were obtained by averaging 3 measurements or calculations from 3 ECG or spectral Doppler cycles. Doppler variables were measured by use of the onboard computer.

Pulsatility index was determined by use of the following equation[29]:

$$PI = (PSV - \text{end diastolic velocity})/TAV_{mean}$$

Resistive index was determined by use of the following equation[29]:

$$RI = (PSV - \text{end diastolic velocity})/PSV$$

Blood flow was computed by use of the following equation[30]:

$$\text{Blood flow} = \text{cross-sectional area} \times TAV_{mean}$$

Congestion index was calculated by use of the following equation[31]:

$$CI = \text{cross-sectional area}/TAV_{mean}$$

Results of each experiment were entered into a computer spreadsheet program[b] on a personal computer. All ultrasonographic procedures were recorded on videotape for possible reevaluation and future reference. All data were tested for normality by use of the Shapiro-Wilk test. Values of data

that were normally distributed were reported as mean ± SD, and those that were not normally distributed were reported as median and range. Values for Doppler variables for dogs in each anemic state were compared with the value for the physiologic (control) state by use of paired *t* tests for data that were normally distributed or the Wilcoxon signed-rank test for data that were not normally distributed. Differences were considered to be significant at $P \leq 0.05$. A statistical software program[c] was used to perform the data analysis.

3.4 RESULTS

3.4.1 Severe acute anemia—Mean ± SD Hct was 16.0 ± 0.77% after blood removal for 3 to 5 days. Dogs were lethargic, and a few had a reduced appetite during a 12-hour period. Dogs had extremely pale mucous membranes and a fast and weak pulse, but rectal temperature was within the reference range. The spleen was significantly ($P = 0.005$) thinner (mean thickness was 17.0 ± 1.9 mm and 13.9 ± 0.5 mm for the control state and severe anemia, respectively [18.1%]; Figure 3.1). Subjectively, splenic echogenicity was frequently increased. There was a significant reduction ($P = 0.025$) in mean cross-sectional area of the HSV (control state, 0.046 ± 0.021 mm^2; severe anemia, 0.024 ± 0.009 mm^2; [47.8%]). There was no significant change in mean cross-sectional area of the MPV. There was a significant increase in mean HR for all observations during severe anemia (25.2% to 70.1%; Figure 3.2, Table 3.1).

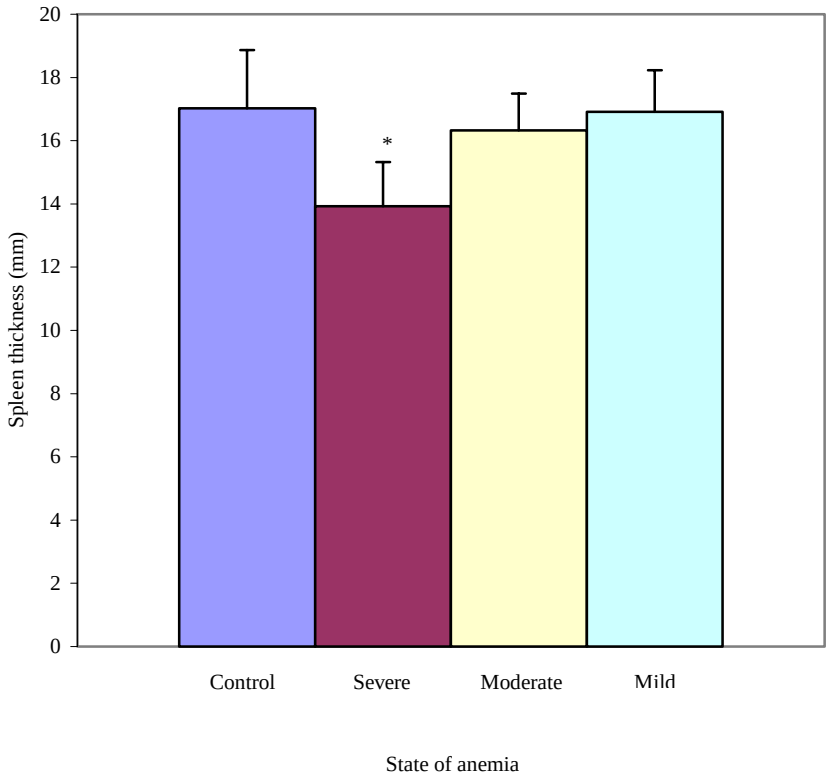

Figure 3.1—Mean ± SD splenic thickness in dogs before removal of blood to create anemia (control state), after removal of blood to create severe anemia, and during moderate and mild anemia in the recovery period. *Value differs significantly (P = 0.005) from the value for the control state.

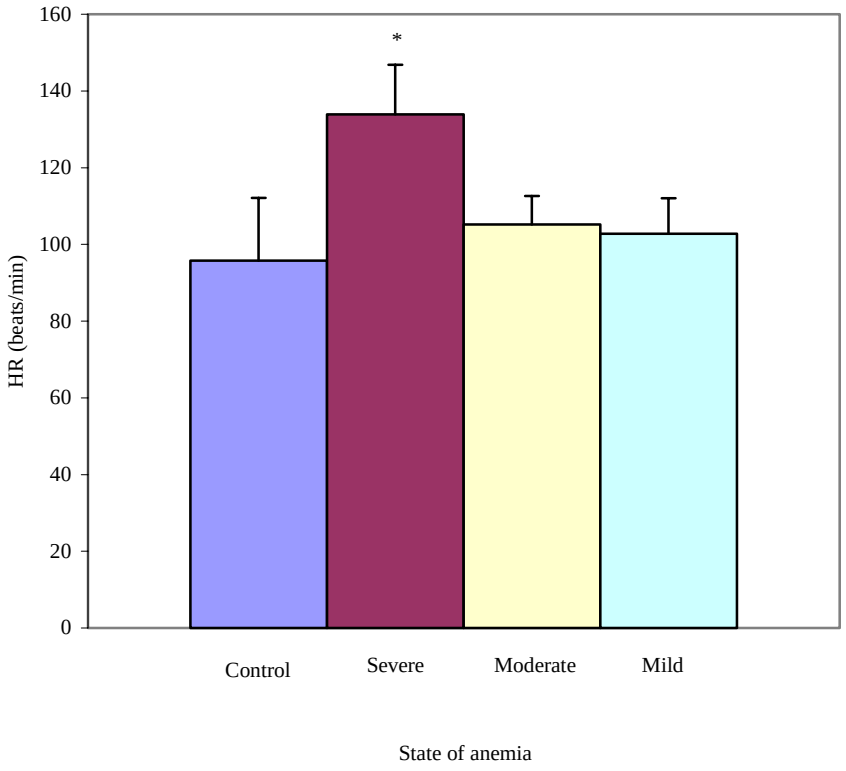

Figure 3.2—Mean ± SD heart rate (HR) in dogs during various states of anemia. * Value differs significantly ($P < 0.001$) from the value for the control state.

Spectral Doppler patterns of the AAo, CMA, CA, and MPV during severe anemia resembled the corresponding patterns for clinically normal dogs described elsewhere.[32] However, adjacent arterial systolic peaks were more regularly and closely spaced (Figures 3.3 and 3.4). The overall duration of the cardiac cycle, in particular that of the diastolic phase was remarkably shortened. Frequently, a single conical velocity pattern was the only feature that formed the diastolic segment of the Doppler spectrum because any extra horizontal or conical segment had been lost. In 1 case, only half of a cone representing an increasing diastolic velocity remained toward the end of the diastolic phase; therefore, a biphasic (instead of triphasic) velocity pattern was seen in the aortic Doppler spectrum. A triphasic velocity pattern was seen less frequently in the CMA spectrum of anemic dogs than in that of control dogs.

We detected a significant increase in mean PSV (AAo, 45.8%; CMA, 56.1%; and CA, 41.9%), in mean PV (MPV, 84.2%) and in mean TAV_{mean} (AAo, 69.4%; CMA, 64.3%; CA, 29.7%; and MPV, 76.9%; Figure 3.5). A significant decrease in mean PI was seen only in the AAo (20.5%) and HSA (19.3%), whereas mean PI in the CMA and CA was unchanged (Figure 3.6). No significant change was found in mean RI of any artery. Mean CI was significantly reduced (45.2%). Portal blood flow increased by 67.7%, although this was not a significant change.

3.4.2 Moderate anemia—Mean ± SD Hct was 26.3 ± 0.74% after dogs were allowed to recover for 5 to 7 days. Dogs were active and physically strong. Mucous membranes were pale to pale-pink, and pulse was slightly weak and fast. Rectal temperature was within the reference range. Splenic echogenicity was subjectively increased, but we did not detect a significant change in splenic thickness or cross-sectional area of the HSV or MPV. Significantly higher mean HR was observed during some measurements (20%; Table 3.1).

Table 3.1—Comparison of heart rate and Doppler variables for the abdominal aorta and splanchnic vessels in 11 Beagles during various states of experimentally induced anemia.

		Control state		Severe anemia			Moderate anemia			Mild anemia		
Vessel	Variable	Mean ± SD	n	Mean ± SD	*P**	n	Mean ± SD	*P**	n	Mean ± SD	*P**	n
	HR (beats/min)	103.3 ± 19.8	10	136.2 ± 18.7	< 0.001	10	110.7 ± 10.7	0.225	10	105.9 ± 10.5	0.796	10
	PSV (cm/s)	127.1 ± 33.7	11	185.3 ± 40.4	0.002	11	149.1 ± 24.0	0.074	11	145.7 ± 29.4	0.077	11
AAo	TAV_{mean} (cm/s)	22.9 ± 7.6	11	38.8 ± 11.8	0.003	11	33.8 ± 3.3	0.002	11	32.6 ± 5.5	0.002	11
	PI	3.22 ± 0.91	11	2.38 (2.04–3.51)†	0.033	11	2.47 ± 0.49	0.059	11	2.23 (2.13–3.20)†	0.006	11
	RI	0.84 ± 0.04	11	0.84 ± 0.04	0.665	11	0.82 ± 0.04	0.341	11	0.83 ± 0.02	0.756	11
	HR (beats/min)	106.6 (57.0-117.6)†	10	133.5 ± 12.1	0.005	10	108.0 ± 11.4	0.475	10	114.7 (87.8–124.1)†	0.445	10
	PSV (cm/s)	103.4 ± 20.2	11	161.4 ± 17.2	< 0.001	11	123.9 ± 19.8	0.012	11	114.3 ± 14.0	0.182	11
CMA	TAV_{mean} (cm/s)	21.0 ± 5.8	11	34.5 ± 6.4	< 0.001	11	31.4 ± 7.8	0.003	11	29.4 ± 5.0	0.003	11
	PI	2.66 ± 0.63	11	2.08 (1.78–3.61)†	0.110	11	2.10 ± 0.56	0.017	11	2.01± 0.31	0.004	11
	RI	0.82 ± 0.04	11	0.83 ± 0.04	0.577	11	0.81 (0.69–0.87)†	0.449	11	0.79 ± 0.03	0.030	11
	HR (beats/min)	96.7 ± 16.2	10	137.4 (99.4–142.9)†	0.005	10	114.0 (86.1–118.4)†	0.028	10	106.7 ± 13.7	0.178	10
	PSV (cm/s)	115.2 ± 27.8	11	163.5 ± 34.6	0.002	11	129.9 ± 17.9	0.080	10	112.6 ± 17.0	0.747	11
CA	TAV_{mean} (cm/s)	25.9 ± 9.0	11	33.6 ± 6.2	0.015	11	30.8 (27.0–46.3)†	0.028	10	26.8 ± 5.3	0.762	11
	PI	2.25 ± 0.51	11	2.23 ± 0.52	0.950	11	1.78 ± 0.27	0.024	10	2.03 ± 0.47	0.388	11
	RI	0.79 ± 0.04	11	0.82 ± 0.06	0.102	11	0.75 ± 0.04	0.041	10	0.78 ± 0.06	0.756	11
	HR (beats/min)	91.9 ± 22.7	9	133.7 ± 14.0	0.001	9	94.2 ± 12.4	0.833	9	104.7 ± 23.6	0.298	9
HSA	PI	1.35 ± 0.45	10	1.09 ± 0.25	0.044	10	1.11 ± 0.22	0.172	10	1.07 ± 0.21	0.040	10
	RI	0.66 ± 0.10	10	0.64 ± 0.07	0.638	10	0.63 ± 0.04	0.568	10	0.62 ± 0.09	0.259	10
	HR (beats/min)	81.1 ± 20.1	7	138.5 ± 22.0	0.002	7	96.3 ± 15.6	0.245	7	80.2 ± 18.5	0.790	7
	PV (cm/s)	19.0 (15.1-45.7)†	9	42.0 ± 14.8	0.005	9	34.5 ± 16.5	0.079	9	22.7 ± 9.2	0.986	9
MPV	TAV_{mean} (cm/s)	10.6 ± 2.8	9	19.1 ± 7.3	0.017	8	18.7 ± 8.8	0.034	9	13.5 ± 3.8	0.059	7
	BF (mL/min/kg)	36.6 ± 13.0	9	61.2 ± 39.7	0.123	8	65.1 ± 36.3	0.048	9	46.4 ± 21.4	0.137	7
	CI	0.066 ± 0.019	9	0.034 ± 0.013	0.010	8	0.044 ± 0.021	0.057	9	0.051± 0.016	0.097	7

The Hct for the various states of anemia were as follows: control state, 45% to 52%; severe anemia, 15% to 17%; moderate anemia, 25% to 27%; and mild anemia, 31% to 37%. *For each variable, *P* values represent comparison with the control state; values were considered significant at $P \leq 0.05$. †Values reported are median (range) because the data were not normally distributed as determined by use of the Shapiro-Wilk test. AAo = Abdominal aorta. CMA = Cranial mesenteric artery. CA = Celiac artery. HSA = Hilar splenic artery. MPV = Main portal vein. HR = Heart rate. PSV = Peak systolic velocity. PV = Peak velocity. TAV_{mean} = Time-averaged mean velocity. BF = Blood flow. PI = Pulsatility index. RI = Resistive index. CI = Congestion index. Number of dogs may be < 11 because of ECG malfunction, gastrointestinal gas, excessive splenic mobility, or the fact that evaluations were not performed because of time constraints.

Arterial and portal vein spectral Doppler patterns were similar to corresponding patterns described elsewhere in clinically normal dogs.[32] A significant increase in mean PSV persisted only in the CMA (19.8%), whereas the AAo, CA, and MPV did not have significant changes (Table 3.1). Mean TAV_{mean} remained significantly higher in all vessels (AAo, 47.6%; CMA, 50.0%; CA, 26.7%; and MPV, 76.4%). There was significant reduction in mean PI of the CMA (21.2%) and CA (21.0%), however, there was no significant change in mean PI of the AAo or HSA. Mean RI of the CA (4.8%) was significantly reduced, but we did not detect a change in mean RI of the AAo, CMA, or HSA. There was a significant increase in mean portal blood flow (77.9%) but no significant change in mean CI.

3.4.3 Mild anemia—Mean ± SD Hct was 34.4 ± 1.9% after dogs were allowed to recover for 12 to 16 days. Dogs were active and physically strong. Mucous membranes were pale to pale-pink. Pulse and rectal temperature were within the reference ranges. Splenic echogenicity was still subjectively increased. Arterial and venous Doppler spectra were similar to those obtained during the control state.

Mean TAV_{mean} remained significantly increased in the AAo (42.8%) and CMA (40.0%), but there was no significant change in the CA or MPV (Table 3.1). Significant reduction in mean PI was evident in the AAo (24.0%), CMA (24.5%), and HSA (21.2%) but not in the CA. Mean RI of the CMA (3.7%) was significantly lower while there was no change in the AAo, CA or HSA. No significant change was detected in splenic size, HR, or PSV, PV, CI, blood flow, or CSA in any vessel.

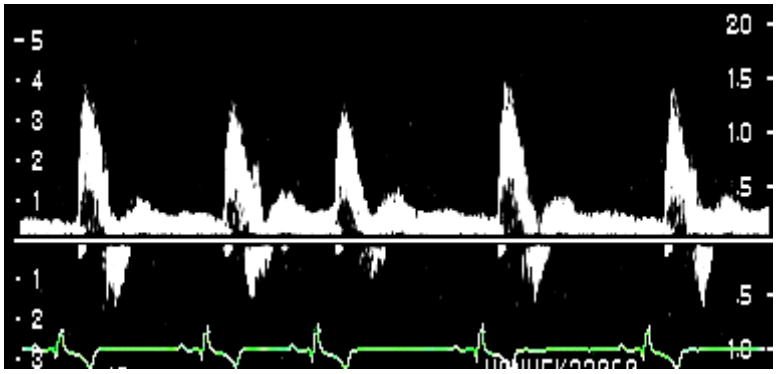

Figure 3.3—Doppler spectrum of the abdominal aorta obtained from a position cranial to the origin of the left renal artery in a clinically normal Beagle. Notice the reverse flow in early diastole followed by a peak forward flow. Forward diastolic flow continues after the peak, diminishing gradually over time. Flow velocity in early diastole defined a conical outline, followed by a horizontal outline from mid- to end diastole. Heart rate was 67 beats/min.

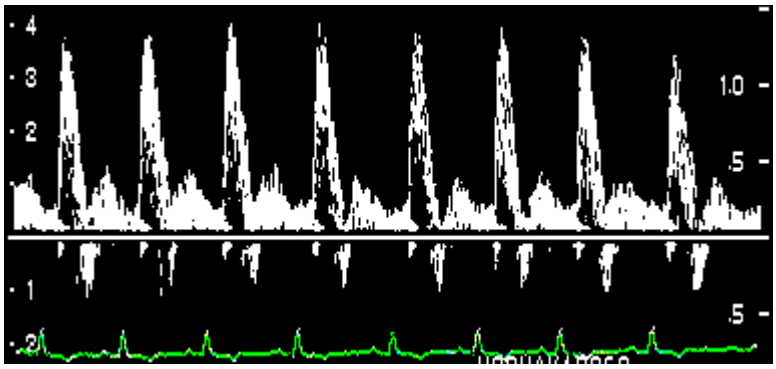

Velocity (M/s)

0 Time (milliseconds) 4

A.

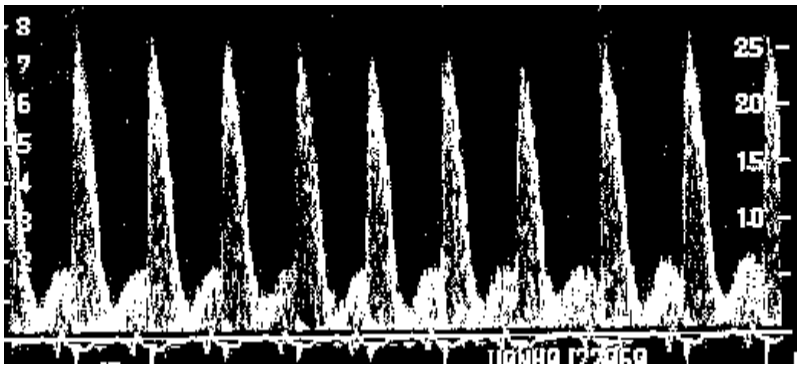

Velocity (M/s)

0 Time (milliseconds) 4

B.

Figure 3.4—Doppler spectrum of the abdominal aorta obtained from a position cranial to the origin of the left renal artery in a Beagle during experimentally induced severe anemia. In panel A, notice the closely spaced systolic peaks and loss of the horizontal segment in the mid- to late diastolic wave. In panel B, notice the lack of reverse flow in early diastole in addition to the closely spaced systolic peaks. Only half a cone represents the early diastolic wave, with the next systolic peak beginning at peak diastolic flow. Heart rate was 114 and 171 beats/min for panels A and B, respectively.

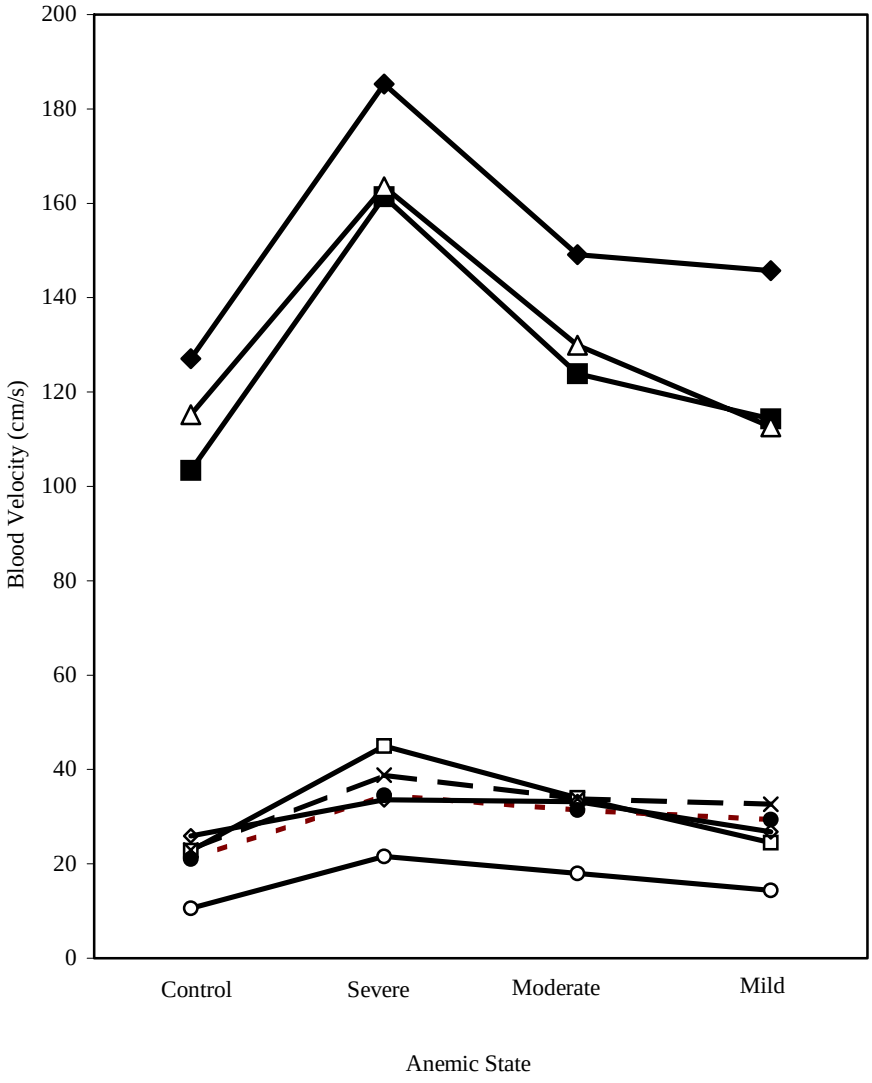

Figure 3.5—Mean ± SD peak systolic velocity in the abdominal aorta (solid diamond), cranial mesenteric artery (solid square), and celiac artery (open triangle); peak velocity in the main portal vein (open square), and time-averaged mean velocity in the abdominal aorta (cross), cranial mesenteric artery (solid circle), celiac artery (open diamond) and main portal vein (open circle) in dogs during various states of anemia. *See* Figure 1 for remainder of key.

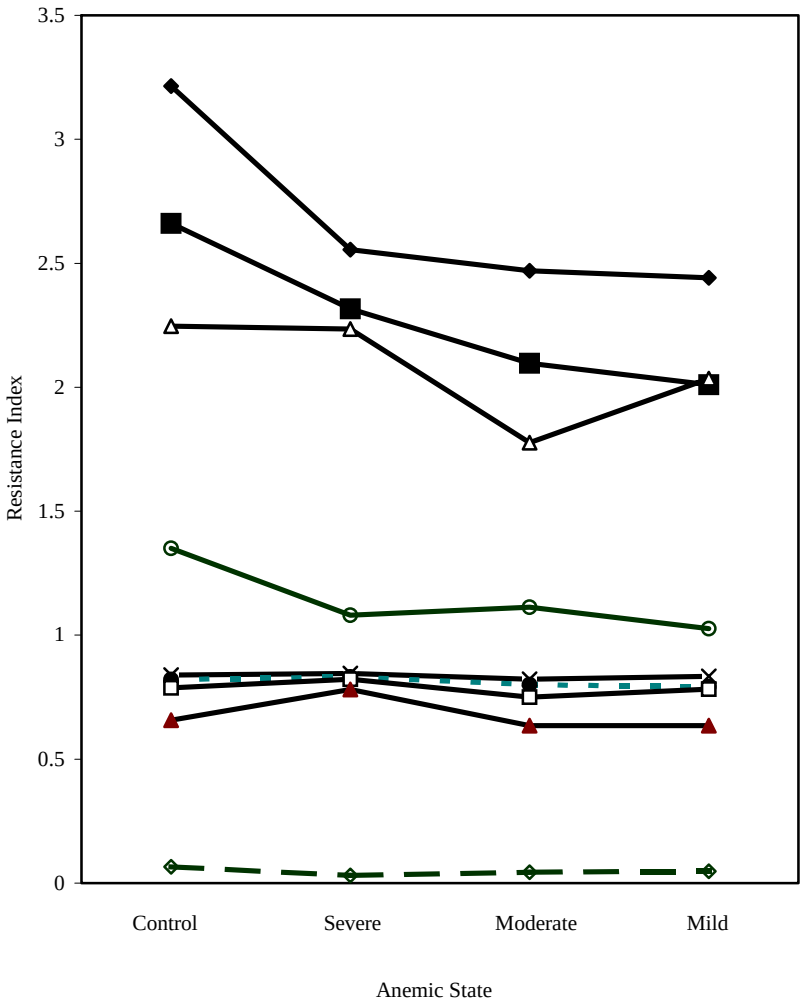

Figure 3.6—Mean ± SD pulsatility index for the abdominal aorta (solid diamond), cranial mesenteric artery (solid square), celiac artery (open triangle), and hilar splenic artery (open circle); resistive index for the abdominal aorta (cross), cranial mesenteric artery (solid circle), celiac artery (open square), and hilar splenic artery (solid triangle); and congestion index for the main portal vein (open diamond) in dogs during various states of anemia. *See* Figure 1 for remainder of key.

3.4.4 All anemic states—A significant increase in HR was consistent for all observations during severe anemia, but was evident in only about 20% of the observations during moderate anemia, and HR did not change significantly during mild anemia. Heart rate progressively decreased from the highest values during severe anemia toward the baseline value during mild anemia. Changes in peak velocities almost paralleled those of HR. Peak systolic velocity of all arteries and PV of the portal vein were significantly increased during severe anemia, was significantly increased only in the CMA during moderate anemia, and thereafter progressively returned toward values similar to those of the control state during mild anemia. The TAV_{mean} values of all vessels were significantly higher during all states of anemia, except in the CA and MPV in which no significant change was detected during mild anemia. This variable had a consistent pattern and decreased progressively from a high level during severe anemia toward baseline values during mild anemia.

With regard to the Doppler indices of vascular resistance, significant changes varied on the basis of the particular index, vessel, and degree or duration of anemia. A significant reduction in PI was seen during severe and mild states of anemia in the AAo and HSA; during moderate and mild anemia in the CMA; and only during moderate anemia in the CA. A significant reduction in RI value was observed in the CMA during mild anemia and in the CA during moderate anemia. No significant change in RI was found in the AAo or HSA during any state of anemia. Portal vein CI was significantly lower during severe state of anemia but not during moderate or mild anemia. Patterns of change in PI and RI values also varied among vessels, although values were generally lower for PI and RI during mild anemia than during severe anemia (Table 3.1).

3.5 DISCUSSION

Analysis of the results reported here provides evidence of significant changes in various Doppler variables among vessels during severe anemia as well as during moderate and mild anemia. There was a significant increase in TAV_{mean} (mean flow velocity) for all states of anemia and in all vessels that were evaluated, except in the CA and MPV during mild anemia. On the other hand, significant increases in arterial PSV or portal vein PV was found only during severe anemia, except in the CMA during moderate anemia when a significant increase persisted. Current knowledge on relationships between Doppler variables and anemia is based on results for fetal anemia in humans attributable to RBC alloimmunization or parvovirus infection. Findings of the study reported here correlate with observations of the human fetus during severe anemia in which significant increases of peak and mean blood flow velocities of various vessels have been reported.[7-12]

Analysis of results of the study reported here also indicates a significant increase in portal blood flow during moderate anemia. Although specific reference to the portal vein was not found, this result corroborates with findings in other vessels by noninvasive hemodynamic studies of human patients[6] and by invasive studies of animals[1,2] with anemia. Doppler evaluations in human fetuses with severe anemia have revealed significant increases in blood flow of the umbilical vein.[6] Similar observations were made by use of invasive techniques in dogs with normovolemic anemia that reportedly caused an increased blood flow in the AAo and various splanchnic vessels or vascular beds during severe anemia[1,2]. Failure to detect a significant change during severe, moderate or mild states of anemia in the study reported here may have been attributable to a small sample.

Few Doppler evaluations conducted in human fetuses with anemia have investigated vascular resistance by use of PI or RI. No significant change has been found in PI or RI of the umbilical or uterine artery,[7,33] but RI of the splenic artery in hydropic fetuses (severe anemia) is significantly increased.[d] The increase in splenic RI is believed to be attributable to congestion of the splenic capillary bed with trapped RBCs.[d] Analysis of results of our study revealed a reduction in vascular resistance during severe anemia in the AAo, HSA, and MPV as indicated by a significant reduction in PI or CI. A reduction in vascular resistance in the CMA and CA was detected later, indicated by a significant reduction in PI or RI. The reason for this delayed reduction in resistance is not clear, but it may have been associated with redistribution of blood from the splanchnic bed during the acute onset of severe anemia. A variation was also observed with regard to the specific resistance index that changed in response to anemia. A significant reduction in PI was the major finding, whereas a reduction in RI was seen in fewer instances (CMA and CA).

Arterial flow velocity and direction is sensitive to peripheral vascular resistance.[34] When resistance is decreased, forward flow velocity is increased and reverse flow velocity is decreased in a linear relationship, and vice versa.[34] In the study reported here, the transformation of an aortic or CMA velocity pattern from triphasic to biphasic, increase of systolic and diastolic velocities, and increase in TAV_{mean} support observations of other investigators. A significant increase in portal vein TAV_{mean} with no change in cross-sectional area resulted in a significant reduction in CI, further suggesting that flow resistance by the portal vein was also reduced.

Two mechanisms are probably involved in the reduction of vascular resistance. First, a reduction in RBC mass leads to a significant decrease in blood viscosity in dogs.[3] Second,

reduced hemoglobin content during anemia results in increased activity of endothelial-derived relaxing factor (ie, nitric oxide), leading to arteriolar vasodilation.[35,36] Theoretically, increased perfusion pressure or blood volume can cause similar changes in vascular resistance and blood velocity, although a significant change in mean arterial pressure was not found in patients with normovolemic or hypervolemic anemia.[35] There is no evidence to suggest that the circulating blood volume or arterial pressure of the subjects increased in the dogs of our study; however, caution should be exercised in interpreting the results because these variables were not measured.

A remarkable degree of regularity and shortening in R–R intervals during severe anemia, correlating with a regular cardiac rhythm and significant increase in HR, was found in the dogs of our study. With the exception of approximately 20% of the observations during moderate anemia, these changes did not persist beyond the severely anemic state. An echocardiographic study evaluating left ventricular function performed in the same dogs revealed a significant increase in cardiac output, fractional shortening, ejection fraction, and HR during the severely anemic state (data not shown). The observation conforms to findings of other investigations that used invasive techniques and revealed an increase in HR[2,35] and cardiac output[1,3] as components of the hyperdynamic cardiovascular response during acute and chronic severe normovolemic anemia in dogs. Increased cardiac output has also been documented in humans with severe chronic anemia.[36] In 1 study,[35] investigators found that an increase in HR provided a greater contribution to an increase in cardiac output, compared with the contribution provided by an increase in stroke volume. However, in hemodilution experiments in which dextran or other similar fluids were exchanged for blood without a volume deficit, a hyperdynamic state was created without any significant change in HR.[4] It is believed that the increase in cardiac output in severe anemia is the result of reduced total systemic

vascular resistance resulting in increased venous return.[35] Heart rate reportedly influences Doppler variables.[37, 38] In 1 study, [38] investigators found an inverse relationship between HR and PI of the descending aorta and other arteries in growth-retarded human fetuses. Significant reduction in PI of the AAo and HSA was seen in the study reported here, with a significant increase in HR in severely anemic dogs. However, although HR began to return to normal values, and HR during the moderately anemic state was no longer significantly different from that during the control state, PI values decreased still further and were significantly lower during moderate (CMA, CA) and mild (AAo, CMA, HSA) states of anemia. In human fetuses from hypertensive pregnancies and in patients who had renal allografts with acute rejection, investigators did not find significant changes in PI values following correction for low HRs.[39] The increase in HR in our study may have contributed, as a function of severe anemia, to changes in absolute values of some Doppler variables, but it cannot account for the general pattern of other observed changes.

A significant reduction in splenic thickness and cross-sectional area of the HSV during severe acute anemia suggests contraction of the spleen and veins that drain it. It is recognized that the venous system, including splanchnic beds in the intestines, liver, and spleen, forms a large reservoir of blood volume with a capacity for rapid response.[40-42] A decrease in circulating blood volume or blood pressure evokes immediate, diffuse sympathetic discharge, probably from various afferent locations including the cardiopulmonary area and baroreceptors in the aortic and carotid sinuses, leading to venocontraction.[40,42] Venous wall tension increases promptly and progressively during hemorrhage, remains increased as long as there is a volume deficit, and decreases promptly after restoration of normal blood volume.[40] The venous reservoir is believed to accommodate up to 70% of blood volume and is effective in stabilizing circulating volume during conditions of moderate volume depletion.[40] In dogs, the splanchnic

bed can decrease its blood volume by up to 50% and the spleen has the greatest capacity to release blood, compared with the liver and intestines.[40,42] Splenic blood is also more viscous because of a higher percentage of RBCs.[41] On the basis of observations of other investigators, it has been suggested that a decrease in blood volume during the short time lag between blood removal and volume replacement in the study reported here triggered reflex contraction of the venous system. No significant change was seen in cross-sectional area of the MPV during any state of anemia, indicating a normal circulating blood volume. Significant reduction in splenic size and cross-sectional area of the HSV observed during the severely anemic state may have been attributable to depletion of stored RBCs. The spleen gradually regained size, probably as a result of an enhanced erythropoiesis, which was evidenced by increased numbers of reticulocytes, thus making available a reserve of RBCs for storage. Splenic thickness during the moderately anemic state was no longer significantly different from that for the control state.

It is possible that assumptions made for, and methods used in, our study may have introduced errors in the results that we considered insignificant. Examinations and measures obtained on dogs before commencement of experiments were considered adequate, and all dogs were considered to be in good health with normally functioning organs. Specific tests for organ function, such as glomerular filtration rate or plasma erythropoietin concentrations for the kidneys, were not conducted because of financial limitations. For a similar reason, a rather small sample was used in the study. This may have contributed to failure to detect significant changes, especially those with marginal significance. Measurements to confirm normal circulating blood volume and arterial pressure were not performed following induction of anemia because the study was designed along a clinical line intended to conform, as much as possible, to routine clinical practice at our facility. A deficit in circulating volume or arterial pressure would decrease blood flow and flow velocities and increase values of resistive

indices.[43] There was no evidence to suggest that dogs had such a deficit. Instead, lack of a significant reduction in cross-sectional area of the portal vein suggested that there was a normal circulating blood volume during all anemic states.

The large number of vessels examined, including those whose data were not reported here, the need for a precise sample collection technique, and differences in patient cooperation resulted in time constraints that may have influenced accuracy of certain measurements. In 1 dog, HR could not be determined during the control state because the dog would not tolerate placement of ECG pads. In addition, the HR, together with Doppler measurements of the CA and HSA were not done in 1 dog each, and of the MPV in 4 dogs because of various reasons. In the case of the CA, it was obscured by gastrointestinal gas. Examination of the HSA represented a special problem because the spleen moved constantly during normal respiratory excursions. Splenic mobility worsened in dogs that struggled. For these conditions, it was impossible to obtain good spectral tracings because the splenic artery was oscillating in and out of the sample window. Obtaining 3 consecutive cycles of the Doppler spectrum of the HSA was particularly difficult. Sometimes we obtained only 1 cycle of the spectrum with varying intensity or even an incomplete cycle of the spectrum. A poor spectral tracing may yield inaccurate measurements of Doppler variables.[44]

The MPV was usually evaluated last, and it was evaluated in fewer dogs because of time constraints. Additionally, examining the MPV required considerable effort when manipulating the transducer within a limited intercostal space to obtain an optimal insonation angle. The procedure was often uncomfortable to the dogs, forcing them to move. Vessel movements also were evident with respiration, and vessels sometimes were obscured by gastrointestinal gas.

Other limitations, and sources of systematic and random errors encountered with Doppler hemodynamic measurements despite technologic advancements in ultrasound equipment include estimation of vessel cross-sectional area, angle of insonation, and mean velocity from which Doppler blood flow measurements are derived.[28,29,39,43] In the study reported here, estimation of cross-sectional area was required for measurement of portal vein blood flow and CI. The problem of small vessel size was not encountered, and there was good resolution of the inner circumference of the MPV in the cross-sectional view. However, the MPV was not perfectly circular in cross section, and its diameter varied with respiratory movements, and gas from the stomach or lungs sometimes made viewing difficult. The technique used in this study for estimating portal cross-sectional area may have resulted in overestimation of blood flow and CI of the MPV because the true mean cross-sectional area would have been less than the estimated value.

Cross-sectional area of the HSV was estimated only for comparison of vessel size between control and anemic states. Cross-sectional area was calculated from the diameter measured by use of a long-axis view because it was difficult to obtain images of the vessel in a short-axis view.

Variation was evident between 0^{o} and 60^{o} for the estimated intersection angle between the ultrasound beam and long axis of each vessel when obtaining a Doppler spectrum. Moreover, it was unlikely that the scan plane and long-axis plane of a vessel were always aligned when estimating the insonation angle.[28] Random and systematic errors in estimation of the insonation angle may have contributed to variation in estimating angle and blood flow velocities. The modified technique of uniform insonation used in the study reported here may have further

resulted in overestimation of TAV_{mean} and blood flow because some low-velocity components of flow may have been excluded.

Despite the assumptions and modifications made in measurements and limitations of the DUS technique, the changes reported in this study appear to reflect the true influence of normovolemic anemia on Doppler variables. Collection of data from a homogenous population by the same investigator and use of the same machine for all evaluations greatly minimized variations attributable to those factors. However, caution should be exercised for use of these data because they are likely to vary with the study population, equipment, and techniques used.

Noninvasive Doppler ultrasonography documented hyperdynamic circulation in the AAo and splanchnic vessels in dogs with experimentally induced normovolemic anemia. Analysis of the results indicates that anemia significantly reduces arterial and venous DUS resistance indices and increases blood velocities and blood flow. This should be taken into consideration when interpreting results of DUS investigations of any physiologic or pathologic state with concurrent anemia. Lack of DUS evidence of abdominal splanchnic hyperdynamic circulation or evidence of a change in the opposite direction (eg, an increase in RI or PI) in dogs with conditions that have coexisting anemia, such as babesiosis, should raise the suspicion for other important pathologic processes.

3.6 FOOTNOTES

[a]Sonoline Omnia, Siemens Medical Systems Inc, Ultrasound Group, Erlangen, Germany.

[b]MS Excel, Microsoft Corp, Redmond, Wash.

[c]Stata Release 7, Stata Press, College Station, Tex.

[d]Bahado-Singh R, Pirhonen J, Rahman F, *et al*. Effect of fetal anemia on splenic artery resistance index in red cell isoimmunization. *J Soc Gynecol Invest* 1995;2:146.

3.7 REFERENCES

1. Race D, Dedichen H, Schenk JWR. Regional blood flow during dextran-induced normovolemic hemodilution in the dog. *J Thorac Cardiovasc Surg* 1967;53:578–586.

2. Vatner SF, Higgins CB, Franklin D. Regional circulatory adjustments to moderate and severe chronic anemia in conscious dogs at rest and during exercise. *Circ Res* 1972;30:731–740.

3. Fowler NO, Holmes JC. Blood viscosity and cardiac output in acute experimental anemia. *J Appl Physiol* 1975;39:453–456.

4. Doss DN, Estafanous FG, Ferrario CM, *et al*. Mechanism of systemic vasodilation during normovolemic hemodilution. *Anesth Analg* 1995;81:30–34.

5. Grupp I, Grupp G, Holmes JC, *et al*. Regional blood flow in anemia. *J Appl Physiol* 1972;33:456–461.

6. Kirkinen P, Jouppila P, Eik-Nes SH. Umbilical vein blood flow in rhesus isoimmunization. *Br J Obstet Gynaecol* 1983;90:640–643.

7. Rightmire DA, Nicolaides KH, Rodeck CH, *et al*. Fetal blood velocities in Rh isoimmunization: relationship to gestational age and to fetal hematocrit. *Obstet Gynecol* 1986;68:223–226.

8. Mari G, Adrignolo A, Abuhamad AZ, *et al.* Diagnosis of fetal anemia with Doppler ultrasound in the pregnancy complicated by maternal blood group immunization. *Ultrasound Obstet Gynecol* 1995;5:400–404.

9. Cosmi E, Mari G, Chiaie LD, *et al.* Noninvasive diagnosis by Doppler ultrasonography of fetal anemia resulting from parvovirus infection. *Am J Obstet Gynecol* 2002;187:1290–1293.

10. Nishie EN, Brizot ML, Liao AW, *et al.* A comparison between middle cerebral artery peak systolic velocity and amniotic fluid optical density at 450 nm in the prediction of fetal anemia. *Am J Obstet Gynecol* 2003;188:214–219.

11. Bahado-Singh R, Oz U, Deren O, *et al.* Splenic artery Doppler peak systolic velocity predicts severe fetal anemia in rhesus disease. *Am J Obstet Gynecol* 2000;182:1222–1226.

12. Abdel-Fattah SA, Soothill PW, Carroll SG, *et al.* Middle cerebral artery Doppler for the prediction of fetal anemia in cases without hydrops: a practical approach. *Br J Radiol* 2002;75:726–730.

13. Taylor GA, Hudak ML. Color Doppler ultrasound changes in small vessel diameter and cerebral blood flow during acute anemia in the newborn lamb. *Invest Radiol* 1994;29:188–194.

14. Reyers F, Leisewitz AL, Lobetti RG, *et al.* Canine babesiosis in South Africa: more than one disease. Does this serve as a model for falciparum malaria? *Ann Trop Med Parasitol* 1998;92:503–511.

15. Newton CR, Marsh K, Peshu N, *et al.* Perturbations of cerebral hemodynamics in Kenyans with cerebral malaria. *Pediatr Neurol* 1996;15:41–49.

16. Wright IG, Kerr JD. Hypotension in acute *Babesia bovis* (*B. argentina*) infections of splenectomized calves. *J Comp Pathol* 1977;87:531–537.

17. Maegraith B, Gilles HM, Devakul K. Pathological processes in *Babesia canis* infections. *Z Tropenmed Parasitol* 1957;8:485–514.

18. Welzl C, Leisewitz AL, Jacobson LS, *et al.* Systemic inflammatory response syndrome and multiple-organ damage/dysfunction in complicated canine babesiosis. *J S Afr Vet Assoc* 2001;72:158–162.

19. Jacobson LS, Lobetti RG, Vaughan-Scott T. Blood pressure changes in dogs with babesiosis. *J S Afr Vet Assoc* 2000;71:14–20.

20. Kantrowitz BM, Nyland TG, Fisher P. Estimation of portal blood flow using duplex real-time and Doppler ultrasound imaging in the dog. *Vet Radiol Ultrasound* 1989;30:222–226.

21. Nyland TG, Fisher PE. Evaluation of experimentally induced canine hepatic cirrhosis using duplex Doppler ultrasound. *Vet Radiol* 1990;31:189–194.

22. Lamb CR, Mahoney PN. Comparison of three methods for calculating portal blood flow velocity in dogs using duplex Doppler ultrasonography. *Vet Radiol Ultrasound* 1994;35:190–194.

23. Mwanza T, Miyamoto T, Okumura M, *et al.* Ultrasonographic evaluation of portal vein hemodynamics in experimentally bile duct ligated dogs. *Jpn J Vet Res* 1998;45:199–206.

24. Szatmari V, Nemeth T, Kotai I, *et al.* Doppler ultrasonographic diagnosis and anatomy of congenital intrahepatic arterioportal fistula in a puppy. *Vet Radiol Ultrasound* 2000;41:284–286.

25. Riesen S, Schmid V, Gaschen L, *et al.* Doppler measurement of splanchnic blood flow during digestion in unsedated normal dogs. *Vet Radiol Ultrasound* 2002;43:554–560.

26. Kircher P, Lang J, Blum J, *et al.* Influence of food composition on splanchnic blood flow during digestion in unsedated normal dogs: a Doppler study. *Vet J* 2003;166:265–272.

27. Lobetti RG. The comparative role of hemoglobinemia and hypoxia in the development of nephropathy in the dog. *J S Afr Vet Assoc* 1996;67:188–198.

28. Gill RW. Measurement of blood flow by ultrasound: accuracy and sources of error. *Ultrasound Med Biol* 1985;11:625–641.

29. Nelson TR, Pretorius DH. The Doppler signal: where does it come from and what does it mean? *Am J Roentgenol* 1988;151:439–447.

30. Moriyasu F, Ban N, Nishida O, *et al.* Clinical application of an ultrasonic duplex system in the quantitative measurement of portal blood flow. *J Clin Ultrasound* 1986;14:579–588.

31. Moriyasu F, Nishida O, Ban N, *et al.* "Congestion index" of the portal vein. *Am J Roentgenol* 1986;146:735–739.

32. Szatmari V, Sotonyi P, Voros K. Normal duplex Doppler waveforms of major abdominal blood vessels in dogs: a review. *Vet Radiol Ultrasound* 2001;42:93–107.

33. Copel JA, Grannum PA, Belanger K, *et al.* Pulsed Doppler flow velocity waveforms before and after intrauterine intravascular transfusion for severe erythroblastosis fetalis. *Am J Obstet Gynecol* 1988;158:768–774.

34. Rittenhouse EA, Maixner W, Burr JW, *et al.* Directional arterial flow velocity: A sensitive index of changes in peripheral vascular resistance. *Surgery* 1976;79:350–355.

35. Glick G, Plauth WHJ, Braunwald E. Role of the autonomic nervous system in the circulatory response to acutely induced anemia in unanesthetized dogs. *J Clin Invest* 1964;43:2112–2124.

36. Anand IS, Chandrashekhar Y, Wander GS, *et al.* Endothelium-derived relaxing factor is important in mediating the high output state in chronic severe anemia. *J Am Coll Cardiol* 1995;25:1402–1407.

37. Yarlagadda P, Willoughby L, Maulik D. Effect of fetal heart rate on umbilical arterial Doppler indices. *Br J Surg* 1969;56:676–679.

38. Van den Wijngaard JAGW, van Eyck J, Wladimirroff JW. The relationship between fetal heart rate and Doppler blood flow velocity waveforms. *Ultrasound Med Biol* 1988;14:593–597.

39. Rasmussen K. Non-invasive quantitative measurement of blood flow and estimation of vascular resistance by the Doppler ultrasound method. *Dan Med Bull* 1992;11:625–641.

40. Dow RW, Fry WJ. Venous compensatory mechanisms in acute hypovolemia. *Surg Gynecol Obstet* 1967;September:511–515.

41. Chien S, Dellenback RJ, Usami S, *et al.* Blood volume, hemodynamic and metabolic changes in hemorrhagic shock in normal and splenectomized dogs. *Am J Physiol* 1973;225:866–879.

42. Carneiro JJ, Donald DE. Blood reservoir function of dog spleen, liver and intestine. *Am J Physiol* 1977;232:H67–H72.

43. Pozniak MA, Kelcz F, Stratta RJ, *et al.* Extraneous factors affecting resistive index. *Invest Radiol* 1988;23:899–904.

44. Halpern EJ, Deane CR, Needleman L, *et al.* Normal renal artery spectral Doppler waveform: a closer look. *Radiology* 1995;196:667–673.

CHAPTER 4

DOPPLER ULTRASONOGRAPHIC CHANGES IN THE CANINE KIDNEY DURING NORMOVOLAEMIC ANAEMIA

L.M. Koma, R.M. Kirberger, L. Scholtz

As accepted in December 2004 for publication by the Research in Veterinary Science

4.1 ABSTRACT

The haemodynamics of the canine left renal artery (LRA) and interlobar artery (ILA) were evaluated in eleven fasted, healthy, conscious beagles with severe acute (haematocrit [Hct] 16%), moderate chronic (Hct 26%) and mild chronic (Hct 34%) normovolaemic anaemia using Doppler ultrasound. Heart rate, peak systolic velocity (PSV), end diastolic velocity (EDV), time-averaged mean velocity (TAV_{mean}), pulsatility index (PI) and resistive index (RI) were recorded. Doppler values in the dogs following the induction of anaemia states were compared with corresponding values in the same dogs prior to the induction of anaemia.

Left renal artery mean PSV, mean PI and mean RI were significantly higher and mean EDV was significantly lower in severe acute anaemia. No significant change was seen in mean values of the same parameters in moderate and mild chronic anaemia. There was no significant change in TAV_{mean} of the LRA or mean PI and mean RI of the ILA in any grade of anaemia.

Acute, severe normovolaemic anaemia significantly altered LRA Doppler parameters in resting dogs without influencing those of the ILA. Moderate or mild chronic anaemia had no effect on any renal Doppler parameter.

Key words: anaemia model, canine, Doppler ultrasound, renal haemodynamics

4.2 INTRODUCTION

Non-invasive duplex Doppler ultrasound (DUS) has been used in various studies for investigating renal haemodynamic physiology in the dog (Abildgaard *et al.* 1997; Brown *et al.* 1997; Reid *et al.* 1980). Colour and power Doppler have been used for evaluation of the haemodynamic effects of pharmacological agents (Arger *et al.* 1999; Sehgal *et al.* 2001), toxicity and renal failure in native kidneys (Daley *et al.* 1994), and in acute renal allograft rejection (Takahashi *et al.* 1999). In both humans and animals, various Doppler parameters including blood flow (Reid *et al.* 1980), peak systolic velocity (PSV) (Gaschen *et al.* 2001; Pope *et al.* 1996), mean velocity (Okada *et al.* 2001), end diastolic velocity (Knapp *et al.* 1995), resistive index (RI) (Akihiro *et al.* 2001; Platt 1992; Pozniak *et al.* 1992; Sari *et al.* 1999), and pulsatility index (PI) (Miletic *et al.* 1998) were used to quantify renal haemodynamics. The RI of an intrarenal artery (interlobar or arcuate) probably gives the most reliable results (Knapp *et al.* 1995), and is the Doppler parameter most frequently used in clinical investigations of renal disease. In dogs, intrarenal RI has been used to detect and investigate haemodynamic changes in Addison's disease (Koch *et al.* 1997), renal toxicity (Rivers *et al.* 1996), obstruction (Dodd *et al.* 1991; Nyland *et al.* 1993) and renal failure of various causes (Morrow *et al.* 1996; Rivers *et al.* 1996; Rivers *et al.* 1997). It has also been used for evaluating the performance of renal transplants (Pozniak *et al.* 1992; Pozniak *et al.* 1988).

At the Onderstepoort Veterinary Academic Hospital, University of Pretoria, we are extending the use of DUS for investigating haemodynamic changes in canine babesiosis. About 31% of babesiosis cases presented to the hospital are clinically severe, with complications that are difficult to predict presenting therapeutic challenges (Reyers *et al.* 1998). Renal involvement in babesiosis is well recognised, with clinical signs of dysfunction or even acute renal failure

(Lobetti and Jacobson 2001; Maegraith *et al.* 1957; Malherbe 1966). The underlying pathological mechanism is poorly understood, but it is thought to be associated with reduced renal blood flow (Maegraith *et al.* 1957; Malherbe 1966). The occurrence of systemic hypotension in some cases of severe canine babesiosis has also been reported (Freeman *et al.* 1994; Jacobson *et al.* 2000). However, currently there is no clinical technique for rapidly demonstrating the presence of renal haemodynamic disturbance. It has been suggested that the pathogenesis of renal disease in canine babesiosis and human falciparum malaria may be similar (Clark and Jacobson 1998; Malherbe 1966). In complicated human falciparum malaria, renal dysfunction or acute renal failure can occur (Sitprija *et al.* 1967; Sitprija *et al.* 1977; Stone *et al.* 1972). Decreased mean arterial pressure due to vasodilatation in the acute phase of malaria, and renal hypoperfusion has been observed in some patients with or without acute renal failure (Eiam-ong and Sitprija 1998; Sitprija 1971; Sitprija *et al.* 1975; Sitprija *et al.* 1996).

Anaemia is frequently encountered in canine babesiosis (Reyers *et al.* 1998). Several investigators have suggested that relationships between anaemia and renal haemodynamics in the dog is characterised by significantly increased renal blood flow and reduced vascular resistance, both in severe acute (Grupp *et al.* 1972; Race *et al.* 1967; Schrier and Earley 1970) and severe chronic (Vatner *et al.* 1972) anaemia. All these studies, done more than 30 years ago, measured renal blood flow by means of in-dwelling Doppler ultrasound, electromagnetic flowmeter or by a dye dilution and clearance technique, and obtained vascular resistance as a division of arterial pressure gradient by the blood flow (Grupp *et al.* 1972; Race *et al.* 1967; Schrier and Earley 1970; Vatner *et al.* 1972).

In the limited renal haemodynamic studies using non-invasive DUS, Pozniak *et al.* (1988) reported an elevation of the intrarenal RI in hypotension (hypovolaemic anaemia) in the dog.

The effect of normovolaemic anaemia on renal DUS parameters has not been investigated. Knowledge of the influence of normovolaemic anaemia on renal haemodynamics may permit correct interpretation of DUS results in the investigation of canine babesiosis, and improve an understanding of its pathophysiology, and that of other anaemic conditions. It is hoped that these findings may then help to predict the development of renal complications. The purpose of this study was to determine the influence of: (1) severe, acute normovolaemic anaemia and (2) moderate and mild chronic normovolaemic anaemia on renal DUS parameters in the dog.

4.3 MATERIALS AND METHODS

4.3.1 Experimental design - This study was part of a larger investigation on the influence of normovolaemic anaemia on DUS parameters of abdominal splanchnic haemodynamics, and on left ventricular function. Eleven beagles comprising one intact and three neutered males, and seven intact non-pregnant females were used. Mean and standard deviation (SD) of their body weights was 12.0 ± 1.8 kg. Four males and five females had a mean age of 2.63 years. The exact age of two females could not be established. All beagles were clinically healthy. The Onderstepoort Veterinary Academic Research Unit, Faculty of Veterinary Science, University of Pretoria loaned the dogs. During the active trial period, two to four dogs were transferred and housed in large kennels at the Onderstepoort Veterinary Academic Hospital. Here they were fed a high protein and calorie commercial dog food. In the first week of the study, one dog was introduced to the trial. Subsequently two dogs were introduced each week. The study compared the corresponding renal haemodynamics in physiological and anaemic states in the same dog. Doppler spectra of the left renal artery (LRA) and interlobar artery (ILA) were obtained and baseline DUS parameters measured as detailed in a following paragraph. Measurements were then repeated immediately after induction of severe, acute anaemia

(haematocrit [Hct] 13-17%), and at moderate (Hct 25-27%) and mild (Hct 31-37%) stages during recovery.

Doppler evaluation of abdominal splanchnic haemodynamics lasting between 90-120 minutes and with regular breaks of 5-10 minutes immediately followed an echocardiographic examination on the same animals. At the end of the trial each animal, having recovered sufficiently from the anaemia, was returned to Onderstepoort Veterinary Academic Research Unit. The Animal Use and Care Committee of the Faculty of Veterinary Science, University of Pretoria, approved the study.

4.3.2 Induction of anaemia - The technique used for induction of anaemia was described by Lobetti (1996), and modified so as to be non-fatal. About 20% of the circulating blood volume was removed 1-3 times per day over a 3-4 day period to produce severe acute anaemia with Hct 13-17%. Plasma from the removed blood plus additional Ringer's lactate calculated to replace the volume deficit of red blood cells was infused into the animal in an attempt to maintain a normal circulating blood volume, however, no measurements were carried out to confirm normovolaemia. Doppler measurements in the severely anaemic state commenced at least 16 hours after completion of the volume replacement.

4.3.3 Ultrasonographic examinations - All dogs were fasted for 12 hours before being examined by one investigator (LMK). No anaesthesia or sedation was used. The ventral abdomen and left flank were clipped, cleaned and acoustic coupling gel was applied onto the skin surface. For general abdominal imaging, the dog was positioned in dorsal recumbency. Right lateral recumbency was used for imaging the left kidney in dorsal, transverse and oblique planes in the left cranial quadrant of the abdomen slightly caudal to the spleen. All

ultrasonographic examinations were carried out using a Sonoline Omnia ultrasound-imaging machine (Siemens Medical Systems Inc., Ultrasound Group, Erlangen, Germany), and a linear or curved array transducer. A frequency of 5.0 MHz was used for B-mode examination of the general abdominal cavity and organs, and 7.5 or 5.0 MHz for B-mode evaluation of the left kidney, and identification of its vessels. Machine settings were optimised to give good image quality. Both left and right kidneys were subjectively observed on B-mode. The length, width and height of the left kidney were measured with on-board electronic callipers. Relative echogenicities of the spleen and left kidney were evaluated subjectively, comparing the spleen with renal cortex.

Doppler imaging of the LRA and ILA were performed with 5.2 MHz Doppler frequency. A sample volume was placed within the LRA about 5 mm from its origin at the AAo to obtain its Doppler spectrum. The ILA was sampled within the renal pelvis about 5-10 mm from the renal hilus. A 7.5 MHz transducer for B-mode imaging, and colour Doppler facilitated sampling these vessels. Cursors of sample volumes were oriented transversely across the LRA and ILA as the vessels coursed towards the transducer. In each case, a sample volume size of about 3 mm was used. While obtaining Doppler spectra, attempts were made to avoid wall artefacts from the LRA or spectral contamination from a neighbouring vessel. In the LRA the vessel-beam alignment was angle corrected electronically before recording the spectral tracing. Manual transducer adjustment, and electronic beam steering achieved this, and the vessel-beam angle was below 60 degrees in all cases. Machine settings were optimised for high sensitivity imaging. Doppler spectra of individual vessels were evaluated for their flow patterns, and with the help of a simultaneous ECG tracing various features of the Doppler spectra were categorised. The instantaneous heart rate (HR) at each Doppler cycle sampled was computed from the preceding R-R interval on the ECG. Measurements of PSV, time-averaged mean

velocity (TAV_{mean}), PI and RI were made using the onboard computer, and PI and RI were expressed as (Nelson and Pretorius 1988):

$$PI = \frac{\text{Peak systolic velocity – End diastolic velocity}}{\text{Time-averaged mean velocity}}$$

$$RI = \frac{\text{Peak systolic velocity – End diastolic velocity}}{\text{Peak systolic velocity}}$$

End diastolic velocity (EDV) was calculated by re-arranging the RI equation.

The value recorded for each parameter was an average of measurements or calculations from three ECG or spectral Doppler cycles. Heart rate and Doppler parameters of the LRA were not measured in one dog because of poor cooperation, and the LRA TAV_{mean} was not measured in two other dogs because of arterial wall artefact or spectral contamination from the left renal vein.

4.3.4 Data analysis - Results of each experiment were entered into an MS Excel program (Microsoft Corporation) on a personal computer. All ultrasonographic procedures were recorded on videotape for possible re-evaluation and future reference. All data were found to be normally distributed using the Shapiro-Wilk test, and were presented as mean and standard deviation (SD). Doppler parameters in each grade of anaemia were compared with those in the physiologic state using the paired t-test. Differences were considered to be significant at the 5% level of significance. A Stata Release 7 statistical software program (Stata Press, 702 University Drive East, College Station, Texas 77840, USA) was used to perform the data analysis.

4.4 RESULTS

Haematocrit levels and physical condition of animals following induction of severe acute anaemia, and during recovery are reported elsewhere (Koma *et al.* 2005). Data for linear dimensions of the left kidney are given in Table 4.1, and those of heart rate and renal Doppler parameters are presented in Table 4.2.

4.4.1 Severe acute anaemia - Mean renal length and width were significantly increased while renal height was unchanged. Systolic peaks of the LRA and ILA Doppler spectra were more closely and regularly spaced (Figs. 4.1 and 4.2). Mean HR and mean PSV, PI and RI of the LRA were significantly increased. Mean EDV of the LRA was significantly reduced. There was no significant change in mean TAV_{mean} of the LRA, and in mean PI and RI of the ILA.

4.4.2 Moderate and mild chronic anaemia - Mean renal length and width were significantly increased in mild anaemia but renal height was unchanged. There was no significant change in any renal dimension in moderate anaemia. Heart rates in moderate and mild anaemic states were not significantly different from those in the physiologic state, and the corresponding LRA and ILA Doppler spectra in both states appeared similar. No significant change was found in mean PI and RI of any vessel, or in mean PSV, EDV and TAV_{mean} of the LRA.

Table 4.1 Linear dimensions of the left kidney during physiological and anaemic states

Physical state	Renal length (mm)				Renal width (mm)				Renal height (mm)			
	n	Mean	SD	*P*-value	n	Mean	SD	*P*-value	n	Mean	SD	*P*-value
Baseline	10	48.18	2.79	0.05	10	27.43	2.25	0.02	10	27.63	3.93	0.15
Severe anaemia		50.18	3.47			29.54	2.46			29.63	2.62	
Baseline	11	48.56	2.92	0.40	11	26.75	3.12	0.21	11	27.16	4.03	0.31
Moderate anaemia		48.01	3.23			27.97	1.58			28.12	2.41	
Baseline	10	48.18	2.79	0.03	10	27.43	2.25	< 0.01	9	27.60	4.16	0.41
Mild anaemia		50.46	2.24			29.25	2.07			29.09	2.63	

Hct = haematocrit, mm = millimetres, n = number of observations, SD = standard deviation. Baseline Hct = 47.5%, severe anaemia Hct = 16.0%, moderate anaemia Hct = 26.3%, mild anaemia Hct = 34.4%. Level of significance, α = 5%.

Table 4.2 Heart rate and renal Doppler parameters during physiological and anaemic states

Vessel segment	Parameter	n	Baseline (Hct 47.5%)		Severe anaemia (Hct 16.0%)			Moderate anaemia (Hct 26.3%)			Mild anaemia (Hct 34.4%)		
			Mean	SD	Mean	SD	*P*-value	Mean	SD	*P*-value	Mean	SD	*P*-value
LRA	HR	10	88.5	24.6	136.1	20.8	0.007	96.4	19.2	0.541	79.8	14.1	0.285
	PSV	10	75.2	22.0	105.8	33.2	0.013	72.7	17.0	0.879	74.1	3.4	0.799
	EDV	10	25.7	8.2	21.0	7.7	0.000	22.8	7.5	0.166	21.7	9.9	0.110
	TAV_{mean}	8	24.1	8.6	27.1	9.5	0.484	20.1	6.6	0.735	19.2	9.1	0.161
	PI	10	1.34	.32	1.6	0.38	0.022	1.5	0.27	0.203	1.56	0.38	0.221
	RI	10	0.66	0.07	0.72	0.06	0.005	0.70	0.05	0.445	0.72	0.07	0.114
ILA	HR	10	88.3	29.0	131.0	16.6	0.005	98.2	16.3	0.859	96.2	24.6	0.575
	PI	11	1.2	.25	1.29	0.22	0.424	1.19	0.26	0.477	1.02	0.22	0.131
	RI	11	0.64	0.09	0.70	0.07	0.213	0.66	0.06	0.722	0.61	0.06	0.563

EDV = end diastolic velocity, Hct = haematocrit, SD = standard deviation, n = number of observations, HR = heart rate, PSV = peak systolic velocity, TAV_{mean} = time-averaged mean velocity, PI = pulsatility index, RI = resistive index, LRA = left renal artery, ILA = interlobar artery. Level of significance, α = 5%.

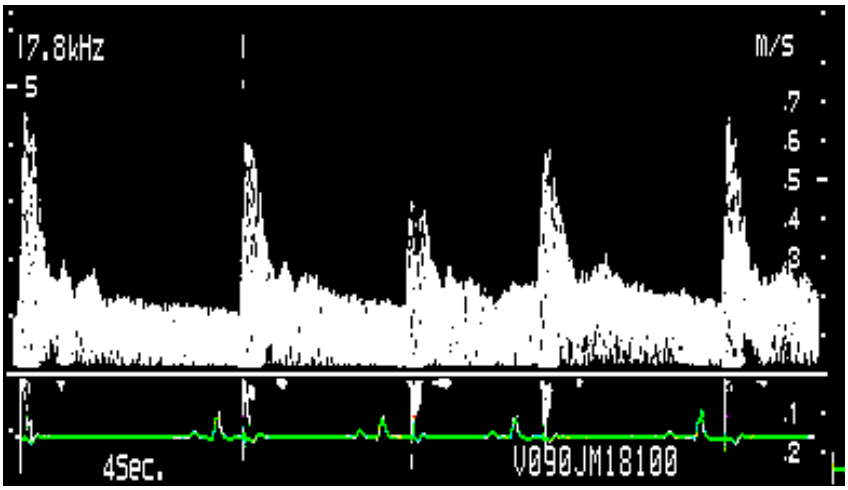

A.

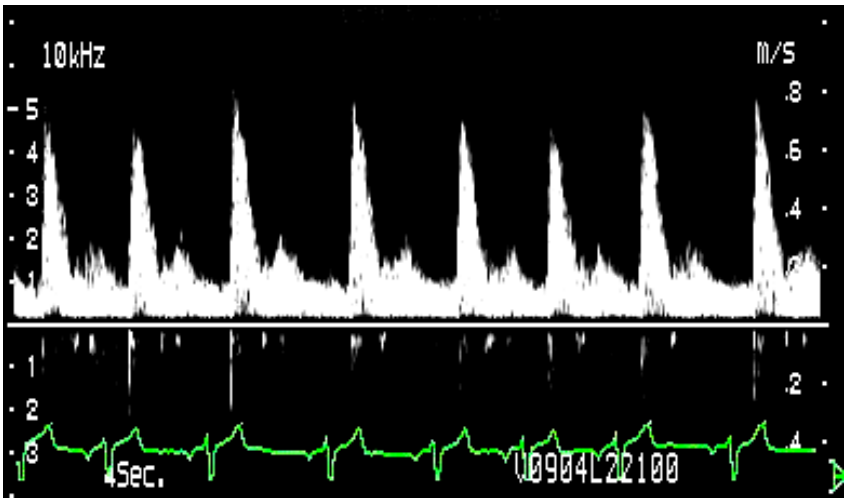

B.

Figure 4.1 - Doppler spectra of the left renal artery obtained from a beagle in (A) physiological state and (B) severe acute anaemia with haematocrit (Hct) of 16%. Notice the closer and more regular spacing of cycles in the anaemic state. Systolic peaks appear higher while end diastolic velocities appear lower than in the physiologic state.

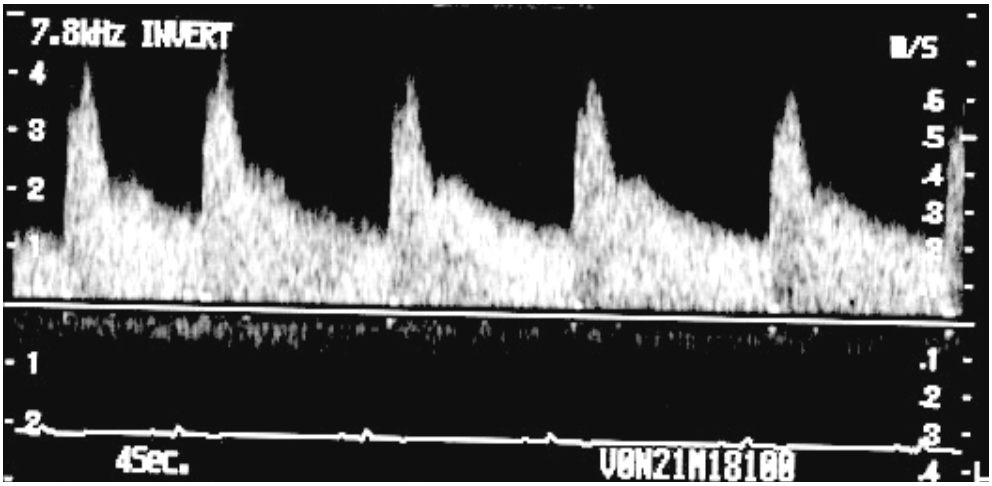

A.

B.

Figure 4.2 - Doppler spectra of an interlobar artery of the left kidney obtained from a beagle in (A) physiological state and (B) severe, acute anaemia with Hct of 16%. Notice the closer and more regular spacing of cycles in the anaemic state. Systolic peaks appear higher while end diastolic velocities are about equal compared with those in the physiologic state.

4.5 DISCUSSION

Significant increase was found in the left renal length and width in severe and mild anaemia. The observed increase in renal size is probably due to increased blood volume within its tissue. Increase in renal blood volume would result from increased renal blood flow that occurs in moderate and severe anaemia (Nashat and Portal 1967; Race *et al.* 1967; Schrier and Earley 1970; Vatner *et al.* 1972).

No specific report could be found in the literature to relate current observations on the renal artery PSV and TAV_{mean}. However, numerous studies in the human foetus have established that PSV and TAV_{mean} in vessels such as middle cerebral artery, aorta and splenic artery are increased in severe anaemia (Abdel-Fattah *et al.* 2002; Bahado-Singh *et al.* 2000; Steiner *et al.* 1995). Increased PSV and TAV_{mean} of the abdominal aorta (AAo), cranial mesenteric artery (CMA) and celiac artery (CA) have also been reported in anaemic dogs (Koma *et al.* 2005). The observed increase in PSV in the present study suggests a renal artery haemodynamic change in anaemia similar to that of other vessels of the dog and human foetus. However, absence of significant change in the renal artery TAV_{mean} in severe anaemia differentiates it from other vessels of the dog and human foetus where significant increase is reported (Abdel-Fattah *et al.* 2002; Koma *et al.* 2005).

Significant elevations in renal artery PI and RI observed in severe, acute anaemia in the current study suggests increased flow resistance by this vessel. The increase in PI and RI was associated with significant reduction in EDV, suggesting presence of renal artery contraction. The pattern of change in renal artery PI and RI in anaemia differed from that observed earlier for the same parameters of the CMA and CA (Koma *et al.* 2005). In severe acute anaemia,

renal artery PI and RI were significantly increased while those of the CMA and CA were unchanged. In moderate and mild anaemia, renal artery PI and RI were unchanged while those of the CMA and CA were either unchanged or significantly reduced. The present finding supports an earlier observation that renal artery resistance increases with increasing flow rate or arterial pressure over the range of 75-200 mm Hg whereas resistance decreases in other vascular beds (Haddy *et al.* 1958). Although we did not measure renal artery pressure, there is no reason to suggest its increase following induction of severe acute anaemia. The observed increase in renal artery resistance is therefore most likely associated with increased velocity of flow within the vessel. The variation in vascular resistance between the renal and other vascular beds such as the gastrointestinal bed may be due to their different functions and responses to anaemia (Vatner *et al.* 1972). The kidney maintains its blood flow by an auto regulation mechanism to a constant level within certain limits of systemic arterial blood pressure and blood flow to maintain a constant glomerular filtration rate (Haddy *et al.* 1958). It appears that contraction of the renal artery leading to increase in PI and RI contributes to this auto regulation mechanism of the kidney that minimises an increase in its blood flow during anaemia. Our observation supports other reports that in severe acute anaemia, in spite of an increased blood flow, renal flow fraction of the cardiac output is reduced (Grupp *et al.* 1972; Race *et al.* 1967). However, our observation on the renal PI and RI appears to contradict reports of other studies that used invasive methods and found significant reduction in renal resistance in severe chronic anaemia (Vatner *et al.* 1972) or in acutely haemodiluted dogs (Schrier and Earley 1970). The apparent contradiction between our study and that of others may be due to differences in anaemia induction and evaluation methods, and the different anaemia types investigated. Vatner *et al*. (1972) induced anaemia gradually over a 2-4 week period and investigated chronic anaemia, progressing from moderate to severe. Such a gradual change is likely to stimulate a different type of renal haemodynamic response in comparison to

the severe, acute anaemia induced within 3-4 days in our study. In their investigation, Schrier and Earley (1970) achieved acute normovolaemic haemodilution by withdrawal of blood and simultaneous replacement with an equal volume of each dog's previously harvested plasma. They calculated renal artery resistance from its blood pressure and blood flow that were measured within 60 minutes of completion of the haemodilution. In contrast, our earliest measurements of renal artery PI and RI were made at least 16 hours following completion of the haemodilution. This difference in timing of measurements most likely is an important factor of variation observed in renal artery haemodynamic response to anaemia. In our case, the kidney would have had sufficient time to permit any intermediate adjustments in response to the effects of acute reduction in Hct level.

Unlike the renal artery, we found no significant change in PI and RI of the ILA at any stage during the normovolaemic anaemia. This implies that any elevation found in intrarenal PI or RI of the dog would be due to disorders other than normovolaemic anaemia. Reference was made to a significantly elevated intrarenal RI in anaemia, but the type of anaemia was not defined (Morrow *et al.* 1996). An experimental study in pigs demonstrated that acute haemorrhagic shock (hypotension) significantly elevated RI of both the renal artery and intrarenal arteries (Clancy *et al.* 1995). Elevation in the intrarenal RI has also been observed in various renal or systemic diseases (Koch *et al.* 1997; Rivers *et al.* 1997).

This study has non-invasively demonstrated renal haemodynamic changes associated with normovolaemic anaemia in the dog. Significant increase in PSV, PI and RI of the renal artery was found in severe acute anaemia whereas the same parameters were not changed in mild or moderate chronic anaemia. No change in PI or RI of the ILA was found at any stage during

anaemia. Renal artery response to severe acute normovolaemic anaemia was different from those of other vessels such as the AAo, CMA and CA.

4.6 ACKNOWLEDGEMENTS

Makerere University, Uganda, and University of Pretoria, South Africa, provided the funding for this study. Siemens Co., South Africa, loaned an ultrasound machine.

4.7 REFERENCES

Abdel-Fattah, S.A., Soothill, P.W., Carroll, S.G., Kyle, P.M., 2002. Middle cerebral artery Doppler for the prediction of foetal anaemia in cases without hydrops: a practical approach. British Journal of Radiology 75, 726-730.

Abildgaard, A., Klow, N.-E., Jakobsen, J.A., Egge, T.S., Eriksen, M., 1997. Effect of ultrasound contrast medium in colour Doppler and power Doppler visualisation of blood flow in canine kidneys. Acta Radiologica 38, 445-453.

Akihiro, K., Yutaka, Y., Osamu, U., Kazumi, K., Jintetsu, S., Tsuneharu, M., 2001. Evaluation of reflux kidney using renal resistive index. Journal of Urology 165, 2010-2012.

Arger, P.H., Sehgal, C.M., Pugh, C.R., Kirchoffer, J.I., Kotlar, E.Y., Bovee, K.C., 1999. Evaluation of change in blood flow by contrast-enhanced power Doppler imaging during norepinephrine-induced renal vasoconstriction. Journal of Ultrasound in Medicine 18, 843-851.

Bahado-Singh, R., Oz, U., Deren, O., Kovanchi, E., Hsu, C.D., Copel, J.A., Mari, G., 2000. Splenic artery Doppler peak systolic velocity predicts severe foetal anaemia in rhesus disease. American Journal of Obstetrics and Gynaecology 182, 1222-1226.

Brown, J.M., Quedens-Case, C., Alderman, J.L., Greener, Y., Taylor, K.J.W., 1997. Contrast enhanced sonography of visceral perfusion defects in dogs. Journal of Ultrasound in Medicine 16, 493-499.

Clancy, M.J., Alderman, J.L., Case, C., Taylor, K.J.W., 1995. The use of ultrasound in the noninvasive detection of changes in the renal circulation in response to blood loss using an animal model. Resuscitation 30, 161-167.

Clark, I.A., Jacobson, L.S., 1998. Do babesiosis and malaria share a common disease process? Annals of Tropical Medicine and Parasitology 92, 483-488.

Daley, C.A., Finn-Bodner, S.T., Lenz, S.D., 1994. Contrast-induced renal failure documented by colour Doppler imaging in a dog. Journal of American Animal Hospital Association 30, 33-37.

Dodd, G.D., Kaufman, P.N., Bracken, R.B., 1991. Renal arterial duplex Doppler ultrasound in dogs with urinary obstruction. Journal of Urology 145, 644-646.

Eiam-ong, S., Sitprija, V., 1998. Falciparum malaria and the kidney: a model of inflammation. American Journal of Kidney Diseases 32, 361-375.

Freeman, M.J., Kirby, B.M., Panciera, D.L., Henik, R.A., Rosin, E., Sullivan, L.J., 1994. Hypotensive shock syndrome associated with acute Babesia canis infection in a dog. Journal of the American Veterinary Medical Association 204, 94-96.

Gaschen, L., Audet, M., Menninger, K., Schuurman, H.-J., 2001. Ultrasonographic findings of functioning renal allografts in the cynomolgus monkey (*Macaca fascicularis*). Journal of Medical Primatology 30, 46-55.

Glick, G., Plauth, W.H.J., Braunwald, E., 1964. Role of the autonomic nervous system in the circulatory response to acutely induced anaemia in unanaesthetised dogs. Journal of Clinical Investigation 43, 2112-2124.

Grupp, I., Grupp, G., Holmes, J.C., Fowler, N.O., 1972. Regional blood flow in anaemia. Journal of Applied Physiology 33, 456-461.

Haddy, F.J., Scott, J., Fleischman, M., Emanuel, D., 1958. Effect of change in flow rate upon renal vascular resistance. American Journal of Physiology 195, 111-119.

Jacobson, L.S., Lobetti, R.G., Vaughan-Scott, T., 2000. Blood pressure changes in dogs with babesiosis. Journal of the South African Veterinary Association 71, 14-20.

Knapp, R., Plotzeneder, A., Frauscher, F., Helweg, G., Judmaier, W., Zurnedden, D., Recheis, W., Bartsch, G., 1995. Variability of Doppler parameters in the healthy kidney: An anatomic-physiologic correlation. Journal of Ultrasound in Medicine 14, 427-429.

Koch, J., Jensen, A.L., Wenck, A., Iversen, L., Lykkegaard, K., 1997. Duplex Doppler measurements of renal blood flow in a dog with Addison's disease. Journal of Small Animal Practice 38, 124-126.

Koma, L.M., Spotswood, T.C., Kirberger, R.M., Becker, P., 2005. Influence of normovolaemic anaemia on Doppler characteristics of the abdominal aorta and splanchnic vessels in beagles. American Journal of Veterinary Research 66,187-195.

Lobetti, R.G., 1996. The comparative role of haemoglobinaemia and hypoxia in the development of nephropathy in the dog. Journal of the South African Veterinary Association 67, 188-198.

Lobetti, R.G., Jacobson, L.S., 2001. Renal involvement in dogs with babesiosis, Journal of the South African Veterinary Association 72, 23-28.

Maegraith, B., Gilles, H.M., 1957. Devakul, K., Pathological processes in *Babesia canis* infections. Zeitschrift Fur Tropenmedizin und Parasitologie 8, 485-514.

Malherbe, W.D., 1966. Clinicopathological studies of Babesia canis infection in dogs. V. The influence of the infection on kidney function. Journal of the South African Veterinary Medical Association 37, 261-264.

Miletic, D., Fuckar, Z., Sustic, A., Mozetic, V., Smokvina, A., Stancic, M., 1998. Resistance and pulsatility indices of acute renal obstruction. Journal of Clinical Ultrasound 26, 79-84.

Morrow, K.L., Salman, M.D., Lappin, M.R., Wrigley, R.H., 1996. Comparison of the resistive index to clinical parameters in dogs with renal disease. Veterinary Radiology & Ultrasound 37, 193-199.

Nashat, F.S., Portal, R.W., 1967. Effects of changes in haematocrit on renal function. Journal of Physiology 193, 513-522.

Nelson, T.R., Pretorius, D.H., 1988. The Doppler signal: Where does it come from and what does it mean? American Journal of Roentgenology 151, 439-447.

Nyland, T.G., Fisher, B.S., Doverspike, M., Hornof, W.J., Olander, H.J., 1993. Diagnosis of urinary tract obstruction in dogs using duplex Doppler ultrasonography. Veterinary Radiology & Ultrasound 34, 348-352.

Okada, T., Yoshida, H., Iwai, J., Matsunaga, T., Yoshino, K., Ohtsuka, Y., Kouchi, K., Tanabe, M.O., N., 2001. Pulsed Doppler sonography of the hilar renal artery: differentiation of obstructive from nonobstrucive hydronephrosis in children. Journal of Paediatric Surgery 36, 416-420.

Platt, J.F., 1992. Duplex Doppler evaluation of native kidney dysfunction: obstructive and nonobstructive disease. American Journal of Roentgenology 58, 1035-1042.

Pope, J.C., Hernanzschulman, M., Showalter, P.R., Cole, T.C., Schrum, F.F., Szurkus, D., Brock, J.W., 1996. The value of Doppler resistive index and peak systolic velocity in the evaluation of porcine renal obstruction. Journal of Urology 156, 730-733.

Pozniak, M.A., Kelcz, F., D'Alessandro, A., 1992. Sonography of renal transplants in dogs: The effect of acute tubular necrosis, cyclosporine nephrotoxicity, and acute rejection on resistive index and renal length. American Journal of Roentgenology, 158, 791-797.

Pozniak, M.A., Kelcz, F., Stratta, R.J., Oberley, T.D., 1988. Extraneous factors affecting resistive index. Investigative Radiology 23, 899-904.

Race, D., Dedichen, H., Schenk, J.W.R., 1967. Regional blood flow during dextran-induced normovolaemic haemodilution in the dog. Journal of Thoracic and Cardiovascular Surgery 53, 578-586.

Reid, M.H., Mackay, R.S., Lantz, M.T., 1980. Noninvasive blood flow measurements by Doppler ultrasound with applications to renal artery flow determination. Investigative Radiology 15, 323-331.

Reyers, F., Leisewitz, A.L., Lobetti, R.G., Milner, R.J., Jacobson, L.S., van Zyl, M., 1998. Canine babesiosis in South Africa: more than one disease. Does this serve as a model for falciparum malaria? Annals of Tropical Medicine and Parasitology 92, 503-511.

Rivers, B.J., Walter, P.A., Letourneau, J.G., Finlay, D.E., Ritenour, E.R., King, V.L., O'Brien, T.D., Polzin, D.J., 1996. Estimation of arcuate resistive index as a diagnostic tool for aminoglycoside-induced acute renal failure in dogs. American Journal of Veterinary Research 57, 1536-1544.

Rivers, B.J., Walter, P.A., Polzin, D.J., King, V.L., 1997. Duplex Doppler estimation of intrarenal Pourcelot resistive index in dogs and cats with renal disease. Journal of Veterinary Internal Medicine 11, 250-260.

Sari, A., Dinc, H., Zibandeh, A., Telatar, M., Gumele, H.R., 1999. Value of resistive index in patients with clinical diabetic nephropathy. Investigative Radiology 34, 718-721.

Schrier, R.W., Earley, L.E., 1970. Effects of haematocrit on renal haemodynamics and sodium excretion in hydropenic and volume-expanded dogs. Journal of Clinical Investigation 49, 1656-1667.

Sehgal, C.M., Arger, P.H., Silver, A.C., Patton, J.A., Saunders, H.M., Bhattacharyya, A., Bell, C.P., 2001. Renal blood flow changes induced with endothelin-1 and fenoldopam mesylate at quantitative Doppler US: Initial results in a canine study. Radiology 219, 419-426.

Sitprija, V., 1971. Urinary excretion patterns in renal failure due to malaria: The effects of phenoxybenzamine in two cases. Australian and New Zealand Journal of Medicine 1, 44.

Sitprija, V., Arthachinta, S., Kashemsant, U., Poshyiachinda, V., 1975. Renal blood flow study in acute renal failure. Chula University Research Journal 2, 103-119.

Sitprija, V., Indraprasit, S., Pochanugool, C., Benyajati, C., Piyaratn, P., 1967. Renal failure in malaria. Lancet 1, 185.

Sitprija, V., Napathorn, S., Laorpatanaskul, S., Suithichaiyakul, T., Moollaor, P., Suwangool, P., Sridama, V., Thamaree, S., Tankeyoon, M., 1996. Renal and systemic haemodynamics in falciparum malaria. American Journal of Nephrology 16, 513-519.

Sitprija, V., Vongsthongsri, M., Poshyiachinda, V., Arthachinta, S., 1977. Renal failure in malaria: A pathophysiologic study. Nephron 18, 277-287.

Steiner, H., Schaffer, H., Spitzer, D., Batka, M., Graf, A.H., Staudach, A., 1995. The relationship between peak velocity in the foetal descending aorta and haematocrit in rhesus isoimmunisation. Obstetrics and gynaecology 85, 659-662.

Stone, W.J., Hanchett, J.E., Knepshell, J.H., 1972. Acute renal insufficiency due to falciparum malaria. Archives of Internal Medicine 129, 620.

Takahashi, S., Narumi, Y., Takahara, S., Suzuki, S., Kyo, M., Cruz, M., Takamura, M., Kokado, Y., Ichimaru, N., Toki, K., Nakamura, H., Okuyama, A., 1999. Acute renal allograft rejection in the canine: Evaluation with serial duplex Doppler ultrasonography. Transplantation Proceedings 31, 1731-1734.

Vatner, S.F., Higgins, C.B., Franklin, D., 1972. Regional circulatory adjustments to moderate and severe chronic anaemia in conscious dogs at rest and during exercise. Circulation Research 30, 731-740.

CHAPTER 5

INFLUENCE OF NORMOVOLEMIC ANEMIA ON DOPPLER-DERIVED BLOOD VELOCITY RATIOS OF ABDOMINAL SPLANCHNIC VESSELS IN CLINICALLY NORMAL DOGS

Lee M Koma, MPhil, Robert M Kirberger, MMed Vet (Rad), Leonie Scholtz, MMed (Rad D), Paul Bland-van den Berg, PhD

As accepted on 5 January 2005 for publication by the Veterinary Radiology & Ultrasound

5.1 ABSTRACT

Doppler spectra of the abdominal aorta (AAo), cranial mesenteric artery (CMA), celiac artery (CA) and left renal artery (LRA) were obtained from eleven fasted, clinically healthy, conscious Beagles before and after inducing severe acute normovolemic anemia (mean ± SD Hct 16.0 ± 0.77%). Peak systolic, end diastolic and time-averaged mean velocities were measured. Velocities and velocity ratios of splanchnic vessels to the AAo were compared during physiologic and anaemic states. There was no difference between LRA and AAo, CMA or CA regarding time-averaged mean velocity, time-averaged mean velocity ratio or end diastolic velocity during the physiological state. During the anemic state, LRA mean time-averaged mean velocity ($P \leq 0.008$) and mean end diastolic velocity ($P \leq 0.041$) were significantly lower than those of AAo, CMA and CA. Mean time-averaged mean velocity ratio of the LRA was also significantly ($P \leq 0.004$) lower than the CMA and CA ratios, and significantly ($P = 0.014$) lower during anemic state than physiologic state of the same vessel. End diastolic and time-averaged mean velocities of the AAo, CMA and CA increased proportionally during anemia, but there was a relatively less increase in the same variables of the LRA, suggesting less increase in blood flow. Doppler ratios allowed a non-invasive comparison between splanchnic and aortic hemodynamics. Velocity ratios might be useful for clinical detection of relative hemodynamic changes between different vessels. (*Veterinary Radiology & Ultrasound 2005; vol: pp*)

Key words: anemia model, aorta, celiac artery, cranial mesenteric artery, renal artery, Doppler velocity ratios

5.2 INTRODUCTION

Various invasive techniques have been used in the dog to quantify the hemodynamic physiology and pathophysiology of digestion[1] and renal function.[2] Hemodynamic pathophysiology of normovolemic hemodilution (anemia) in the dog has also been studied extensively using invasive methods.[3-9] The introduction of duplex Doppler ultrasound marked a new era in the investigation of the hemodynamic physiology of digestion,[10,11,12] and renal function.[13-15] Quantitative and semi-quantitative Doppler ultrasound methods have been used to assess intrarenal arteries (interlobar and arcuate artery) in the dog to investigate renal hhemodynamic physiology and pathophysiology.[16-21] Hepatic,[22,23] aortic and digestive[24,25] hemodynamics have also been investigated. Results of hemodynamic measurements using Doppler ultrasound correlate well with those of different invasive methods, making it a reliable tool.[25]

Quantification of hemodynamics by estimation of blood flow using Doppler ultrasound is used more frequently in animals[22,24,26,27] than the congestion index to estimate venous resistance.[22,27] Measurement of these parameters require estimation of the Doppler angle of alignment and vessel cross sectional area that are subject to systematic and random errors.[22,27-29] Resistive index,[16-21,23-25] and pulsatility index,[24,25] are frequently used to provide information on downstream arterial vascular resistance to blood flow from the sampling point. Because resistive index and pulsatility index are ratios of the Doppler shift components of a spectrum, there is no requirement for estimation of the Doppler angle or vessel cross sectional area. These indices are therefore most useful for investigating the microcirculation within organs or tissues where estimation of both the Doppler angle and vessel cross sectional area would be difficult or impossible. However, resistive index is used less frequently for investigating hemodynamic alterations in abdominal viscera such as liver, spleen, stomach and

intestines.[23-25,30] One reason may be the high degree of mobility of these organs, making it difficult to obtain complete cycles of good quality Doppler tracings from their microcirculation for resistive index measurement.

Investigators quantifying hemodynamics in severe human fetal anemia due to red blood cell alloimmunization or parvovirus infection have reliably used peak systolic velocity of vessels such as the middle cerebral artery, aorta and splenic artery to predict or diagnose anemia.[31-34] Peak systolic velocity ratio, a fraction of the lowest prestenotic or poststenotic velocity to an intrastenotic velocity, appears to be useful for quantifying arterial stenosis in human patients.[35,36] Peak systolic velocity and end diastolic velocity have been used occasionally to quantify arterial hemodynamics in the dog.[23,24] In acute, severe normovolemic anemia in the dog, significant increase in peak systolic velocity or time-averaged mean velocity of the AAo, CMA and CA was reported.[37] Measurements of peak systolic velocity or time-averaged mean velocity do not require estimation of vessel cross sectional area, although estimation of the Doppler angle is necessary. Time-averaged mean velocity is regarded to have a linear relationship with blood flow, and could be a good estimate of hemodynamic alterations where vessel cross-sectional areas remain constant.[4] In those abdominal viscera where measurement of resistive index of vessels of the parenchyma or hollow organ walls is difficult, e.g. the liver, spleen and intestines, expressing the velocity of a main artery of the organ as a ratio of the AAo would permit a comparison of their hemodynamics; might detect the presence of a relative hemodynamic alteration; and might complement the more frequently used Doppler parameters in hemodynamic evaluation. The influence of different machines, operators or subjects on variability of ratios might be less than that on absolute values of Doppler parameters. Differences between physiologic and anemic states of individual abdominal splanchnic vessels (within vessel comparison) based on absolute Doppler value have been reported.[37] The purpose of the current study is to compare the hemodynamics of selected abdominal

splanchnic vessels, i.e. CMA, CA and LRA, with each other and with that of the AAo (i.e. between vessel comparison) based on absolute values and on peak systolic velocity and time-averaged mean velocity ratios as Doppler indices in the dog. Comparison of regional abdominal hemodynamics by use of Doppler ratios may provide a means of early detection of hemodynamic abnormality and impending organ malfunction before biochemical changes are detectable in the liver, or of the spleen or gastrointestinal tract where biochemical tests are not available.

5.3 MATERIALS AND METHODS

5.3.1 Experimental design - Eleven Beagles (one intact and three neutered males, and seven intact non-pregnant females) were studied. Mean ± SD (standard deviation) of body weight was 12.0 ± 1.8 Kg. Four males and five females had a mean ± SD age of 2.63 ± 0.05 years. The exact age of two females could not be established. All Beagles were in good physical condition, and clinically healthy. The Onderstepoort Veterinary Academic Research Unit, Faculty of Veterinary Science, University of Pretoria loaned the dogs. Before the trial, blood was sampled and baseline Hct of each dog determined. Fecal analysis, urinalysis, routine serum biochemistry, echocardiography, thoracic radiographs and abdominal ultrasonography were done to test for normality. Details of the tests are given elsewhere.[38] Systemic blood pressure and circulating blood volume were not measured, partly because our study was designed for conformity with the routine clinical practice at our facility whereby these variables are not evaluated. Variability of blood pressure, low reliability of tests such as plasma osmolality estimation, and time and financial constraints were other factors that influenced our decision. We recognise that assumption of a normal circulating blood volume and systemic blood pressure could have introduced errors in our results, as discussed in a previous report.[37]

During the active trial period, two to four dogs were transferred and housed in large kennels at the Onderstepoort Veterinary Academic Hospital. In the first week of the study, one dog was introduced to the trial. Subsequently two dogs were introduced each week.

The study was self-controlled, comparing blood flow velocities of physiologic and anemic states in the same subject. Physiologic and anemic velocities of the AAo, CMA, CA and LRA were measured using Doppler ultrasound immediately before and after induction of severe, acute normovolemic anemia (Hct 13-17%), as outlined in a following paragraph. The abdominal Doppler ultrasound evaluation immediately followed an echocardiographic examination of the same animals in another study that examined normal left ventricular function as part of a larger study. The echocardiographic examination was completed within 45-60 minutes, and the abdominal splanchnic Doppler ultrasound examination lasted between 90-120 minutes depending on patient cooperation. Regular breaks of 5-10 minutes were permitted during each examination. At the end of the study each animal was returned to Onderstepoort Veterinary Academic Research Unit. The Animal Use and Care Committee of the Faculty of Veterinary Science, University of Pretoria, approved this study.

5.3.2 Induction of anemia – A published technique used for induction of anemia was modified so as to be non-terminal.[39] About 20% of the circulating blood volume was removed 1-3 times per day over a 3-4 day period to produce severe acute anemia with Hct 13-17%. Plasma from the removed blood plus additional Ringer's lactate calculated to replace the volume deficit of red blood cells was infused into the animal in an attempt to maintain a normal circulating blood volume. However, no measurements were carried out to confirm normovolemia. Doppler measurements in the severely anemic state commenced at least 16 hours after completion of the volume replacement.

5.3.3 Ultrasonographic examinations - All dogs were fasted for 12-hours before being examined by one investigator (LMK). No anesthesia or sedation was used. The ventral and left lateral abdomen was clipped, cleaned and covered with acoustic gel. Right lateral recumbency was used for imaging the AAo, CMA, CA and LRA. All examinations were carried out using a Sonoline Omnia ultrasound-imaging machine (Siemens Medical Systems Inc., Ultrasound Group, Erlangen, Germany) with a convex or linear array transducer. B-mode identification of the AAo, CMA, CA and LRA was done with a 5.0 MHz convex array transducer, or with a 7.5 MHz linear array transducer for the LRA. All machine settings, including overall gain, depth compensation gain, edge enhancement, focus and line density were adjusted during each examination to obtain optimal image quality. Doppler examinations of the AAo, CMA and CA were performed at 3.5 MHz Doppler frequency. Within the AAo, Doppler sample volume was located anywhere along its length cranial to the origin of the LRA. Excluding vessel walls from the sample volume modified the technique of uniform insonation.[28,29,40] This kept the sample volume size within at least two thirds of the vessel diameter and avoided wall artefacts and spectral contamination from neighboring vessels. Evaluation of the LRA, and sometimes CMA and CA, was performed at 5.2 MHz Doppler frequency. Doppler sample volume in the CMA, CA or LRA was located about 5 mm away from the vessel's aortic origin. Cursors were oriented transversely, their lengths spanning across the vessel diameter due to the vessel coursing towards the transducer. In each dog, a sample volume width of about 3 mm was used. The vessel-beam alignment was angle corrected before recording a spectral tracing. Angle correction was assisted by manual adjustment of the transducer, or by electronic steering of the linear array transducer. The vessel-beam alignment angle was less than 60 degrees in all examinations. Machine settings were optimized for high sensitivity imaging in the Doppler mode. All spectral tracings were obtained with a simultaneous electrocardiograph (ECG). All Doppler measurements were obtained from spectral cycles whose preceding R-R intervals

were approximately equal, excluding obvious sinus arrhythmias. The instantaneous heart rate at each Doppler cycle sampled was computed from the preceding R-R interval on the ECG. The value recorded for heart rate, peak systolic velocity, end diastolic velocity or time-averaged mean velocity was obtained by averaging measurements or calculations from three ECG or spectral Doppler cycles. Peak systolic velocity and time-averaged mean velocity were measured with the onboard computer. Peak systolic velocity ratio and time-averaged mean velocity ratio were calculated by dividing the peak systolic velocity and time-averaged mean velocity of a splanchnic artery with the corresponding velocity of the AAo. End diastolic velocity was calculated from the resistive index by re-arranging the following equation:[41]

$$\text{Resistive index} = \frac{\text{Peak systolic velocity} - \text{End diastolic velocity}}{\text{Peak systolic velocity}}$$

Values for all velocities were recorded in centimetres per second (cm/s). Data for the LRA could not be obtained from one dog because of poor cooperation, and time-averaged mean velocity could not be measured in two other dogs because of arterial wall movement artefact or spectral contamination from the left renal vein.

5.3.4 Data analysis - Results of each experiment were entered into an MS Excel (Microsoft Corporation, Redmond, Washington) program on a personal computer. All ultrasonographic procedures were recorded on videotape for possible re-evaluation and future reference. All data were tested for normality with the Shapiro-Wilk test and were normally distributed. All vessels were compared with one another with respect to their peak systolic velocity, end diastolic velocity, time-averaged mean velocity, peak systolic velocity ratio and time-averaged mean velocity ratio during physiologic and anemic states using the paired t-test. In addition, peak systolic velocity ratio and time-averaged mean velocity ratio of each vessel were compared between the physiologic and anemic states using the paired t-test. A 5% level of

significance was used. SPSS version 12 (SPSS Inc., Chicago, IL 60606) statistical software program was used to perform the data analysis.

5.4 RESULTS

Representative Doppler spectra of the AAo, CMA and LRA obtained during physiologic and anemic states are given in Figures 5.1-5.3. Data comparing different vessels are given in Tables 5.1-5.3, and comparison of anemic and physiologic states is given in Table 5.4. The LRA had significantly lower mean peak systolic velocity and mean peak systolic velocity ratio during both physiologic and anemic states than each of the other three vessels investigated (Table 5.1). The CMA had significantly lower mean peak systolic velocity than that of the AAo during the physiologic but not anemic state. There was no significant difference between CA and AAo, CA and CMA regarding peak systolic velocity, or between CA and CMA regarding peak systolic velocity ratio during any state. Also during the physiologic state, no significant difference was found in mean time-averaged mean velocity or mean time-averaged mean velocity ratio between any vessel pair (Table 5.2). However, during the anemic state, the same variables of the LRA were significantly lower than that of each of the AAo, CMA and CA. During the physiologic state, only mean end diastolic velocity of the CMA was significantly lower than that of the CA, with no other significant difference between the remaining vessel pairs (Table 5.3). However, during the anemic state, mean end diastolic velocity of the LRA was significantly lower than that of each of the AAo, CMA and CA that did not significantly differ from each other. There was no significant difference between anemic and physiologic values of mean peak systolic velocity ratio or mean time-averaged mean velocity ratio of any vessel, except the LRA anemic mean time-averaged mean velocity ratio was significantly lower than the physiologic value (Table 5.4).

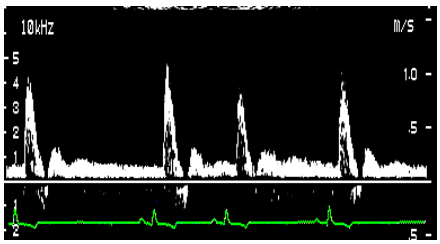

Figure 5.1A

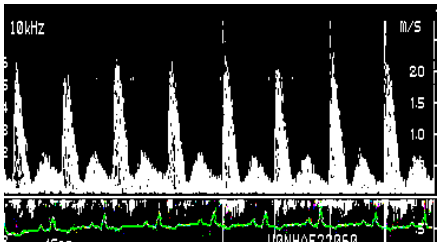

5.1B.

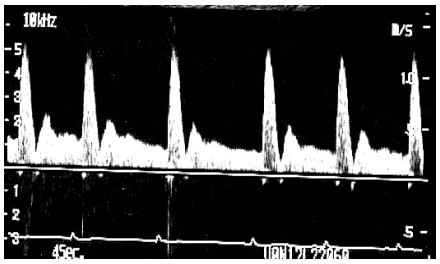

Figure 5.2A

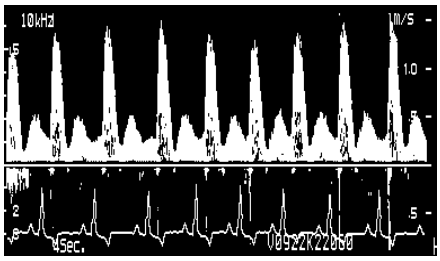

5.2B

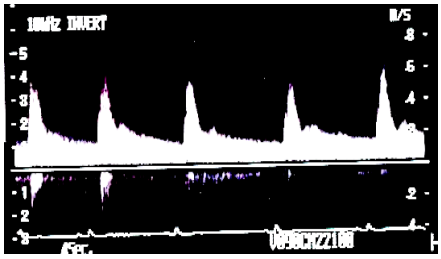

Figure 5.3A

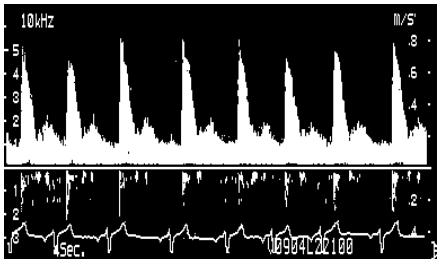

5.3B

Figures 5.1-5.3 Doppler spectra of the abdominal aorta, celiac artery and left renal artery respectively, during (A) physiologic state and (B) anemic state. Note closer spacing, and higher systolic peaks during the anemic state compared to the corresponding physiologic state.

Table 5.1 - Comparison of peak systolic velocity and peak systolic velocity ratio between vessels during physiologic and anemic states

Variable	Vessel pair	Physiologic state n	Mean ± SD	*P*-value	Anemic state n	Mean ± SD	*P*-value
Peak systolic velocity (cm/s)	AAo	11	127.1 ± 33.7	0.046	11	185.3 ± 40.4	0.081
	CMA	11	103.4 ± 20.2		11	161.4 ± 17.2	
	AAo	11	127.1 ± 33.7	0.329	11	185.3 ± 40.4	0.104
	CA	11	115.2 ± 27.8		11	163.5 ± 34.6	
	AAo	10	130.4 ± 33.6	0.000	11	185.3 ± 40.4	0.000
	LRA	10	75.2 ± 22.0		11	103.8 ± 32.1	
	CMA	11	103.4 ± 20.2	0.180	11	161.4 ± 17.2	0.818
	CA	11	115.2 ± 27.8		11	163.5 ± 34.6	
	CMA	10	102.7 ± 21.1	0.000	11	161.4 ± 17.2	0.000
	LRA	10	75.2 ± 22.0		11	103.8 ± 32.1	
	CA	10	116.9 ± 28.8	0.002	11	163.5 ± 34.6	0.000
	LRA	10	75.2 ± 22.0		11	103.8 ± 32.1	
Peak systolic velocity ratio	CMA	11	0.86 ± 0.24	0.163	11	0.90 ± 0.19	0.925
	CA	11	0.95 ± 0.26		11	0.91 ± 0.24	
	CMA	10	0.83 ± 0.23	0.001	11	0.90 ± 0.19	0.000
	LRA	10	0.59 ± 0.13		11	0.57 ± 0.16	
	CA	10	0.94 ± 0.27	0.001	11	0.91 ± 0.24	0.000
	LRA	10	0.59 ± 0.13		11	0.57 ± 0.16	

AAo = abdominal aorta. CA = celiac artery. CMA = cranial mesenteric artery. LRA = left renal artery. SD = standard deviation. Level of significance, α = 5%. Peak systolic velocity ratio = peak systolic velocity of a splanchnic vessel (CMA, CA or LRA) divided by that of the AAo.

Table 5.2 - Comparison of time-averaged mean velocity and time-averaged mean velocity ratio between vessels during physiologic and anemic states

Variable	Vessel pair	Physiologic state n	Mean ± SD	*P*-value	Anemic state n	Mean ± SD	*P*-value
Time-averaged mean velocity (cm/s)	AAo CMA	11 11	22.9 ± 7.6 21.0 ± 5.8	0.455	11 11	38.8± 11.8 34.5 ± 6.4	0.193
	AAo CA	11 11	22.9 ± 7.6 25.9 ± 9.1	0.234	11 11	38.8 ± 11.8 33.6 ± 6.2	0.116
	AAo LRA	8 8	24.9 ± 7.5 24.1 ± 8.6	0.827	11 11	38.8 ± 11.8 24.8 ± 9.0	0.001
	CMA CA	11 11	21.0 ± 5.8 25.9 ± 9.1	0.099	11 11	34.5 ± 6.4 33.6 ± 6.2	0.684
	CMA LRA	8 8	21.1 ± 5.6 24.1 ± 8.6	0.248	11 11	34.5 ± 6.4 24.8 ± 9.0	0.008
	CA LRA	8 8	28.0 ± 9.7 24.1 ± 8.6	0.282	11 11	33.6 ± 6.2 24.8 ± 9.0	0.002
Time-averaged mean velocity ratio	CMA CA	11 11	0.99 ± 0.37 1.19 ± 0.36	0.126	11 11	0.94 ± 0.24 0.92 ± 0.27	0.794
	CMA LRA	8 8	0.91 ± 0.38 1.00 ± 0.30	0.494	11 11	0.94 ± 0.24 0.67 ± 0.24	0.004
	CA LRA	8 8	1.17 ± 0.39 1.00 ± 0.30	0.262	11 11	0.92 ± 0.27 0.67 ± 0.24	0.002

AAo = abdominal aorta. CA = celiac artery. CMA = cranial mesenteric artery. LRA = left renal artery. SD = standard deviation. Level of significance, α = 5%. Time-averaged mean velocity ratio = time-averaged mean velocity of a splanchnic vessel (CMA, CA, or LRA) divided by that of the AAo.

Table 5.3 - Comparison of end diastolic velocity between vessels during physiologic and anemic states

Variable	Vessel pair	Physiologic state n	Mean ± SD	*P*-value	Anemic state n	Mean ± SD	*P*-value
End diastolic velocity (cm/s)	AAo CMA	11 11	20.1 ± 6.6 18.3 ± 4.5	0.422	11 11	28.6 ± 10.9 27.1 ± 6.6	0.505
	AAo CA	11 11	20.1 ± 6.6 24.5 ± 8.0	0.107	11 11	28.6 ± 10.9 28.3 ± 8.6	0.923
	AAo LRA	11 11	20.1 ± 6.6 23.4 ± 11.0	0.231	10 10	29.7 ± 10.8 21.0 ± 7.8	0.004
	CMA CA	11 11	18.3 ± 4.5 24.5 ± 8.0	0.038	11 11	27.1 ± 6.6 28.3 ± 8.6	0.530
	CMA LRA	11 11	18.3 ± 4.5 23.4 ± 11.0	0.212	10 10	28.0 ± 6.1 21.0 ± 7.8	0.015
	CA LRA	11 11	24.5 ± 8.0 23.4 ± 11.0	0.764	10 10	28.3 ± 9.1 21.0 ± 7.8	0.041

AAo = abdominal aorta. CA = celiac artery. CMA = cranial mesenteric artery. LRA = left renal artery. SD = standard deviation. Level of significance, α = 5%.

Table 5.4 - Comparison of peak systolic velocity ratio and time-averaged mean velocity ratio within vessels during physiologic and anemic states

Variable	Vessel	Physiologic state		Anemic state	
		n	Mean ± SD	Mean ± SD	*P*-value
Peak systolic velocity ratio	CMA	11	0.858 ± 0.243	0.902 ± 0.189	0.701
	CA	11	0.950 ± 0.255	0.906 ± 0.238	0.705
	LRA	10	0.587 ± 0.127	0.575 ± 0.165	0.865
Time-averaged mean velocity ratio	CMA	11	0.993 ± 0.370	0.939 ± 0.244	0.719
	CA	11	1.186 ± 0.358	0.923 ± 0.275	0.095
	LRA	8	1.004 ± 0.299	0.724 ± 0.240	0.014

AAo = abdominal aorta, CA = celiac artery, CMA = cranial mesenteric artery, LRA = left renal artery, SD = standard deviation. Level of significance, α = 5%. Time-averaged mean velocity ratio = time-averaged mean velocity of a splanchnic vessel (CMA, CA, or LRA) divided by that of the AAo.

5.5 DISCUSSION

Parenchymal pathology can compromise organ perfusion if, for example, interstitial effusion or infiltration exerts increased external pressure on its microcirculation. Organ intravascular pressure may be raised reducing perfusion pressure gradient between the heart and the diseased organ, and increasing resistance to flow. Congestion of capillaries with blood would produce a similar result. Blood velocity, as a function of perfusion pressure and vascular resistance would be reduced. The frequently used Doppler ultrasound method for detecting such hemodynamic alterations, especially in parenchymatous organs such as the kidney, is by estimating the resistance to blood flow with resistive index.[14,20,21] Increased tissue resistance to perfusion slows diastolic velocity more than systolic velocity, causing resistive index to increase. However, in animals resistive index of small vessels of visceral parenchyma (e.g. liver and spleen) or hollow organ walls (e.g. stomach and intestines) is more difficult to measure due to a high degree of mobility of these organs and poor quality of Doppler tracings. Moreover resistive index is known to vary with anatomic position of the sample volume, giving less consistent results with samples obtained farther away from the parenchymal microcirculation.[13] In such instances other velocity derivatives such as ratio of the closest accessible artery or arterial trunk of an organ to that of the AAo may be beneficial. Since the CMA and CA run almost parallel to the Doppler beam when using the imaging technique described earlier, accurate estimates of peak systolic velocity and time-averaged mean velocity of these vessels can be obtained using Doppler ultrasound. Similarly, good estimates of the aortic velocities can be obtained with Doppler angles below 60 degrees. A potential advantage of peak systolic velocity ratio or time-averaged mean velocity ratio might be lesser variability from the influence of different machines, operators, or populations under investigation.

A major drawback with this technique would be lack or difficulty of locating a specific artery for a splanchnic organ, both CMA and CA being non-specific arterial trunks supplying vast areas of the gastrointestinal tract or several organs respectively.

This preliminary study was designed to investigate the influence of acute, severe normovolemic anemia on hemodynamics of the spleen, kidneys, liver and gastrointestinal tract in the dog by comparing velocities of the different supply arteries. Results of paired comparisons of the AAo, CMA and CA during physiologic and anemic states were similar with no significant difference between corresponding velocities of vessel pairs, except peak systolic velocity of the AAo and CMA, and end diastolic velocity of the CMA and CA. This observation plus lack of significant difference in velocity ratios of the CMA and CA between anemic and physiologic states, suggest proportional increase in peak systolic velocity and time-averaged mean velocity of these vessels compared to those of the AAo. The proportional increase in velocities supports earlier reports that gastrointestinal blood flow increases more or less proportionally with cardiac output in acute normovolemic hemodilution in the dog.[3,6] Differences in results between physiologic and anemic states in the two exceptions mentioned above may be due to statistical errors related to small sample size, large standard deviations and a weak power of the statistical test.

The left renal peak systolic velocity and peak systolic velocity ratio were significantly lower than the corresponding values of each of the AAo, CMA and CA in both physiologic and anemic states. While no significant difference was found during the physiologic state between the LRA and each of the remaining vessels based on time-averaged mean velocity, time-averaged mean velocity ratio and end diastolic velocity, the same renal variables were significantly lower during the anemic state. Unpublished observations by these authors revealed a significant

reduction in renal end diastolic velocity during severe acute anemia with no significant change in the renal time-averaged mean velocity. These observations support an earlier report that the renal flow fraction of the cardiac output in acute normovolemic hemodilution is significantly reduced.[3]

Time-averaged velocity and time-averaged velocity ratio have revealed a relative reduction in renal hemodynamics during anemia compared to other abdominal splanchnic vessels and aortic hemodynamics. Velocity ratios may be useful for quantifying hemodynamics of highly mobile abdominal organs such as the spleen and liver in animals. The influence of different machines, operators, or populations investigated on values of peak systolic velocity ratio or time-averaged mean velocity ratio might be lower than on absolute values of Doppler parameters.

5.6 REFERENCES

1. Fronek K, Stahlgren LH. Systemic and regional hemodynamic changes during food intake and digestion in nonanesthetized dogs. Circ Res 1968;23:687-692.

2. Haddy FJ, Scott J, Fleischman M, *et al.* Effect of change in flow rate upon renal vascular resistance. Am J Physiol 1958;195:111-119.

3. Grupp I, Grupp G, Holmes JC, *et al.* Regional blood flow in anemia. J Appl Physiol 1972;33:456-461.

4. Vatner SF, Higgins CB, Franklin D. Regional circulatory adjustments to moderate and severe chronic anemia in conscious dogs at rest and during exercise. Circ Res 1972;30:731-740.

5. Fan F-C, Chen RYZ, Schuessler GB, *et al.* Effects of hematocrit variations on regional hemodynamics and oxygen transport in the dog. Am J Physiol 1980;238:H545-H552.

6. Race D, Dedichen H, Schenk JWR. Regional blood flow during dextran-induced normovolemic hemodilution in the dog. J Thorac Cardiovasc Surg 1967;53:578-586.

7. Wright CJ. The effect of severe progressive hemodilution on regional blood flow and oxygen consumption. Surgery 1976;79:299-305.

8. Rosberg B, Wulff K. Regional blood flow in normovolemic and hypovolemic hemodilution. An experimental study. Br J Anesth 1979;51:423-430.

9. Crystal GJ, Rooney MW, Salem MR. Regional hemodynamics and oxygen supply during isovolemic hemodilution alone and in combination with Adenosine-induced controlled hypotension. Anesth Analg 1988;67:211-218.

10. Barber FE, Baker DW, Nation AWC, *et al.* Ultrasonic duplex echo Doppler scanner. IEEE Trans Biomed Eng 1974;109-113.

11. Qamar MI, Read AE, Skidmore R, *et al.* Transcutaneous Doppler ultrasound measurement of celiac axis blood flow in man. Br J Surg 1985;72:391-393.

12. Maconi G, Parente F, Bollani S, *et al.* Factors affecting splanchnic hemodynamics in Crohn's disease: a prospective controlled study using Doppler ultrasound. Gut 1998;43:645-650.

13. Knapp R, Plotzeneder A, Frauscher F, *et al.* Variability of Doppler parameters in the healthy kidney: An anatomic-physiologic correlation. J Ultrasound Med 1995;14:427-429.

14. Sari A, Dinc H, Zibandeh A, *et al.* Value of resistive index in patients with clinical diabetic nephropathy. Invest Radiol 1999;34:718-721.

15. Rivolta R, Cardinale L, Lovaria A, *et al.* Variability of renal echo-Doppler measurements in healthy adults. J Nephrol 2000;13:110-115.

16. Pozniak MA, Kelcz F, D'Alessandro A. Sonography of renal transplants in dogs: The effect of acute tubular necrosis, cyclosporine nephrotoxicity, and acute rejection on resistive index and renal length. Am J Roentgenol 1992;158:791-797.

17. Nyland TG, Fisher BS, Doverspike M, *et al.* Diagnosis of urinary tract obstruction in dogs using duplex Doppler ultrasonography. Vet Radiol Ultrasound 1993;34:348-352.

18. Morrow KL, Salman MD, Lappin MR, *et al.* Comparison of the resistive index to clinical parameters in dogs with renal disease. Vet Radiol Ultrasound 1996;37:193-199.

19. Rivers BJ, Walter PA, Letourneau JG, *et al.* Estimation of arcuate artery resistive index as a diagnostic tool for aminoglycoside-induced acute renal failure in dogs. Am J Vet Res 1996;57:1536-1544.

20. Koch J, Jensen AL, Wenck A, *et al.* Duplex Doppler measurements of renal blood flow in a dog with Addison's disease. J Small Anim Pract 1997;38:124-126.

21. Rivers BJ, Walter PA, Polzin DJ, *et al.* Duplex Doppler estimation of intrarenal Pourcelot resistive index in dogs and cats with renal disease. J Vet Intern Med 1997;11:250-260.

22. Nyland TG, Fisher PE. Evaluation of experimentally induced canine hepatic cirrhosis using duplex Doppler ultrasound. Vet Radiol 1990;31:189-194.

23. Lamb CR, Burton CA, Carlisle CH. Doppler measurement of hepatic arterial flow in dogs: technique and preliminary findings. Vet Radiol Ultrasound 1999;40:77-81.

24. Riesen S, Schmid V, Gaschen L, *et al.* Doppler measurement of splanchnic blood flow during digestion in unsedated normal dogs. Vet Radiol Ultrasound 2002;43:554-560.

25. Kircher P, Lang J, Blum J, *et al.* Influence of food composition on splanchnic blood flow during digestion in unsedated normal dogs: a Doppler study. Vet J 2003;166:265-272.

26. Lamb CR, Mahoney PN. Comparison of three methods for calculating portal blood flow velocity in dogs using duplex Doppler ultrasonography. Vet Radiol Ultrasound 1994;35:190-194.

27. Mwanza T, Miyamoto T, Okumura M, *et al.* Ultrasonographic evaluation of portal vein hemodynamics in experimentally bile duct ligated dogs. Jpn J Vet Res 1998;45:199-206.

28. Gill RW. Measurement of blood flow by ultrasound: Accuracy and sources of error. Ultrasound Med Biol 1985;11:625-641.

29. Rasmussen K. Methodological problems related to measurement of quantitative blood flow with the ultrasound Doppler technique. Scand J Clin Lab Invest 1987;47:303-309.

30. Bahado-Singh R, Pirhonen J, Rahman F, *et al.* Effect of fetal anemia on splenic artery resistance index in red cell isoimmunization. J Soc Gynecol Invest 1995;2:146.

31. Bahado-Singh R, Oz U, Deren O, *et al.* Splenic artery Doppler peak systolic velocity predicts severe fetal anemia in rhesus disease. Am J Obstet Gynecol 2000;182:1222-1226.

32. Cosmi E, Mari G, Chiaie LD, *et al.* Noninvasive diagnosis by Doppler ultrasonography of fetal anemia resulting from parvovirus infection. Am J Obstet Gynecol 2002;187:1290-1293.

33. Nishie EN, Brizot ML, Liao AW, *et al.* A comparison between middle cerebral artery peak systolic velocity and amniotic fluid optical density at 450 nm in the prediction of fetal anemia. Am J Obstet Gynecol 2003;188:214-219.

34. Segata M, Mari G. Fetal anemia: New technologies. Curr Opin Obstet Gynecol 2004;16:153-158.

35. Schwartz SW, Chambless LE, Baker WH. Consistency of Doppler parameters in predicting arteriographically confirmed carotid stenosis. Stroke 1997;28:343-347.

36. Turck J. Peripheral arteries In: M. Hofer, ed. Teaching Manual of Color Duplex Sonography. New York: Thieme New York, 2001;69-76.

37. Koma LM, Spotswood TC, Kirberger RM, *et al.* Influence of normovolemic anemia on Doppler characteristics of the abdominal aorta and splanchnic vessels in Beagles. Am J Vet Res 2005;66:187-195.

38. Spotswood TC, Kirberger RM, Koma LM, *et al.* A canine normovolemic acute anemia model. Onderstepoort J Vet Res 2005;72:135-143.

39. Lobetti RG. The comparative role of hemoglobinemia and hypoxia in the development of nephropathy in the dog. J S Afr Vet Assoc 1996;67:188-198.

40. Eik-Nes SH, Marsal K, Kristoffersen K. Methodology and basic problems related to blood flow studies in human fetus. Ultrasound Med Biol 1984;10:329-337.

41. Nelson TR, Pretorius DH. The Doppler signal: Where does it come from and what does it mean? Am J Roentgenol 1988;151:439-447.

CHAPTER 6

Comparison of effects of uncomplicated canine babesiosis and canine normovolaemic anaemia on abdominal splanchnic Doppler characteristics – A preliminary investigation

L M Koma[a*], R M Kirberger[a], A L Leisewitz[a], L S Jacobson[a], P J Becker[b] and P Bland van den Berg[c]

Based on an article submitted in May 2005 to the South African Journal of Veterinary Association

[a] Department of Companion Animal Clinical Studies, Faculty of Veterinary Science, University of Pretoria, Private Bag X04, Onderstepoort, 0110 Republic of South Africa.

[*] Author for correspondence: Department of Surgery and Reproduction, Faculty of Veterinary Medicine, Makerere University, P.O. Box 7062 Kampala, Uganda.
E-mail: lee.koma@vetmed.mak.ac.ug

[b] Medical Research Council, University of Pretoria, Private Bag X385, 1 Soutpansberg Road, Pretoria, 0001, Republic of South Africa.

[c] Onderstepoort Veterinary Academic Hospital, Faculty of Veterinary Science, University of Pretoria, Private Bag X04, Onderstepoort, 0110 Republic of South Africa.

6.1 ABSTRACT

A preliminary study was conducted to compare uncomplicated canine babesiosis (CB) and experimentally induced normovolaemic anaemia (EA) using Doppler ultrasonography of abdominal splanchnic vessels. Fourteen dogs with uncomplicated CB were investigated together with 11 healthy Beagles during severe EA, moderate EA and the physiological state as a control group. Canine babesiosis was compared with severe EA, moderate EA and the physiological state using Doppler variables of the abdominal aorta, cranial mesenteric artery (CMA), coeliac, left renal and interlobar, and hilar splenic arteries, and the main portal vein. Patterns of haemodynamic changes during CB and EA were broadly similar and were characterised by elevations in velocities, and reductions in resistance indices in all vessels except the renal arteries when compared with the physiological state. Aortic and CMA peak systolic velocities, and CMA end diastolic and time-averaged mean velocities in CB were significantly lower ($P < 0.023$) than those in severe EA. Patterns of renal haemodynamic changes during CB and EA were similar. However, the renal patterns differed from those of aortic and gastrointestinal arteries, having elevations in vascular resistance indices, a reduction in end diastolic velocity and unchanged time-averaged mean velocity. The left renal artery resistive index in CB was significantly higher ($P < 0.025$) than those in EA and the physiological state. Renal interlobar artery resistive and pulsatility indices in CB were significantly higher ($P < 0.016$) than those of moderate EA and the physiological state. The similar haemodynamic patterns in CB and EA are attributable to anaemia, while significant differences may be attributed to pathophysiological factors peculiar to CB.

Key words: anaemia, canine babesiosis, haemodynamics, Doppler ultrasonography, renal artery, resistive index.

6.2 INTRODUCTION

The virulent canine hemoprotozoan parasite, Babesia canis rossi, is widespread in South Africa[30]. It has long been recognised that the disease caused by this parasite can involve multiple organs or systems, and result in a wide variety of clinical manifestations[28,29]. Typical canine babesiosis (CB) manifests as fever, anorexia and anaemia, with parasites readily demonstrated in infected red blood cells of a peripheral blood smear[29]. Atypical forms of CB may manifest as a chronic disease, or may involve one or more organs such as the blood, spleen, kidney, liver, gastrointestinal tract, eyes or body systems such as cardiovascular, respiratory, nervous and musculoskeletal[3,29]. Parasites may be difficult to demonstrate in peripheral blood smears from atypical forms of the disease[29]. More recently the terms uncomplicated and complicated CB have been used in preference to typical and atypical CB respectively, and the involvement of multiple organs is referred to as multiple organ damage / dysfunction syndrome[17,19,29, 42]. Despite years of dedicated research, disease mechanisms leading to multiple organs dysfunction syndrome remains subjects of investigation[5,17,18,25,36,40].

Systemic[19] and microvascular (arterioles, capillaries and postcapillary venules[10])[28,29] haemodynamic disturbances are thought to play significant roles in the pathophysiology and outcome of CB due to B. c. rossi infection. Hypotension is known to occur in some forms of the disease, and reduction in mean systemic arterial pressure in dogs with severe and complicated disease provides evidence of disturbed systemic haemodynamics[19]. Haemoconcentration[5] and the occurrence of ascites, and oedema at various locations such as the subcutis or joints[28,29] are also evidence of systemic haemodynamic alterations. Blockage of microvessels through sequestration of erythrocytes in various organs e.g. the brain, liver, kidney, and spleen has been frequently reported at postmortem[3,29]. Hypotension may favour sequestration within microvessels[36]. The occurrence of sequestration led to a hypothesis of hypoperfusion in

microvessels that is thought to contribute to the development of multiple organs dysfunction syndrome in complicated CB[3,29]. Many pathologic processes and clinical manifestations of CB correlate with those of bovine babesiosis caused by Babesia bovis[36], or human malaria caused by Plasmodium falciparum[6,28,29,36]. In human cerebral malaria, evidence of localised hypoperfusion in microvessels has been shown by single photon emission computed tomography[21] and electron microscopy[11]. Further, cases of falciparum malaria presented with renal failure were reported to have compartmentalised reduction of renal cortical perfusion, and reduced or normal total renal blood flow as determined by scintigraphy[38]. In some malaria patients without renal failure, reduced mean systemic arterial pressure and renal vascular resistance, and increased renin activity have been reported[37]. In cerebral malaria, trans-cranial Doppler ultrasonography showed normal or hyperdynamic circulation of the middle cerebral artery[7,21] despite the presence of localised hypoperfusion in cerebral microvessels[21].

Little attention has been paid to the investigation of haemodynamic pathophysiology of CB, or its clinical evaluation in uncomplicated and complicated diseases. No report on microvascular or global haemodynamics of the commonly affected organs could be found. Knowledge of organ haemodynamic changes in CB will improve our understanding of the disease pathophysiology. Clinical evaluation of haemodynamics may permit early identification of potential complications or improve management of complicated cases, and monitor the disease response to therapy. The aim of this study was to investigate abdominal splanchnic haemodynamics in uncomplicated CB by use of Doppler ultrasonography, and compare these with the haemodynamics of a control group of normal dogs in various states of experimentally induced normovolaemic anaemia (EA). We hypothesised that there would be a significant increase in abdominal splanchnic haemodynamics during EA compared to the physiological state, and haemodynamic differences between uncomplicated CB and EA, and the physiological state.

6.3 MATERIALS AND METHODS

Fourteen dogs of various breeds and ages, diagnosed with uncomplicated CB by microscopic detection of B. canis parasites within red blood cells of a thin capillary blood smear (from the tip of the pinna), and with no evidence of confirmed or suspected concurrent ehrlichiosis were examined. Presence of moderate to severe lymphadenopathy of the mandibular, parotid and popliteal lymph nodes; epistaxis; petechial hemorrhages of the oral and conjunctival mucosae; neutropenia seen in a peripheral thin blood smear or presence of morulae in monocytes were considered suspicious for concurrent ehrlichiosis (A L Leisewitz, Onderstepoort Veterinary Animal Hospital, pers. comm., 2003). All dogs were seen as outpatients at the Onderstepoort Veterinary Academic Hospital during one season from September 2003 to May 2004. Any dog that received treatment other than, or in addition to, diminazene aceturate (Dimisol, Virbac Animal Health, Halfway House, Republic of South Africa) was excluded from the study. Other exclusion criteria were clinical collapse (non-ambulatory), positive in-saline agglutination (indicating concurrent secondary immune-mediated haemolytic anaemia.[8]), haematocrit (Hct) greater than 37% or lower than 14%, or Dobermans, Spaniels, Great Danes and Irish Wolfhounds that are predisposed to dilated cardiomyopathy. All dogs were first treated with diminazene aceturate and then admitted to the study for Doppler examinations. Owner consent was obtained in all cases. The Animal Use and Care Committee of the University of Pretoria approved the study.

After admission, dogs were excluded if found with any disorder of the respiratory, cardiovascular or gastrointestinal system, or of the liver, spleen or kidneys that was unrelated to CB (such as congenital renal hypoplasia, hydronephrosis, neoplasia or intussusception as determined by thoracic radiography, echocardiography or abdominal ultrasound). Blood smear

examination was repeated to confirm the presence of Babesia parasites. Full blood count was performed to screen haemograms for any abnormalities that were unrelated to CB. Total serum protein, creatinine and blood urea nitrogen levels were recorded in all dogs.

Doppler examinations of the abdominal aorta (AAo), cranial mesenteric artery (CMA), coeliac artery (CA), left renal artery (LRA), one of the renal interlobar arteries (ILA), one of the hilar splenic arteries (HSA) and main portal vein (MPV) were then performed on all selected dogs, commencing within 1-2 hours after treatment, and completed within 4 hours. Dogs were discharged the next day.

One investigator (LMK) carried out all examinations without administering any anaesthesia or sedation. The ventral and left lateral abdomen, and right lateral thorax from the 9th to 13th ribs were clipped, cleaned and covered with acoustic gel. For general abdominal imaging dogs were placed in dorsal recumbency. The spleen was imaged in parasagittal, transverse, and oblique planes, and the left kidney was imaged in dorsal, transverse, and oblique planes slightly caudal in position to that of the spleen. Right lateral recumbency was used for imaging the AAo, CMA, CA, LRA, ILA and HSA in a parasagittal or dorsal plane. Dogs were then turned into left lateral recumbency to image the MPV in dorsal and transverse planes through the right 9-12th intercostal spaces caudal to the liver. All the examinations were carried out using an ultrasound-imaging machine (Sonoline Omnia, Siemens Medical Systems Inc., Ultrasound, Erlangen, Germany) with a convex array, linear array or phased array transducer. B-mode examination of the general abdominal cavity, organs and AAo were done with a 5.0 MHz convex array transducer; identification and evaluation of the vessels was done with a 7.5 MHz linear array transducer or sometimes with a convex array transducer. The MPV was identified with a 6.0 MHz phased array transducer. All machine settings, including overall gain, depth compensation gain, edge enhancement, focus and line density were adjusted during each examination to obtain optimal image quality.

Doppler examinations of the AAo and MPV were performed at 3.5 MHz Doppler frequency. Within the AAo the sample window was placed anywhere along its length cranial to the origin of the left renal artery. The sample window for the MPV was placed at the best location in the vessel, usually just caudal to the liver, where a long axis vessel-beam intercept angle of 60° or less could be obtained from the intercostal approach. Evaluation of the CMA, CA, LRA, ILA and HSA were performed at 5.2 MHz Doppler frequency, or sometimes at 3.5 MHz for the CMA and CA. The sample window in the CMA, CA or LRA was placed within the vessel about 5 mm away from the aortic origin. The sample window for the ILA was placed within the renal pelvis 5-10 mm from the hilus, and for the HSA was placed about 5 mm from the splenic hilus, within or outside the parenchyma. Using a 7.5 MHz frequency on B-mode and colour Doppler facilitated the placement of these sample windows.

In the AAo and MPV, placing one cursor of the sample window close to each inner surface of the opposite vessel walls was done as a modification of the technique of uniform insonation[14]. This kept the size of the sample window within at least two thirds of the vessel diameter and avoided wall artefacts or spectral contamination from adjacent vessels. In the CMA, CA and LRA cursors of the sample window were positioned transversely across each vessel diameter as it coursed towards the transducer. In all cases, except the ILA and HSA, the vessel-beam alignment was angle-corrected before recording the spectral tracing. Angle correction was assisted by manual adjustment of the transducer, and by the electronic steering capacity of the linear array transducer. The vessel-beam angle achieved was recorded. Machine settings were optimised for high sensitivity imaging in the Doppler mode. Doppler variables recorded were resistive index and pulsatility index for all arteries, and additionally peak systolic velocity, end diastolic velocity and time-averaged mean velocity for the larger arteries. Ratios of peak systolic velocity and time-averaged mean velocity of a splanchnic

artery to the corresponding variables of the AAo were calculated. In the MPV, peak velocity time-averaged mean velocity, blood flow and congestion index were recorded. All Doppler examinations had a simultaneous electrocardiographic (ECG) tracing, from which heart rate was calculated.

For some variables fewer observations were recorded than the number of dogs investigated for various reasons. These were ECG malfunctioning or animal's intolerance to placement of ECG pads (heart rate), excessive vessel mobility (HSA), or obscurity by lung or gastrointestinal gas (MPV, CA) and time constraints.

Abdominal organs were evaluated on B-mode. Echogenicity of the spleen, liver and kidneys were subjectively compared to each other. Renal function was estimated by plasma creatinine level. Measurement of the thickest area of the spleen estimated its size. The diameter of the largest splenic vein branch in the splenic body region was measured at the hilus from a long axis view, and its cross sectional area was calculated. The largest short axis cross sectional area of the MPV was obtained by using the cine loop function for up to about 120 frames, and utilising the elliptical program of the onboard computer. This minimised errors of variation in the cross sectional area with time due to respiration. Doppler spectra of individual vessels were evaluated for their flow patterns with the help of a simultaneous ECG tracing.

During each examination, an attempt was made to obtain measurements from spectral cycles whose preceding R-R intervals were approximately equal, excluding obvious sinus arrhythmias. The value recorded for heart rate and each Doppler variable was obtained by averaging three measurements or calculations from three ECG or Doppler spectral cycles. Doppler variables were measured with the onboard computer. Pulsatility index (PI) was calculated from the equation[33]:

PI = (Peak systolic velocity – end diastolic velocity)/ Time-averaged mean velocity.

Resistive index (RI) was calculated from the equation[33]:

RI = (Peak systolic velocity – end diastolic velocity) / Peak systolic velocity.

Blood flow was computed using the equation[31]:

Blood flow = cross sectional area x time-averaged mean velocity.

Congestion index was calculated using the equation[32]:

Congestion index = cross sectional area / Time-averaged mean velocity.

Results of each examination were entered into a spreadsheet program (MS Excel, Microsoft Corporation, Redmond, Washington, USA) on a personal computer. All ultrasonographic procedures were recorded on videotape for possible re-evaluation and future reference. All data were tested with the Shapiro-Wilk test and were normally distributed. The data are presented as mean ± standard deviation (SD).

Data from uncomplicated CB were compared with similar data from 11 healthy Beagles obtained before withdrawal of blood (mean ± SD Hct 47.5 ± 2.2%, physiological state), after repetitive blood withdrawal to produce acute severe normovolaemic anaemia (mean ± SD Hct 16.0 ± 0.77%, severe EA), and during recovery (mean ± SD Hct 26.3 ± 0.74%, moderate EA). Comparison was done using the two-group *t*-test providing for unequal variances (Welch *t*-test) at the 0.05 level of significance. A statistical software program (Stata Release 8, Stata Press, 702 University Drive East, College Station, Texas 77840, USA) was used to perform the data analysis.

6.4 RESULTS

Eighteen dogs with uncomplicated CB were admitted to the study. Four of the 18 dogs were excluded because they were in-saline agglutination positive, had Hct higher than 37% or had clinical complications a week later. Of the remaining 14, there were 8 males and 6 females comprising of 7 large breeds, 4 small to medium breeds and 3 crossbreeds. Mean ± SD age

was 17.8 ± 14.9 months (range 2-56 months), mean ± SD body weight was 17.7 ± 13.1 Kg (range 5.4-30.6 Kg), and mean ± SD Hct was 21.3 ± 5.1% (14.6-32.4%).

Mean ± SD total serum protein levels in uncomplicated CB, severe EA and moderate EA were all within the normal reference range. Mean ± SD creatinine and blood urea nitrogen of uncomplicated CB dogs were also within the normal reference ranges (Table 1).

Comparisons of severe and moderate EA with the physiological state using Doppler variables were reported elsewhere[22, 23]. The current study revealed that uncomplicated CB, severe EA and moderate EA had similar patterns of haemodynamic changes (Figs. 1-5) when compared to the physiological state. Within this broad picture, patterns of renal haemodynamic changes involving all Doppler variables, except the peak systolic velocity, differed from those in the AAo, CMA, CA, HSA and MPV as detailed in the following paragraphs.

Table 6.1: Hematocrit, heart rate, and total serum protein, creatinine and urea levels in uncomplicated canine babesiosis, experimentally induced normovolemic anemia, and the physiologic state

Group	Hematocrit (%)		Heart rate (b/m)		Total serum protein (g/l)		Creatinine (µmol/l)		Blood urea nitrogen (mmol/l)	
	n	Mean ± SD	n	Mean ± SD	n	Mean ± SD	n	Mean ± SD	n	Mean ± SD
Uncomplicated CB	14	21.3 ± 5.1	12	114.0 ± 23.8	14	61.9 ± 13.0	14	67.1 ± 20.7	14	6.1 ± 3.2
Severe EA	11	16.0 ± 0.8	11	134.0 ± 13.0	10	54.0 ± 3.2	-	-	-	-
Moderate EA	11	26.3 ± 0.7	11	105.4 ± 7.5	5	61.8 ± 3.0	-	-	-	-
Physiologic state	11	47.5 ± 2.2	10	95.9 ± 16.3	11	59.8 ± 3.0	11	68.4 ± 8.1	3	4.5 ± 0.7
Normal reference ranges						53-75		40-133		3.6-8.9

CB = canine babesiosis. EA = experimentally induced normovolemic anemia. n = sample size. SD = standard deviation.

There was no discernible pattern for haemodynamic change, or significant difference between uncomplicated CB and severe EA or moderate EA regarding resistive indices of the AAo, CMA, CA and HSA when compared to the physiological state (Fig. 1, Table 2). In the LRA, the resistive index increased from 0.656 during the physiological state through 0.723 during severe EA to 0.779 during uncomplicated CB. Left renal artery mean resistive index during uncomplicated CB was significantly higher than those during severe EA (P = 0.014), moderate EA (P = 0.025) and the physiological state (P < 0.001). Renal ILA mean resistive index during uncomplicated CB was significantly higher than those during moderate EA (P = 0.009) and the physiological state (P = 0.01), but was not significantly different from that during severe EA.

There was a tendency for pulsatility indices of the AAo, CMA, CA and HSA to decrease during uncomplicated CB, severe and moderate EA, but a tendency towards increases for pulsatility indices of the LRA and ILA (Fig. 2, Table 2). Mean pulsatility index of the AAo during uncomplicated CB was significantly (P = 0.029) lower than that during the physiological state but was not significantly different from those during severe or moderate EA. The LRA and ILA mean pulsatility indices during uncomplicated CB were significantly ($P \leq 0.016$) higher than the corresponding variables during the physiological state. Additionally, the ILA mean pulsatility index during uncomplicated CB was significantly (P = 0.014) higher than that during moderate EA. There was no significant difference between uncomplicated CB and severe EA based on pulsatility indices of the LRA and ILA, or between uncomplicated CB and moderate EA regarding pulsatility index of the LRA. Also, no significant difference was found between uncomplicated CB and severe EA, moderate EA or the physiological state based on mean pulsatility indices of the CMA, CA or HSA.

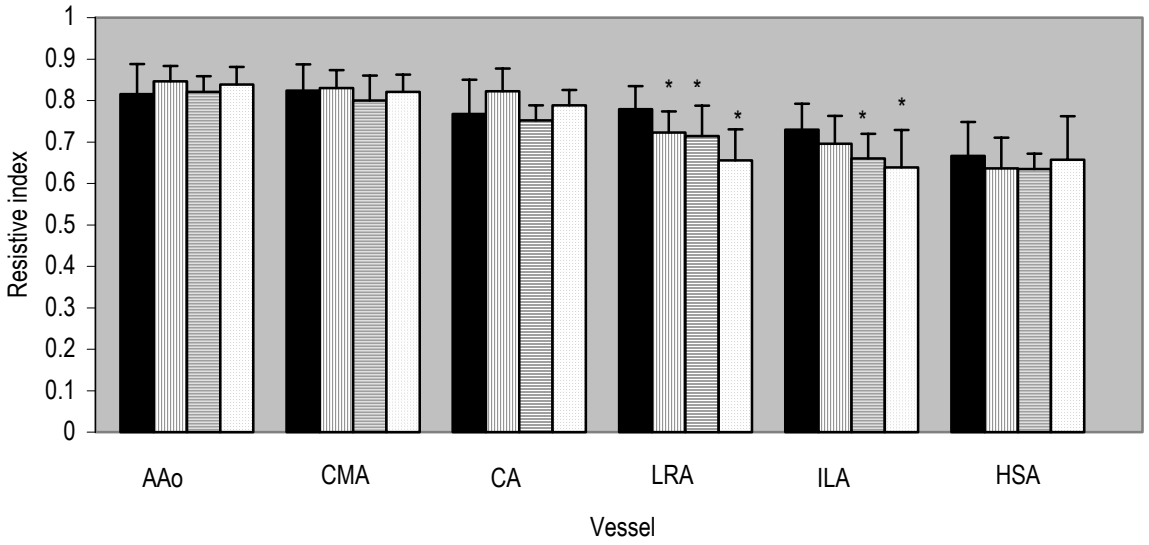

Fig. 6.1: Resistive index in dogs with uncomplicated CB, severe EA, moderate EA, and the physiologic state. Data are shown as mean ± SD.

Uncomplicated CB. Severe EA.

Moderate EA. Physiologic state.

*Denotes a significant difference between uncomplicated CB and the marked group.

Table 6.2: Resistive index, pulsatility index and congestion index during uncomplicated babesiosis, experimental anemia and the physiologic state.

Variable	Vessel	n	Uncomplicated CB Mean ± SD	n	Severe EA Mean ± SD	*P*	n	Moderate EA Mean ± SD	*P*	n	Physiologic state Mean ± SD	*P*
Resistive index	AAo	14	0.816 ± .072	11	0.846 ± .037	0.184	11	0.821 ± .038	0.819	11	0.839 ± .042	0.334
	CMA	14	0.824 ± .063	11	0.830 ± .043	0.790	11	0.800 ± .060	0.335	11	0.821 ± .042	0.860
	CA	13	0.768 ± .083	11	0.823 ± .055	0.064	10	0.752 ± .037	0.550	11	0.788 ± .037	0.431
	LRA	14	0.779 ± .055	11	0.723 ± .051	0.014	11	0.715 ± .073	0.025	10	0.656 ± .074	< 0.001
	ILA	14	0.730 ± .062	11	0.695 ± .068	0.205	11	0.660 ± .060	0.009	11	0.638 ± .090	0.010
	HSA	14	0.667 ± .082	11	0.636 ± .074	0.346	11	0.635 ± .037	0.210	10	0.657 ± .105	0.818
Pulsatility index	AAo	14	2.409 ± .770	11	2.555 ± .517	0.576	11	2.470 ± .494	0.813	11	3.214 ± .912	0.029
	CMA	14	2.296 ± .611	11	2.316 ± .566	0.933	11	2.096 ± .561	0.403	11	2.661 ± .632	0.160
	CA	13	1.965 ± .619	11	2.235 ± .518	0.256	10	1.776 ± .267	0.335	11	2.246 ± .510	0.236
	LRA	14	1.807 ± .391	11	1.566 ± .378	0.131	11	1.650 ± .554	0.433	10	1.343 ± .317	0.004
	ILA	14	1.487 ± .303	11	1.285 ± .221	0.066	11	1.191 ± .258	0.014	11	1.202 ± .249	0.016
	HSA	14	1.191 ± .319	11	1.081 ± .242	0.336	11	1.112 ± .216	0.467	10	1.351 ± .445	0.346
Congestion index	MPV	11	0.043 ± .022	9	0.030 ± .013	0.158	10	0.045 ± .020	0.818	9	0.066 ± .019	0.028

For each variable *P* value represents comparison of uncomplicated CB with the group represented in the preceding column. Significance was set at $P \leq 0.05$. CB = canine babesiosis. EA = experimentally induced normovolemic anemia. AAo = abdominal aorta. CMA = cranial mesenteric artery. CA = celiac artery. LRA = left renal artery. ILA = interlobar artery. HSA = hilar splenic artery. MPV = main portal vein.

Congestion index of the MPV had a tendency to decrease in all groups when compared to the physiological state. Mean MPV congestion index during uncomplicated CB was significantly (P = 0.028) lower than that during the physiological state but was not significantly different from that during severe or moderate EA (Table 2).

Peak velocities (peak systolic velocity and peak velocity) of all the vessels had a tendency to increase in all groups when compared to the physiological state. Peak velocities during uncomplicated CB were significantly ($P \leq 0.014$) lower than those during severe EA but not significantly different from those of moderate EA or the physiological state in the AAo, CMA and MPV (Fig. 3, Table 3). Left renal artery mean peak systolic velocity during uncomplicated CB was significantly ($P \leq 0.011$) higher than those during moderate EA and the physiological state, but was not significantly different from that during severe EA. There was no significant difference between uncomplicated CB and severe EA, moderate EA or the physiological state based on mean peak systolic velocity of the CA.

The aortic, CMA and CA mean end diastolic velocities had a tendency to increase, but the same variable in the LRA tended to decrease in all groups when compared to the physiological state (Fig. 4, Table 3). The CMA mean end diastolic velocity during uncomplicated CB was significantly (P = 0.023) lower than that during severe EA but was not significantly different from that during moderate EA or the physiological state. There was no significant difference between uncomplicated CB and any group based on mean end diastolic velocities of the AAo, CA and LRA.

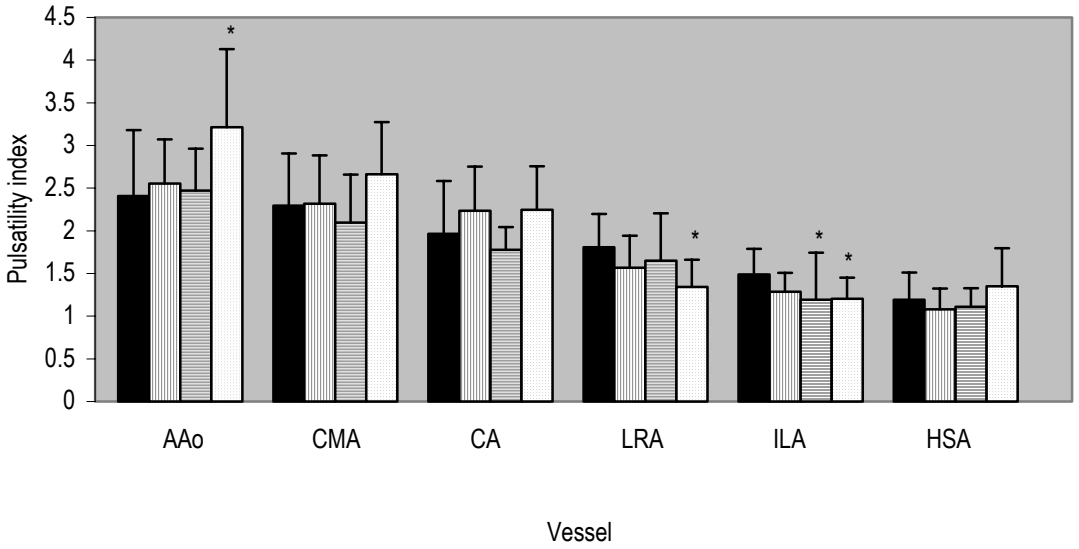

Figure 6.2: Pulsatility index in dogs with uncomplicated CB, severe EA, moderate EA, and the physiologic state. Data are shown as mean ± SD.

Uncomplicated CB. Severe EA.

Moderate EA. Physiologic state.

*Denotes a significant difference between uncomplicated CB and the marked group.

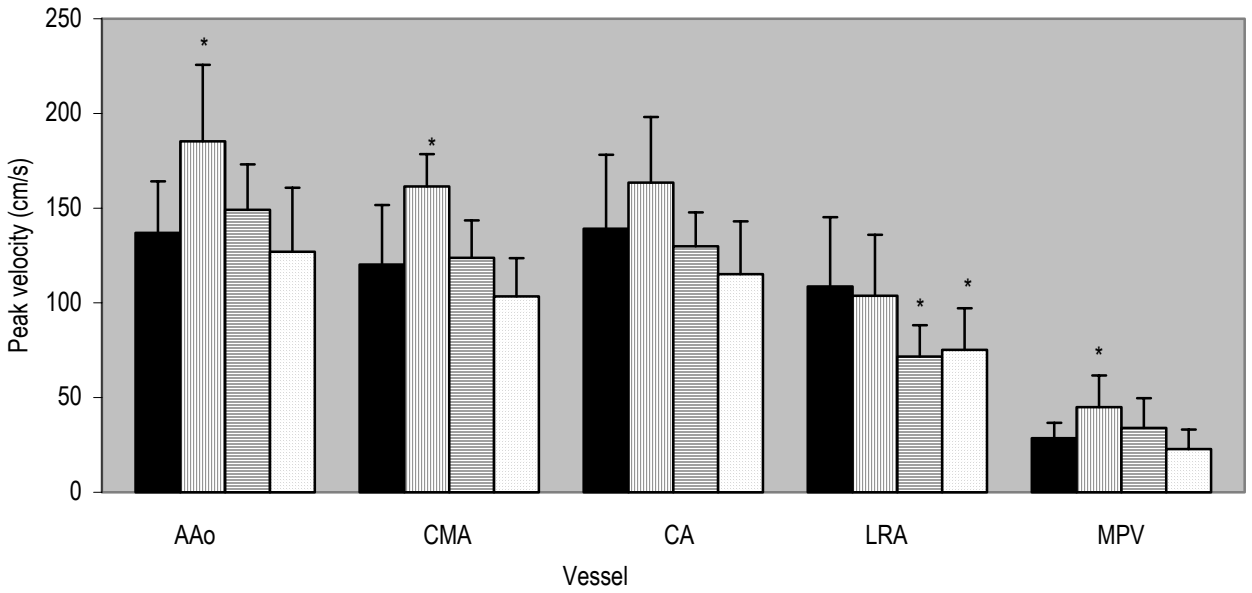

Figure 6.3: Peak velocities in dogs with uncomplicated CB, severe EA, moderate EA, and the physiologic state. Data are shown as mean ± SD.

Uncomplicated CB. Severe EA.

Moderate EA. Physiologic state.

*Denotes a significant difference between uncomplicated CB and the marked group.

Table 6.3: Blood velocities during uncomplicated canine babesiosis, experimental anemia and the physiologic state.

Variable	Vessel	Uncomplicated CB		Severe EA		*P*	Moderate EA		*P*	Physiologic state		*P*
		n	Mean ± SD	n	Mean ± SD		n	Mean ± SD		n	Mean ± SD	
Peak systolic velocity (cm/s)	AAo	14	137.0 ± 27.4	11	185.3 ± 40.4	0.003	11	149.1 ± 24.0	0.250	11	127.1 ± 33.7	0.437
	CMA	14	120.3 ± 31.3	11	161.4 ± 17.2	< 0.001	11	123.9 ± 19.8	0.730	11	103.4 ± 20.2	0.115
	CA	13	139.1 ± 39.1	11	163.5 ± 34.6	0.118	10	129.9 ± 17.9	0.458	11	115.2 ± 27.8	0.095
	LRA	14	108.6 ± 36.7	11	103.8 ± 32.1	0.731	11	71.7 ± 16.5	0.003	10	75.2 ± 22.0	0.011
Peak velocity (cm/s)	MPV	12	28.5 ± 8.0	10	45.0 ± 16.8	0.014	10	34.0 ± 15.7	0.334	9	22.8 ± 10.3	0.185
End diastolic velocity (cm/s)	AAo	14	24.8 ± 9.1	11	28.6 ± 10.9	0.368	11	25.9 ± 3.7	0.693	11	20.1 ± 6.6	0.142
	CMA	14	20.5 ± 6.6	11	27.1 ± 6.6	0.023	11	25.1 ± 9.8	0.205	11	18.3 ± 4.5	0.324
	CA	13	32.0 ± 12.1	11	28.3 ± 8.6	0.398	10	32.4 ± 6.6	0.903	11	24.5 ± 8.0	0.084
	LRA	14	23.9 ± 9.5	10	21.0 ± 7.8	0.427	10	22.8 ± 7.5	0.765	10	25.7 ± 8.2	0.616
Time averaged mean velocity (cm/s)	AAo	14	32.3 ± 10.3	11	38.8 ± 11.8	0.161	11	33.8 ± 3.3	0.605	11	22.9 ± 7 .6	0.015
	CMA	14	25.8 ± 6.8	11	34.5 ± 6.4	0.003	11	31.4 ± 7.8	0.069	11	21.0 ± 5.8	0.068
	CA	13	37.3 ± 16.3	11	33.6 ± 6.2	0.464	10	33.2 ± 7.2	0.424	11	25.9 ± 9.0	0.042
	LRA	14	25.5 ± 9.8	11	24.8 ± 9.0	0.845	10	17.7 ± 6.8	0.031	8	24.1 ± 8.6	0.734
	MPV	11	16.6 ± 6.0	9	21.6 ± 10.1	0.210	10	18.0 ± 8.6	0.685	9	10.6 ± 2.8	0.009

For each variable *P* value represents comparison of uncomplicated CB with the group represented in the preceding column. Significance was set at $P \leq 0.05$. CB = canine babesiosis. EA = experimentally induced normovolemic anemia. AAo = abdominal aorta. CMA = cranial mesenteric artery. CA = celiac artery. LRA = left renal artery. MPV = main portal vein.

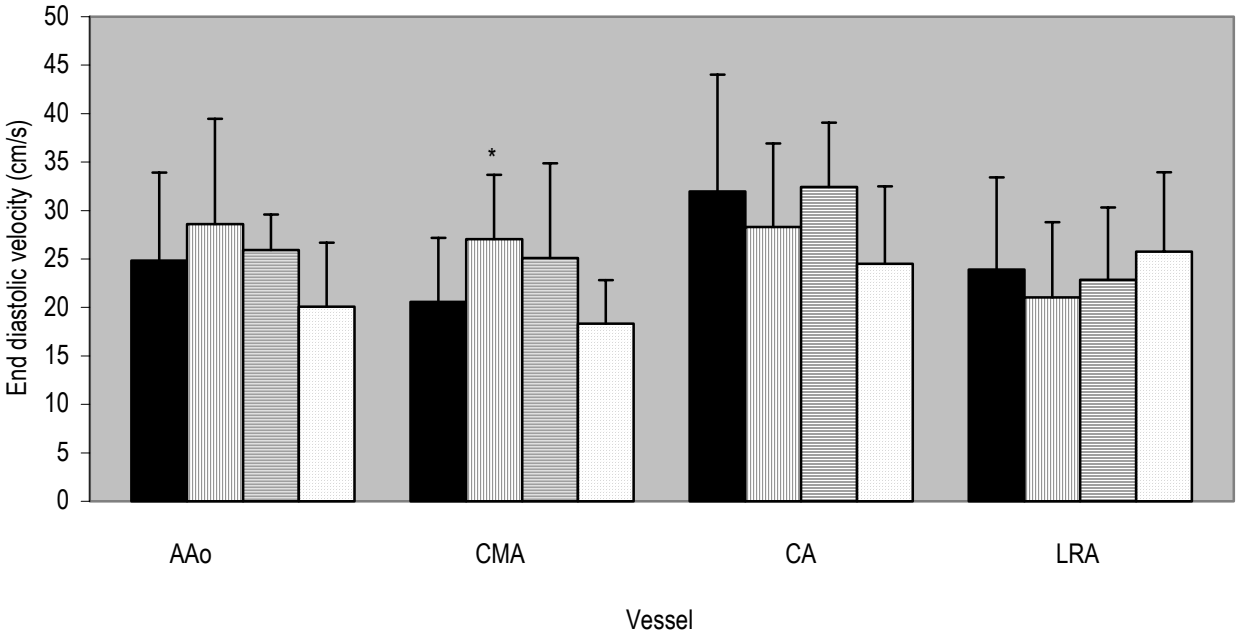

Figure 6.4: End diastolic velocity in dogs with uncomplicated CB, severe EA, moderate EA, and the physiologic state. Data are shown as mean ± SD.

Uncomplicated CB. Severe EA.

Moderate EA. Physiologic state.

*Denotes a significant difference between uncomplicated CB and the marked group.

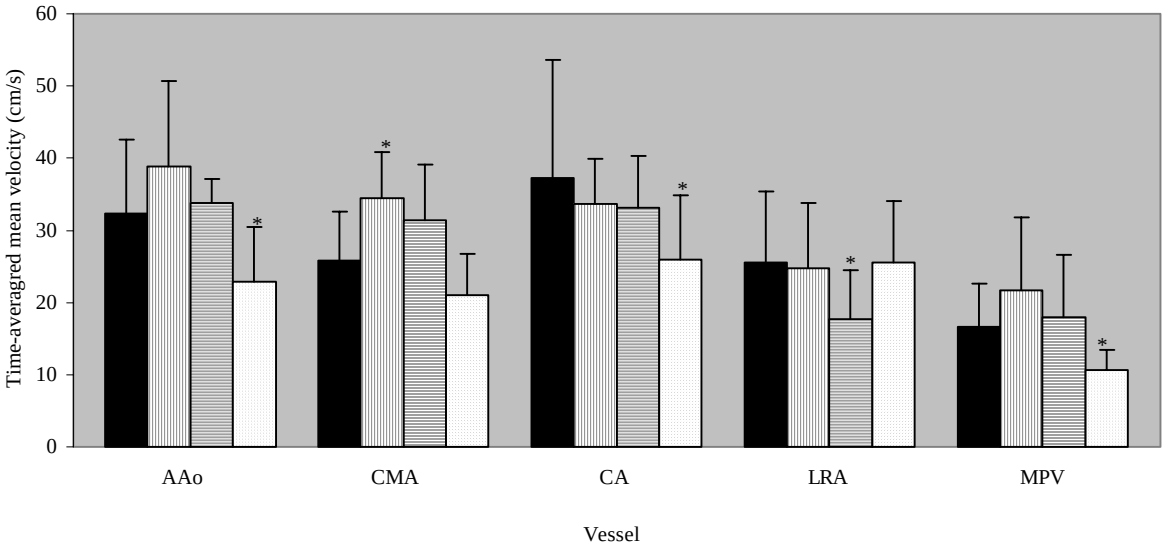

Figure 6.5: Time-averaged mean velocity in dogs with uncomplicated CB, severe EA, moderate EA, and the physiologic state. Data are shown as mean ± SD.

Uncomplicated CB.

Severe EA.

Moderate EA.

Physiologic state.

*Denotes a significant difference between uncomplicated CB and the marked group.

Table 6.4: Velocity ratios and blood flow during uncomplicated canine babesiosis, experimental anaemia and the physiologic state.

Variable	Vessel	Uncomplicated CB		Severe EA		*P*	Moderate EA		*P*	Physiologic state		*P*
		n	Mean ± SD	n	Mean ± SD		n	Mean ± SD		n	Mean ±SD	
Peak systolic velocity ratio	CMA	14	0.888 ± .220	11	0.902 ± .189	0.853	11	0.849 ± .186	0.650	11	0.858 ± .243	0.762
	CA	13	1.024 ± .262	11	0.906 ± .238	0.261	10	0.859 ± .083	0.049	11	0.950 ± .255	0.492
	LRA	14	0.813 ± .305	11	0.570 ± .158	0.018	11	0.488 ± .119	0.002	10	0.587 ± .127	0.022
Time averaged mean velocity ratio	CMA	14	0.889 ± .412	11	0.939 ± .244	0.706	11	0.935 ± .236	0.729	11	0.993 ± .370	0.511
	CA	13	1.198 ± .475	11	0.923 ± .275	0.092	10	0.984 ± .225	0.170	11	1.186 ± .358	0.944
	LRA	13	0.755 ± .298	11	0.668 ± .235	0.435	10	0.515 ± .193	0.029	8	1.004 ± .299	0.081
Blood flow (ml/kg/min)	MPV	11	73.9 ± 25.4	9	66.2 ± 38.8	0.616	10	61.5 ± 34.1	0.361	9	36.8 ± 13.0	0.001

For each variable *P* value represents comparison of uncomplicated CB with the group represented in the preceding column. Significance was set at $P \leq 0.05$. CB = canine babesiosis. EA = experimentally induced normovolemic anaemia. AAo = abdominal aorta. CMA = cranial mesenteric artery. CA = celiac artery. LRA = left renal artery. MPV = main portal vein.

Mean time-averaged mean velocities of the AAo, CMA, CA and MPV had a tendency to increase in all groups when compared to the physiological state, but that of the LRA tended to decrease during moderate EA (Fig. 5, Table 4). The aortic, CA and MPV mean time-averaged mean velocities during uncomplicated CB were significantly ($P \leq 0.042$) higher than those during the physiological state but were not significantly different from those during severe or moderate EA. The LRA mean time-averaged mean velocity during uncomplicated CB was significantly ($P = 0.031$) higher than that during moderate EA but was not significantly different from that during severe EA or the physiological state. The CMA mean time-averaged mean velocity during uncomplicated CB was significantly ($P = 0.003$) lower than that during severe EA but was not significantly different from that during moderate EA or the physiological state.

Mean peak systolic velocity ratios of the CMA, CA and LRA had a tendency to increase during uncomplicated CB and severe EA but a tendency to fall during moderate EA when compared to the physiological state (Table 4). Mean peak systolic velocity ratio of the LRA during uncomplicated CB was significantly ($P \leq 0.022$) higher than that during severe EA, moderate EA and the physiological state. Mean peak systolic velocity ratio of the CA during uncomplicated CB was significantly ($P = 0.049$) higher than that during moderate EA but was not significantly different from that during severe EA or the physiological state.

Mean time-averaged mean velocity ratios of all the vessels had a tendency to decrease in all groups when compared to the physiological state, except that the CA ratio during uncomplicated CB had a tendency to increase (Table 4). The LRA mean time-averaged mean velocity ratio during uncomplicated CB was significantly ($P = 0.029$) higher than that during moderate EA. No significant difference was found between other groups based on mean time-averaged mean velocity ratio.

Blood flow of the MPV had a tendency to increase in all groups when compared to the physiological state (Table 4). Blood flow during uncomplicated CB was significantly (*P* = 0.001) higher than that during the physiological state, but was not significantly different from that during severe or moderate EA.

6.5 DISCUSSION

6.5.1 Aortic, gastrointestinal and splenic haemodynamics

The similarity between uncomplicated CB and EA regarding patterns of change in Doppler variables is most likely attributable to a common mechanism. It is well established that moderate to severe acute normovolaemic haemodilution in animals[13,35,41], or chronic anaemia in human patients[1] induces a hyperdynamic cardiovascular response both systemically and regionally, characterised among other things by a reduction in vascular resistance and an increase in blood flow. The lowered vascular resistance during anaemia is mainly due to a reduction in blood viscosity as a result of reduced Hct[10]. In uncomplicated CB, we anticipated mild or no hypovolaemia, hypotension or hyperviscosity - pathophysiological changes that may be seen in the complicated disease. This means any change in Doppler variables during uncomplicated CB would mainly be due to the concurrent anaemia, and should be proportional to the Hct levels. This would explain the modest differences observed between uncomplicated CB and severe or moderate EA in the AAo, CMA, CA, HSA and MPV. Another possible reason for lack of significant differences between uncomplicated CB and any of the grades of EA may be due to a small sample of the cases investigated.

In severe human falciparum malaria, pathophysiological changes associated with systemic inflammatory response leading to hypovolaemia, hypotension, or an increase in plasma fibrinogen levels occur in addition to anaemia. Rheologic changes involving red blood

cell (RBC) cytoadherence (sequestration), reduced deformability and aggregation also occur[10]. Plasma hyperviscosity and the RBC changes would lead to an increase in peripheral vascular resistance[10]. All of the above changes singly or in combination would in turn lead to hypoperfusion. These changes are of particular significance in the microvessels[10]. In the larger vessels, plasma hyperviscosity is often counterbalanced by hypoviscosity due to reduced Hct such that the net effect is often little or no change in whole blood viscosity[38]. Finding normal or increased middle cerebral artery haemodynamics by transcranial Doppler in malaria patients that had evidence of hypoperfusion in the cerebral microvessels[21] supports the above argument.

Pathophysiological mechanisms similar to those of complicated malaria have been suggested for complicated CB that is known to cause hypoalbuminaemia[24]. This is thought to be due to the leakage of protein through the endothelium as is characteristic of critical illness[12]. Mild hyperglobinaemia is also a characteristic of CB, which may be due to antigenic stimulation[24]. Our data shows a normal mean total serum protein in the uncomplicated cases of CB although 2 of the 14 dogs had values above and 2 others had values below the normal range. Although hypoalbuminaemia or hyperglobinaemia alone may lower or raise blood viscosity respectively, it is thought that mild changes in the levels of these serum proteins, such as during uncomplicated CB, have little significance for haemodynamics since their effects frequently cancel each other out. Hypotension has also been reported in complicated CB[19]. A reduction in arterial blood pressure or circulating blood volume would be expected to increase peripheral vascular resistance indices. We were unable to confirm such changes since we did not measure blood volume or blood pressure. Another cause of difference between the uncomplicated CB in our study and EA would be due to a possible effect of diminazene administered to the CB dogs on their blood pressure. However, Joubert *et al*[20] found no influence of diminazene aceturate on systemic blood pressure of healthy adult dogs.

6.5.2 Renal haemodynamics

Variations in haemodynamic response among various vascular beds, or due to different degrees or types of normovolaemic haemodilution in animals have been reported[13,15,35,41]. Increases in renal vascular resistance indices during EA reported in our data contradict earlier studies that reported reduced renal vascular resistance in chronic or acute normovolaemic anaemia in the dog[35,41], while supporting a report of an increased renal artery resistance in response to increasing flow rate over an arterial pressure range of 75-200 mm Hg[16]. Another investigator found decreased effective renal blood flow with increasing severity of anaemia[34]. Grupp *et al.*[15] asserted that renal blood flow increased significantly during anaemia, but renal flow fraction of the cardiac output fell significantly. Haemodilution studies in rabbits found no significant change in renal blood flow[4]. The increase in blood flow during anaemia attempts to compensate for reduced oxygen carrying capacity and maintain optimum tissue oxygen delivery[39]. Blood with normal oxygen carrying capacity surpasses the oxygen requirements of the kidney, which experiences an oxygen deficit only during profound anaemia.[34] Renal auto-regulation occurs during an elevated flow rate, probably mediated by vasoconstriction thereby increasing renal vascular resistance[16]. The mechanism of auto-regulation is not clear, but available evidence suggests that the increase in renal blood flow during anaemia is proportionately lower than that in cardiac output determined under similar conditions[15,35]. It is possible that the increased peak systolic velocity during haemodilution or anaemia activates a renal auto-regulatory mechanism leading to an increase in renal artery resistance. This would explain the different patterns of haemodynamic changes between the LRA on one hand and the AAo, CMA, CA and HSA on the other observed in our study. The contradiction between different reports on renal vascular resistance and blood flow may be due

to differences in animal species, anaemia grades investigated, or the staging and methods of measurement.

In spite of having similar renal haemodynamic change patterns, our data shows that the uncomplicated CB group differed significantly from severe EA, moderate EA and the physiological state with respect to LRA resistive index. The higher LRA resistive index in the uncomplicated CB could not be explained on the basis of Hct levels. Also, significant differences between uncomplicated CB and the physiological state, based on resistive and pulsatility indices of the ILA, without a similar difference between severe EA and the physiological state[26] could not be explained by severity of anaemia. The observed differences between uncomplicated CB and severe EA may be explained by the presence of additional factors (pathology) peculiar to the disease. An increase in renal vascular resistance index supports observations of renal microvascular damage, or acute renal failure in uncomplicated or complicated CB respectively[25,26,42].

In human falciparum malaria with renal failure, reduced renal microvascular blood flow leading to ischemia has been attributed to multiple pathophysiological changes including hypovolaemia, hyperviscosity of blood, catecholamine release and renin-angiotensin activation[38], all promoting an increase in renal vascular resistance. High plasma catecholamine levels and renin activity have also been demonstrated in malaria patients without renal failure[37]. In Rhesus-alloimmunised human foetuses, an increase in splenic resistive index was attributed to blockage of splenic microvessels with damaged red blood cells[2]. Observations on haemodynamics of human falciparum malaria[11,21,37] have led to the suspicion that in CB renal microvascular haemodynamics may also be disrupted.

Mild renal damage is seen more frequently in clinically severe CB than a significant damage, or acute renal failure[26]. We did not quantify urine protein, however, previous studies have shown that proteinuria is frequently encountered in CB and is not a good indicator of disturbed renal function[27]. Serum urea may be elevated in complicated or uncomplicated CB[26]. There is a disproportionate rise in urea compared to creatinine probably due to hyperureagenesis[9]. On the other hand, elevated creatinine levels are seen in cases of complicated CB with impaired renal function[26]. Mean values for both urea and creatinine levels were normal in our sample of dogs with uncomplicated CB, although the standard deviations were relatively high. We can therefore assume that no dog in this trial had significant renal disease. This is not surprising considering the selection criteria used. Although elevated creatinine is commonly seen in the complicated form of CB and is a risk factor for death[42], we specifically selected dogs that had no evidence of complicated disease. The fact that renal vascular resistance indices were significantly increased in dogs that had no biochemical evidence of disturbed renal function was particularly interesting. It is possible that the presence of a localised pathophysiological change such as increased renin activity, or a renal pathology in uncomplicated CB, similar to that of human falciparum malaria, may have contributed to the significantly higher renal resistive and pulsatility indices. In human falciparum malaria with evidence of reduced cerebral microcirculation, Doppler ultrasound could not detect evidence of hypoperfusion in the middle cerebral artery. The resistance index of the middle cerebral artery was, however, not reported. Our observation raises hope that Doppler ultrasound may be useful in an early detection of renal involvement in CB.

The low likelihood of hypovolaemia, hypotension or hyperviscosity in our sample of uncomplicated CB may partly explain differences observed between renal and aortic or gastrointestinal haemodynamics. Greater vulnerability of the kidneys to CB, and the fact that renal failure is a more frequent cause of morbidity and mortality when compared to the liver,

spleen or gastrointestinal tract[26] may be another reason for the observed difference in renal haemodynamics. The haemodynamic changes described in this study are those of uncomplicated CB in which we do not see multiple organs dysfunction syndrome. A similar study of complicated forms of the disease with multiple organs dysfunction syndrome is envisaged, and we hypothesize that far more haemodynamic disturbance will be observed. Further investigations of both uncomplicated and complicated forms of CB will improve our understanding of the haemodynamic changes in the disease, and possibly other similar diseases such as human malaria.

In conclusion, this study revealed a similarity between uncomplicated CB and EA regarding patterns of haemodynamic changes in Doppler variables of the abdominal aorta and splanchnic vessels. These were characteristic of a hyperdynamic circulatory state. While the similarity in patterns of haemodynamic changes during uncomplicated CB and EA may be attributable to anaemia, increased renal vascular resistance was suggestive of renal pathology and a hypodynamic state, supporting earlier observations of other investigators[19,29].

6.6 ACKNOWLEDGEMENTS

Supported by Makerere University, and the University of Pretoria. We are grateful to the students and clinicians of the Small Animal Outpatients Section for assisting us in selecting canine babesiosis cases for this study.

6.7 REFERENCES

1. Anand I S, Chandrashekhar Y 1993 Reduced inhibition of endothelial-derived relaxing factor causes the hyperdynamic circulation in chronic severe anaemia. *Medical Hypotheses* 41:225-228
2. Bahado-Singh R, Pirhonen J, Rahman F, Abuhamad A Z, Mari G, Copel J 1995 Effect of foetal anaemia on splenic artery resistance index in red cell isoimmunisation. *Journal of the Society for Gynaecological Investigation* 2:146
3. Basson P A, Pienaar J G 1965 Canine babesiosis: a report on the pathology of three cases with special reference to the cerebral form. *Journal of the South African Veterinary Association* 36:333-341
4. Caron A, Menu P, Faivre-Fiorina B, Labrude P, Alayash A, Vigneron C 2000 Systemic and renal haemodynamics after moderate haemodilution with HbOCs in anaesthetised rabbits. *American Journal of Physiology Heart and Circulatory Physiology* 278:H1974-H1983
5. Clark I A, Chaudri G, Cowden W B 1989 Roles of tumour necrosis factor in the illness and pathology of malaria. *Transactions of the Royal Society for Tropical Medicine & Hygiene* 83:436-440
6. Clark I A, Jacobson L S 1998 Do babesiosis and malaria share a common disease process? *Annals of Tropical Medicine and Parasitology* 92:483-488
7. Clavier N, Rahimy C, Falaga P, Ayivi B, Payen D 1999 No evidence for cerebral hypoperfusion during cerebral malaria. *Critical Care Medicine* 27:628-632
8. Day M J 2000 Immune-mediated haemolytic anaemia. In Feldman B F, Zinkl J G, Jain N C (eds) *Schalm's Veterinary Haematology*. Lippincott Williams & Wilkins, Philadelphia: 799-806

9. de Scally M P, Lobetti R G, Reyers F, Humphris D 2004 Are urea and creatinine values reliable indicators of azotemia in canine babesiosis? *Journal of the South African Veterinary Association* 75:121-124

10. Dondorp A M, Kager P A, Vreeken J, White N J 2000 Abnormal blood flow and red blood cell deformability in severe malaria. *Parasitology Today* 16:228-232

11. Dondorp A M, Pongponratn E, White N J 2004 Reduced microcirculatory flow in severe falciparum malaria: pathophysiology and electron-microscopic pathology. *Acta Tropica* 89:309-317

12. Dormehl I C, Hugo N, Pretorius J P, Redelinghuys I F 1992 In *vivo* assessment of regional microvascular albumin leakage during E.coli septic shock in the baboon model. *Circulatory Shock* 38:9-13

13. Fowler N O, Holmes J C 1975 Blood viscosity and cardiac output in acute experimental anaemia. *Journal of Applied Physiology* 39:453-456

14. Gill R W 1985 Measurement of blood flow by ultrasound: Accuracy and sources of error. *Ultrasound in Medicine and Biology* 11:625-641

15. Grupp I, Grupp G, Holmes J C, Fowler N O 1972 Regional blood flow in anaemia. *Journal of Applied Physiology* 33:456-461

16. Haddy F J, Scott J, Fleischman M, Emanuel D 1958 Effect of change in flow rate upon renal vascular resistance. *American Journal of Physiology* 195:111-119

17. Jacobson L, Clark I A 1994 The pathophysiology of canine babesiosis: New approaches to an old puzzle. *Journal of the South African Veterinary Association* 65:134-145

18. Jacobson L S, Lobetti R G, Becker P, Reyers F, Vaughan-Scott T 2002 Nitric oxide metabolites in naturally occurring canine babesiosis. *Veterinary Parasitology* 104:27-41

19. Jacobson L S, Lobetti R G, Vaughan-Scott T 2000 Blood pressure changes in dogs with babesiosis. *Journal of the South African Veterinary Association* 71:14-20

20. Joubert K E, Kettner F, Lobetti R G, Miller D M 2003 The effects of diminazene aceturate on systemic blood pressure in clinically healthy adult dogs. *Journal of the South African Veterinary Association* 74:69-71

21. Kampfl A, Pfausler B, Haring H -P, Denchev D, Donnemiller E, Schumutzhard E 1997 Impaired microcirculation and tissue oxygenation in human cerebral malaria: A single photon emission computed tomography and near-infrared spectroscopy study. *American Journal of Tropical Medicine & Hygiene* 56:585-587

22. Koma L M, Kirberger R M, Scholtz L Doppler ultrasonographic changes in the canine kidney during normovolaemic anaemia. *Research in Veterinary Science* In press.

23. Koma L M, Spotswood T C, Kirberger R M, Becker P 2005 Influence of normovolaemic anaemia on Doppler characteristics of the abdominal aorta and splanchnic vessels in Beagles. *American Journal of Veterinary Research* 66:187-195

24. Leisewitz A L, Jacobson L S, de Morais H S, Reyers F 2001 The mixed acid-base disturbances of severe canine babesiosis. *Journal of Veterinary Internal Medicine* 15:445-452

25. Lobetti R G 1996 The comparative role of haemoglobinaemia and hypoxia in the development of nephropathy in the dog. *Journal of the South African Veterinary Association* 67:188-198

26. Lobetti R G, Jacobson L S 2001 Renal involvement in dogs with babesiosis. *Journal of the South African Veterinary Association* 72:23-28

27. Lobetti R G, Reyers F, Nesbit J W 1996 The comparative role of haemoglobinaemia and hypoxia in the development of canine babesial nephropathy. *Journal of the South African Veterinary Association* 67:188-198

28. Maegraith B, Gilles H M, Devakul K 1957 Pathologic processes in Babesia canis infections. *Zeits fur Tropenmedizin und Parasitologie* 8:485-514

29. Malherbe W D, Parkin B S 1951 Atypical symptomatology in Babesia canis infection. *Journal of the South African Veterinary Medical Association* 22:25-36

30. Matjila P T, Penzhorn B L, Becker C P J, Nijhof A M, Jongejan F 2004 Confirmation of occurrence of Babesia canis vogeli in domestic dogs in South Africa. *Veterinary Parasitology* 122:119-125

31. Moriyasu F, Ban N, Nishida O, Nakamura T, Miyake T, Uchino H, Kanematsu Y, Koizumi S 1986 Clinical application of an ultrasonic duplex system in the quantitative measurement of portal blood flow. *Journal of Clinical Ultrasound* 14:579-588

32. Moriyasu F, Nishida O, Ban N, Nakamura T, Sakai M, Miyake T, Uchino H1986 "Congestion index" of the portal vein. *American Journal of Roentgenology* 146:735-739

33. Nelson T R, Pretorius D H 1988 The Doppler signal: Where does it come from and what does it mean? *American Journal of Roentgenology* 151:439-447

34. Paterson J C S 1951 Effect of chronic anaemia on renal function in the dog. *American Journal of Physiology* 164:682-685

35. Race D, Dedichen H, Schenk J W R 1967 Regional blood flow during dextran-induced normovolaemic haemodilution in the dog. *Journal of Thoracic and Cardiovascular Surgery* 53:578-586

36. Schetters T P M, Kleuskens J, Scholtes N C, Gorenflot A F 1998 Parasite localisation and dissemination in the Babesia-infected host. *Annals of Tropical Medicine and Parasitology* 92:513-519

37. Sitprija V, Napathorn S, Laorpatanaskul S, Suithichayikul T, Moollaor P, Suwangool P, Sridama V, Thamaree S, Tankeyoon M 1996 Renal and systemic haemodynamics in falciparum malaria. *American Journal of Nephrology* 16:513-519

38. Sitprija V, Vongsthongsri M, Poshyiachinda V, Arthachinta S 1977 Renal failure in malaria: A pathophysiological study. *Nephron* 18:277-287

39. Spahn D R, Leone B J, Reves J G, Pasch T 1994 Cardiovascular and coronary physiology of acute isovolaemic haemodilution: A review of nonoxygen-carrying and oxygen-carrying solutions. *Anaesthesia and Analgesia* 78:1000-1021

40. Taboada J, Merchant S R 1991 Babesiosis of companion animals and man. *Veterinary Clinics of North America Small Animal Practice* 21:103-123

41. Vatner S F, Higgins C B, Franklin D 1972 Regional circulatory adjustments to moderate and severe chronic anaemia in conscious dogs at rest and during exercise. *Circulation Research* 30:731-740

42. Welzl C, Leisewitz A L, Jacobson L S, Vaughan-Scott T, Myburgh E 2001 Systemic inflammatory response syndrome and multiple-organ damage / dysfunction in complicated canine babesiosis. *Journal of the South African Veterinary Association* 72:158-162

CHAPTER 7

GENERAL DISCUSSION

The method described in Appendix A successfully induced a non-terminal, severe, acute anaemia (mean Hct 16.0%) in healthy Beagles within 4 days without any major problem apart from a transient collapse during blood withdrawal on one occasion. Our experience has shown that initially only about one third of dogs require sedation during blood withdrawal, this proportion rising up to three quarters during repeat withdrawals as dogs become increasingly aware and apprehensive of the procedure. A sedative with a significant cardiovascular effect should not be used, especially with deepening level of anaemia to avoid possible cardiovascular collapse. Use of dog's own plasma with additional Ringer's lactate for blood volume replacement was considered satisfactory for our case. Although confirmation of normal blood volume was not done, we estimated that the true volume deficit due to loss of red blood cells was only about 9%. Dextran, the traditional fluid used for volume replacement, was regarded unsuitable because of its hyperoncotic property[1] that could have interfered with natural fluid homeostatic compensatory mechanisms. Since the Doppler measurements were obtained at least 16 hours after the last blood withdrawal, any remaining deficit would probably have been compensated for by normal fluid redistribution between compartments during normal water intake.

The significant increases in blood velocities or in blood flow, concurrent with significant reductions in Doppler resistance indices observed in all abdominal vessels, except the renal artery, during CB and EA suggest the presence of hyperdynamic circulatory states in these conditions. This observation concurs with those reported for moderate to severe acute[2,3] or

chronic[4] anaemia in human patients, and experimental studies in dogs[5-7]. Doppler patterns of renal haemodynamics during both uncomplicated CB and EA differed from the rest of the abdominal vessels, with significant increases in pulsatility and resistive indices suggesting a hypodynamic tendency. Comparisons of the left renal artery with other abdominal vessels as reported in chapter 5 indicated relative reductions in the renal end diastolic and time-averaged mean velocities, and in time-averaged mean velocity ratio. It is interesting to note that a significant difference in left renal artery TAV_{mean} between anaemic and physiologic states was detected by ratios and between vessels paired comparisons but not within vessel comparison. This observation supports an earlier study that reported a significant increase in renal blood flow concurrent with a significant reduction in the renal flow fraction of the cardiac output during EA in the dog[6].

Close similarity between uncomplicated CB and EA haemodynamic change patterns probably suggests that the observed changes in both conditions share a common pathophysiological mechanism, i.e. anaemia. However, a significantly higher resistive and pulsatility indices of the ILA during CB when compared to the physiological state, and significantly higher resistive index of the LRA during CB when compared to severe EA support the view of impaired renal haemodynamics in CB attributable to factors such as congestion of capillaries with sequestered red blood cells[8,9]. This situation may be even more apparent with complicated CB.

The study has proved, to a large extent, the hypothesis that Doppler values during uncomplicated CB or EA are different from those during the physiological state; and to some extent that uncomplicated CB and EA differ from each other. In conclusion, this study has demonstrated that Doppler ultrasonography may be beneficial in the clinical evaluation and management of suspicious or complicated cases of CB.

7.1 REFERENCES

1. Mathews KA. The various types of parenteral fluids and their indications. *Veterinary Clinics of North America. Small Animal Practice*. 1998;28:483-513.
2. Mari G, Adrignolo A, Abuhamad AZ, Pirhonen J, Jones DC, Ludomirsky A, Copel JA. Diagnosis of fetal anemia with Doppler ultrasound in the pregnancy complicated by maternal blood group immunization. *Ultrasound in Obstetrics and Gynecology*. 1995;5:400-404.
3. Cosmi E, Mari G, Chiaie LD, Detti L, Akiyama M, Murphy KJ, Stefos T, Ferguson JE, Hunter D, Hsu CD, Abuhamad AZ, Bahado-Singh R. Noninvasive diagnosis by Doppler ultrasonography of foetal anaemia resulting from parvovirus infection. *American Journal of Obstetrics and Gynecology*. 2002;187:1290-1293.
4. Anand IS, Chandrashekhar Y, Wander GS, Chawla LS. Endothelium-derived relaxing factor is important in mediating the high output state in chronic severe anaemia. *Journal of American College of Cardiologists*. 1995;25:1402-1407.
5. Race D, Dedichen H, Schenk JWR. Regional blood flow during dextran-induced normovolemic hemodilution in the dog. *Journal of Thoracic and Cardiovascular Surgery*. 1967;53:578-586.
6. Grupp I, Grupp G, Holmes JC, Fowler NO. Regional blood flow in anemia. *Journal of Applied Physiology*. 1972;33:456-461.
7. Vatner SF, Higgins CB, Franklin D. Regional circulatory adjustments to moderate and severe chronic anaemia in conscious dogs at rest and during exercise. *Circulation Research*. 1972;30:731-740.
8. Malherbe WD, Parkin BS. Atypical symptomatology in Babesia canis infection. *Journal of the South African Veterinary Medical Association*. 1951;22:25-36.

9. Maegraith B, Gilles HM, Devakul K. Pathological processes in *Babesia canis* infections. *Zeitschrift fur Tropenmedizin und Parasitologie*. 1957;8:485-514.

CHAPTER 8

SUMMARY

This study compared Doppler variables of the abdominal aorta and splanchnic vessels between CB, EA and the physiological state. Part one presents Doppler investigations of abdominal vessels during physiological state and during severe, moderate and mild EA in 11 healthy Beagles. The anaemia induction method is detailed in Appendix A, and Doppler evaluation results are presented in chapters 3-5.

There were significant increases in all velocity components of the AAo, CMA, CA and MPV, and in portal blood flow in anaemic dogs (Chapter 3). Resistance indices of the same vessels, and that of the hilar splenic artery were significantly reduced. The haemodynamic changes were most notable during severe EA. The most consistent change was significant increase in time-averaged mean velocity (TAV_{mean}) during all grades of EA in all relevant vessels, except the CA and MPV during mild EA. Changes involving other Doppler variables varied with the vessel and EA type. These changes were consistent with a hyperdynamic circulatory state.

In renal haemodynamics significant changes were found only during severe EA (Chapter 4). Each velocity component of the LRA responded differently: peak systolic velocity increased significantly, end diastolic velocity decreased significantly, while TAV_{mean} remained unchanged. Also in contrast to other abdominal vessels, pulsatility and resistance indices of the LRA increased significantly during anaemia suggesting a hypodynamic circulatory state, although resistive indices of the renal ILA remained unchanged.

Chapter 5 presents comparisons of corresponding velocities and velocity ratios between splanchnic vessels and the AAo during physiological and anaemic states, and within vessel comparison of the physiological and anaemic states. The LRA TAV_{mean} ($P \leq 0.008$) and end diastolic velocity ($P \leq 0.041$) were significantly lower than the corresponding aortic, CMA and CA variables during the anaemic state. Left renal artery TAV_{mean} ratio was significantly ($P = 0.014$) lower during the anaemic than physiological state, and significantly ($P \leq 0.004$) lower than the corresponding CMA or CA variable in anaemic dogs. These observations suggest presence of absolute and relative reductions in LRA TAV_{mean} ratio, TAV_{mean} or end diastolic velocity during anaemia.

Part two of the study compared data of uncomplicated CB with those of the EA (Chapter 6). There was a striking similarity between CB and EA haemodynamic change patterns involving all Doppler variables in all vessels. In spite of this similarity, renal resistive indices during CB were significantly higher than those during the EA or controls.

The similarity in haemodynamic patterns during CB and EA is attributed to anaemia while significant differences between the groups may be attributable to pathophysiological factors peculiar to CB. Our observations support the view that renal circulation is impaired during CB by various factors such as hypotension, hypovolaemia or blockage of capillaries with sequestered red blood cells. This study has proved, to a large extent, the hypothesis that Doppler values during EA or uncomplicated CB are different from those during the physiological state; and to some extent that EA and uncomplicated CB differ from each other. Doppler ultrasonography is a useful technique for clinical investigation of haemodynamics in CB and related diseases.